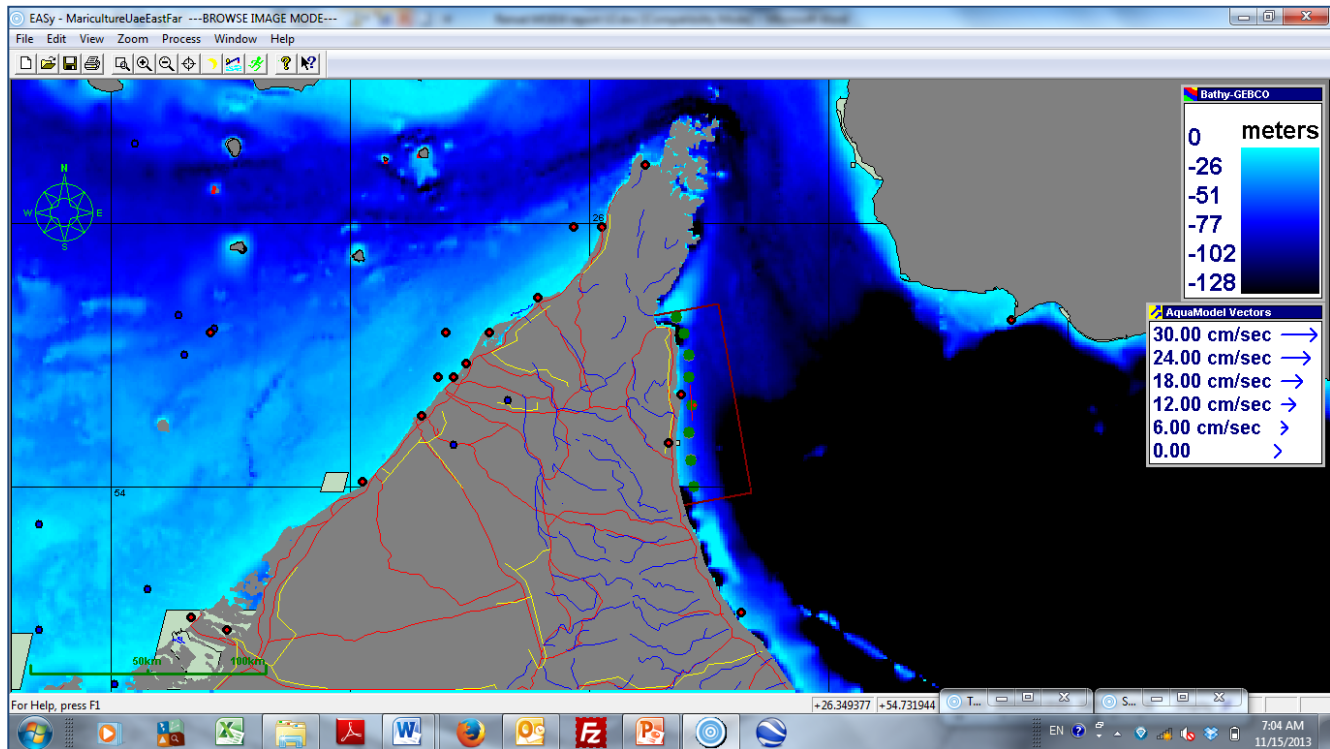


Initial Study of Potential Fish Mariculture near the United Arab Emirates East Coast with AquaModel Software



Prepared for

**United Arab Emirates
Ministry of Environment and Water
and
Dr. Donald Anderson,
Woods Hole Oceanographic Institution**

By

**Jack Rensel, Ph.D., Frank O'Brien and Dale Kiefer, Ph.D
Systems Science Applications, Inc.
Irvine, CA 92620**

November 30, 2013

Table of Content

Executive Summary of Project	1
Executive Summary of AquaModel Software	3
Introduction	4
Objectives, purpose and origin of model	4
Model Description	5
Overview	5
Circulation Module	14
Fish Physiology and Farm Module	16
Outline of AquaModel Fish Physiology Structure.....	19
Plankton Module.....	27
Benthic Module.....	27
Physical Circulation Module	32
Prior Validation	34
Primary AquaModel Coefficients for UAE Simulation	36
Fish Species Selection and fecal Settling Rates	37
Waste fish feed settling rates	37
Waste fish feed loss rates	37
Resuspension threshold.....	38
Deposition threshold	39
Consolidation rate.....	39
Description of Study Sites and Virtual Fish Pens	40
Near Field, Single Fish Farm AquaModel Analysis Results	46
Current Velocity	46
Dissolved Oxygen and Nitrogen.....	47
Benthic Effects	56
Far Field, Eight Fish Farm AquaModel Analysis Results.....	61
Current velocity	61
Current Direction	63
Phytoplankton and Algal Effects.....	65
Decision Matrix for Net Pen Siting.....	69

Summary of Project Achievements	70
Recommendations	71
References Cited	73

List of Figures

Figure 1. EASy software architecture and data integration processes.....	6
Figure 2. Diagrammatic representation of key processes simulated in AquaModel.	7
Figure 3. Array settings for AquaModel such as location of center or farm(s), default bottom depth (if detailed bathymetry not available) and capture cell locations to output spreadsheet or database results.....	8
Figure 4. Pen location, size and initial loading settings (for Pen 1 only).	9
Figure 5. Water column conditions and optional synthetic tidal flow simulation settings, the latter not used when current meter or 3D flow field data are available.	9
Figure 6 Feed rate override settings, compute optimum feed use settings, percent feed loss level, initial pen oxygen and nitrogen settings, fecal and waste feed sinking rate, fish growth range bounds.....	10
Figure 7. Benthic and sediment properties plot ranges, initial values, settling rates of feed and feces and other related controls. The values selected for erosion deposition and erosion threshold in Figure 7 are highly conservative for the present application.	11
Figure 8. Several of the fish physiological parameters and coefficients obtained from best fit to literature values and our growth experiments (developer’s version only).	12
Figure 9. Contouring, current vector display, time stream and other display settings.....	13
Figure 10. NPZ (plankton) model settings, factors, coefficients and rates (developer’s version only).....	14
Figure 11. AquaModel current data input menu for inputting ROMS, ADCIRC and FVCOM circulation model data.	15
Figure 12. Generalized fish metabolic processes described by the routine for fish metabolism. (Background drawing by Duane Raver, USFWS; assimilation factor is adjustable).	18
Figure 13. Logic of Fish Physiological Model.	20
Figure 14. Conceptual diagram of waste transporting model components.....	28
Figure 15. Conceptual model of benthic dynamics processes and respiration. Sulfide inhibits aerobes, oxygen inhibits anaerobic organisms and vice versa. Increased carbon loading leads to domination by anaerobes when the oxygen supply is inadequate for the aerobes.	30
Figure 16. Organic loading to sediments and interstitial oxygen concentration relationship.	31
Figure 17. Growth rate measured in culture versus predicted (P) by model for initial calibration runs.....	34
Figure 18. Laboratory measured vs. model predicted (P) respiration rate for initial calibration runs.....	35

Figure 19	Summary of dissolved oxygen deficit compared to background (upstream) conditions for commercial net pens in prior studies. N = 12.	36
Figure 20.	Summary of dissolved inorganic nitrogen increases inside commercial net pens and immediately downstream relative to ambient conditions as described in text. N = 12.	36
Figure 21.	Landsat image of part of UAE with eight virtual fish farm sites for demonstration purposes only. The authors of this document are not suggesting that fish farms should be placed at these locations as indicated in this document.....	41
Figure 22.	Vicinity map of sites 1 (near field site) and 2 near the shoreline bight of Fujairah.	41
Figure 23.	AquaModel bathymetry and modeling domain (small box to the left) with green net pens in center for Site 1, the near field site that was examined with regard to sediment effects on a fine scale.....	42
Figure 24.	Site 1 net pen fish farm with the eight net pen cages shown within the 1.8 km square modeling domain and with a red transect line drawn across the middle to illustrate the gradually sloping depth profile with the cages at about 42m depth.	42
Figure 25.	AquaModel view of Arabian Gulf (left) and Sea of Oman/Arabian Sea (right) with part of the Arabian Peninsula. United Arab Emirates east coast modeling domain indicated by the rectangular green box and some of the GIS shapefiles turned on to illustrate the GIS functions of the program.....	43
Figure 26.	Closer view of the modeling domain for the far field examination of 8 locations along the UAE east coast with mariculture options showing the basic layout of the array. ...	43
Figure 27.	3D view of the UAE east coast AquaModel bathymetry from using the AquaModel Image Statistics tool.....	45
Figure 28.	3D view of UAE west coast (left side) and east coast (right side) showing profound differences in depth structure.	45
Figure 29.	Beginning of last month of fish culture cycle showing water column and benthic parameters X-Y plots with dissolved nitrogen as the primary image.....	49
Figure 30.	Midway through month 5AM showing a mixture of water column and benthic parameters X-Y plots with dissolved nitrogen as the primary image.....	50
Figure 31.	Mid way through month 6AM showing a mixture of water column and benthic parameters X-Y plots with dissolved nitrogen as the primary image.....	51
Figure 32.	Mid way through month 7AM showing a mixture of water column and benthic parameters X-Y plots with dissolved nitrogen as the primary image.....	52
Figure 33.	Mid way through month 8AM showing a mixture of water column and benthic parameters X-Y plots with dissolved nitrogen as the primary image.....	53
Figure 34.	Midway through Month 10AM showing a mixture of water column and benthic parameters X-Y plots with dissolved nitrogen as the primary image.....	54
Figure 35.	End of Month 4AM showing a mixture of water column and benthic parameters X-Y plots with dissolved nitrogen as the primary image.....	55
Figure 36.	Total organic carbon (percent) from zero to 250 m from net pen Site 1 simulation.	56

Figure 37. Beginning of last month of fish culture cycle showing benthic parameters X-Y plots with fractional amount of total organic carbon as the primary image.	58
Figure 38. Midway through final month of fish culture with very limited benthic effects occurring only below and immediately adjacent to net pens.	59
Figure 39. End of last month of fish culture showing increased rates of processing wastes (i.e., in the aerobic and anaerobic bacterial profiles as well as the sediment CO ₂ and sulfides profiles) but these and other rates and results indicate that benthic carrying capacity has not been exceeded.	60
Figure 40. Average and standard deviation of current velocity for net pen depth from all eight study locations from far field AquaModel analysis of the FVCOM circulation model results.	61
Figure 41. Current velocity frequency diagrams for all eight study sites along the UAE east coast derived from AquaModel tools applied to an FVCOM circulation model prepared by Dr. Rubao Ji, Woods Hole Oceanographic Institution.	62
Figure 42. Frequency of occurrence of water currents in each of the specified direction sectors and velocity classes for a month long period at the simulated Site 1 location, using current velocity data extracted from the FVCOM model by AquaModel utilities with vectors showing the towards direction (not the from direction).	63
Figure 43. Frequency of occurrence of water currents in each of the specified direction sectors and velocity classes for a month long period at the simulated Site 4 location, using current velocity data extracted from the FVCOM model by AquaModel utilities with vectors showing the towards direction (not the from direction).	64
Figure 44. Frequency of occurrence of water currents in each of the specified direction sectors and velocity classes for a month long period at the simulated Site 8 location, using current velocity data extracted from the FVCOM model by AquaModel utilities with vectors showing the towards direction (not from direction).	64
Figure 45. Beginning of last month of fish culture with images from top left to bottom right: Nitrogen transect (red line perpendicular from shore through Site 2, phytoplankton transect, nitrogen profile, phytoplankton profile, main image of phytoplankton standing stock (with very low range of concentration to only 0.42 µg L ⁻¹) and total fish biomass.	66
Figure 46. Midway through final month of fish culture with apparent increase of phytoplankton near shore but actual increase is no more than 0.02 µg L ⁻¹	67
Figure 47. Completion of final month of fish culture with no change from the prior image two weeks before.	68

List of Tables

Table 1. Example AquaModel fish physiology submodel functions (<i>O. mykiss</i>).	21
Table 2. Description of functions for AquaModel fish physiology model	23
Table 3. Example fish physiology coefficients and conversion factors (from <i>O. mykiss</i>)	24

Table 4. Study location sites, cage volume, fish density, weight and biomass at the beginning of the final month of culture for fish farm No. 1 near Fujairah only (above) and eight fish farms spread along the entire east coast UAE (below). All sites were about 40 m deep.	44
Table 5. Summary of single fish farm current velocity, biomass, feed use, growth rate, pen oxygen and dissolved inorganic nitrogen in cages during a final month of growout of sea bream.....	47
Table 6. Total organic carbon at varying distances along primary current vector direction line for Site 1.....	56
Table 7. Current velocity average, standard deviation, 5 th and 95 th percentile for all eight study locations both at net pen depth and seabottom from far field AquaModel analysis of the FVCOM circulation model results.	61
Table 8. Phytoplankton as chlorophyll ($\mu\text{g L}^{-1}$ = micrograms per liter) summary table for final month of fish culture at study sites from far field AquaModel simulation.	65
Table 9. Example site selection matrix for various factors involved in site selection.	69

This report should be cited as:

Rensel, J.E., Kiefer, D.A., and F.J. O'Brien. 2013. Initial AquaModel Study of Potential Fish Mariculture near the United Arab Emirates East Coast. Prepared by Systems Science Applications, Inc. Los Angeles for Dr. Donald Anderson, Woods Hole Oceanographic Institution and the United Arab Emirates, Ministry of Environment and Water. 77 p.

Funding for this study was provided via a subcontract from the Ministry of Environment and Water, United Arab Emirates, through Dr. Donald Anderson.

Dr. Rubao Ji of Woods Hole Oceanographic Institution cheerfully provided FVCOM circulation model output data and assistance in using the data for which we are most grateful.

EASy and AquaModel software products are copyright-protected property of System Science Applications Inc. and no portion of this report may be copied or distributed without the express written permission of System Science Applications Inc., Dr. Don Anderson or the Ministry of Environment and Water of the United Arab Emirates.

For more information about AquaModel, please visit www.AquaModel.org and the underlying GIS system visit www.runEASy.com

Executive Summary of Project

This report documents the initial application of AquaModel fish farm siting and effects simulation software to the east coast waters of the United Arab Emirates (UAE) for the Ministry of Environment and Water. AquaModel software is used to forecast sediment and water quality effects of aquaculture as well as to aid in aquaculture site selection, cage configuration and spacing, fish farm management and carrying capacity estimation. Users include the U.S. government (NOAA-NOS), the Chilean Government's research arm (IFOP), and consultants from many other regions in the world.

The work reported herein was part of a major program of the Ministry to address harmful algae ("red tide") issues following the massive fish killing bloom of 2008-2009 in a project led by Dr. Donald Anderson of the Woods Hole Oceanographic Institution. The overall project involves review and planning for actions to deal with harmful algal effects on fish, shellfish, desalination plants, monitoring, satellite imagery use in the waters of the Arabian Gulf and Sea near UAE.

This fish farm study focused on the UAE east coast as it has an operational fish farm company and appears to be more suited for a marine fish culture industry compared to the UAE west coast because of water quality, current velocity, depth and wind wave conditions discussed herein. The west coast apparently has more frequent and destructive wind wave events and water temperature and salinity maximums that exceed optimum ranges for some types of cultured marine fish such as sea bass (*Dicentrarchus labrax*).

To conduct this study, we wrote and tested software code for AquaModel for use with data from one of the most advanced and powerful ocean circulation models available known as FVCOM (Finite-Volume Coastal Ocean Model). An application of this model was specially constructed for the Arabian Gulf and northern Arabian Sea (i.e., Sea of Oman) by Dr. Rubao Ji of Woods Hole Oceanographic Institution. The circulation model uses an irregular grid with higher resolution near shore and in the zone where future marine fish net pens are likely to be utilized. The data output of the FVCOM model are both complex and extensive, requiring considerable effort to design new code to import into AquaModel, which uses a gridded (Cartesian) coordinate system.

Using data generated by this advanced software that was processed to run in AquaModel by a new utility we built, we were able to perform a virtual survey of the east coast of the United Arab Emirates using AquaModel utilities to gain insight into key factors that would influence the success or failure of large commercial net pen operations in the region.

In the preliminary application of the model, we chose the worst-possible-case time period of the fish culture cycle to model. That would be late summer/early fall, the time period when the fish are the largest, are consuming the most feed and are contributing the most dissolved nitrogen wastes and have the highest oxygen demand of the culture cycle. If impacts are small and not trending upward during this last month of culture during the warm summer months, we could judge the results to indicate a higher probability of no significant adverse effect. In addition to impacts within and near the pens to the fish such as reduced dissolved oxygen or high levels of ammonia nitrogen that would stress the fish, we also considered the possibility of regional eutrophication (significant increase of algal biomass) and epiphytes on nearshore habitats such as coral reefs as a result of fish farm nitrogen flowing toward shore.

Similarly, for seabottom habitats, we conducted a worst case evaluation when fish biomass is the largest and feed use and particulate fish fecal waste products are at their annual maximum. Benthic waste effects can be cumulative over time. Thus, we examined the model to assure that the possible sites produced steady state effects, not a gradually increasing effect on the sea bottom that would indicate that total organic carbon was more rapidly accumulating than being dispersed and assimilated by the benthic food web. Steady state operation is a primary goal of commercial net pens, provided the waste assimilation is done with the surficial layer of the bottom remaining aerobic, not anaerobic without having to “fallow” the seabottom for extended periods after each fish culture cycle.

The results of this preliminary study are encouraging. Current velocity at all the studied areas along the UAE east coast, based on the far field circulation model, are near optimum to allow large cages, modestly high fish stocking rates, good supply of oxygen to the fish and suitable depths to help disperse wastes for assimilation by the aquatic food web. The organisms at greatest risk to compromised water quality in any net-pen fish farm operation are the farmed fish themselves, not wild fishes or invertebrates. Large spacing of cages, strong and persistent currents greatly reduce such risks to minimal at the proposed site, as discussed in this report.

Water column effects of fish farms are much more transitory and in the present case we expect to see very minor decreases of dissolved oxygen and increases of dissolved inorganic nitrogen within the cages and immediately downstream. But nutrient loading can be a cumulative effect of having many fish farms and we demonstrate herein the use of AquaModel to estimate carrying capacity of the UAE east coast in that regard.

At depths of at least 30 m and 40 m or more, there should be no significant, measurable adverse effect of large scale net pen aquaculture provided that operational best management practices such as feed loss monitoring are utilized daily. But the carrying capacity of the area for benthic and water column to accept fish aquaculture is not unlimited. The fish farm sizes were selected to have just the beginning of perturbation to the benthic invertebrate community immediately below the cages but not outside that immediate footprint area. In some cases, beneficial effects such as increased diversity and abundance of benthic organisms are possible at low organic carbon loading rates like this, but it is not possible to predict exactly at this point. Given more accurate calibration than was possible in this preliminary study, carrying capacity estimates are possible by means discussed in this report.

The above optimistic conclusions are tentative because this was a preliminary study. We identify tasks remaining to be completed and include specific short and long term recommendations for proceeding with use of AquaModel to manage mariculture operations in UAE.

We also prepared a separate report dealing with mitigation of the adverse effects of harmful algae (HABs) on fish farms in the region. In other regions of the world mitigation of HABs has not been a major impediment to profitable and sustainable mariculture, provided that plans and equipment are be ready in the event of future blooms.

Executive Summary of AquaModel Software

AquaModel is the first and only comprehensive computer model for net-pen aquaculture that simultaneously calculates and displays real-time feed ingestion, growth, respiration, excretion, and egestion by cultured fish. The model is composed of interlinked submodels of fish physiology, hydrodynamics, water quality, solids dispersion and assimilation. The system provides the user a 3-dimensional simulation of growth, metabolic activity of caged fish, associated flow and transformation of nutrients, oxygen, and particulate wastes in adjacent waters and sediments. AquaModel resides within a Geographic Information System (GIS) program designed for oceanographic use but is compatible with other common 2-dimensional GIS software.

AquaModel is not sold but rather licensed to governments and a limited number of professional users while it is being tested and validated in a number of locations worldwide. Within the software are many data graphic and statistical utilities, water flow rate and direction summary tools, methods to utilize several types of digital bathymetry, and means to import and interactively display GIS, water quality, satellite imagery and other data in a video-like fashion or real time using the polling and processing ability of the software. By combining these diverse sources of information in a GIS-based system, users are able to identify locations for, and configure selected fish farm sites for profitable fish farm businesses while protecting the seabottom and water column habitats of ocean creatures. Our research and the scientific literature in general shows that optimum growing conditions are not only good for the profitability of a fish farm but for the environment as well.

AquaModel calculates and displaying geo-positioned transport and food web assimilation of the particulate and dissolved waste in the benthic and plankton communities, respectively. The system utilizes a user friendly drop-down-menu interface that is designed for coastal managers, planners, biologists and fish farm company managers. The model has been used in several countries from tropical to temperate locations worldwide and continues to be refined and validated where used.

The potential fish farming area extends along the UAE east coast from the Fujairah area to the Oman border on the south that is a relatively uniform shoreline zone. Two applications of AquaModel were produced: a single fish farm with 8 cages near Fujairah and another 8 separate fish farms spaced along the entire coast that also included 8 cages in each fish farm. Each farm was configured to produce about 1,000 metric tons of fish such as gilthead sea bream. The simulations involved the use of a high quality and resolution circulation Finite Volume Ocean Model (FVCOM) model produced by Dr. Rubao Ji of the Woods Hole Oceanographic Institute in 2013. The un-gridded data were reprocessed by AquaModel for conversion into the gridded Cartesian coordinate system used by the model. This involved creation of extensive new software code for AquaModel and the output was checked and compared to hourly average model vectors produced in a video by Dr. J. As there were no high resolution bathymetry data readily available for the subject area, we used data from TCarta Inc. with a resolution of 50m and the AquaModel bathymetry processing routine to produce the needed bathymetry imagery.

The goal of this initial project was to produce the models described above and populate them with preliminary input data and make some general observations about the resulting output. The

benthic effect results indicate that the subject area is well flushed and subject to relatively strong currents. Accordingly, the probable amount of effects on the seabottom would be minimal, i.e., only minor adverse effects if any immediately underneath the farms that would be rapidly mitigated by following the fish farm for short periods. More likely the strong currents will result in no adverse impacts to the seabottom and full assimilation of the particulate waste products. As first described in the classic paper by Pearson and Rosenberg (1978), modestly low enrichment of seabottom areas with organic carbon often results in an increase in species diversity. This measure is widely agreed to represent an environmental benefit as diverse food webs tend to be more stable and sustainable than impoverished food webs. Additional model runs using other initial and boundary conditions should be completed to further validate these conclusions.

The water column results show that waste nitrogen from fish excretion is rapidly dispersed and then over time assimilated by phytoplankton that are consumed by zooplankton. For the period of current flow available (July through December 2008) we did not observe persistent periods of onshore flow. Onshore flow from large commercial fish farms is to be avoided to protect nearshore and shallow habitats of special significance such as coral reefs and sea grass meadows. Excessive nutrients, solids and especially organically rich solids in these areas can foster epiphytic algal growth that could be detrimental to existing food webs (Weber et al. 2012). We also noted that dissolved oxygen concentrations near the fish pens and farms remained replete with oxygen compared to remote locations, indicating that the carrying capacity of each location was not being exceeded by the size of the fish farms.

Introduction

Objectives, purpose and origin of model

The purpose of this report is to document the application of computer simulation software known as AquaModel to simulate the water column and benthic effects of net pen fish culture on the east coast waters of the United Arab Emirates for the Ministry of Environment and Water. The model is a product of Systems Science Applications, Inc. (Dr. Dale Kiefer, Dr. Jack Rensel and Mr. Frank O'Brien) and is used both as a consulting tool by us and is currently being prepared for and by governments for management of net pen industries. The AquaModel team has been involved in modeling aquaculture effects since 1990 (Kiefer and Atkinson, 1988, 1989, Rensel 1987, 1989a, 1989b, and many other more recent reports and publications at the [AquaModel publications](#) page. Dr. Rensel has been involved in study of the environmental effects of aquaculture and related fields since 1976.

The first application of AquaModel was for simulating the water column effects of salmon farming in the Pacific Northwest United States, in work performed for the National Oceanic and Atmospheric Administration and the Washington Fish Growers Association (Rensel et al. 2001, 2002, 2003, 2007). Subsequently, the model was adapted for use in the Caribbean Sea for the culture of a fast-growing fish known as cobia (*Rachycentron canadum*). As of 2013, AquaModel has been used in several other locations worldwide. The program is being used by the U.S. National Ocean Service of NOAA and the Chilean Government's primary research organization, Instituto de Fomento Pesquero.

AquaModel is unique among aquaculture models as it simultaneously calculates and displays real time images of physiological effects of fish aquaculture including their respiration (oxygen consumption), nitrogen excretion (mostly ammonia and minor amounts of urea that both rapidly convert to nitrate in the environment), microalgal (phytoplankton growth) resulting from the nitrogen excretion and zooplankton grazing upon the available stocks of phytoplankton in the modeling domain. Concurrently, it simulates discharge and flux of carbon-containing solids from fish feces and waste feed that eventually sink and are deposited on the seabottom. In physically active locations, the wastes are resuspended, aerated and re-transported laterally when near bottom current velocities exceed threshold values. In these more appropriate locations, the wastes are assimilated by the food web without causing significant change of the seabottom community to anaerobic bacteria; this process is to be avoided as reduces or eliminates benthic invertebrate infauna.

The benthic submodel of AquaModel bears some resemblance to other aquaculture models including DEPOMOD (Cromey et al. 2002a, 2002b) as both were derived in part from the well-known G-model of carbon degradation (Westrich and Bernier 1984) and subsequent studies described herein. No computer code or specific information was borrowed from DEPOMOD. Rather, all algorithms and code were developed independently from the underlying literature and known stoichiometric mass-balance relationships, although some calibration settings are shared from the available scientific literature.

AquaModel may be classified as a multibox model with either 2 or 3 dimensional (2D or 3D) hydrodynamic flow options. It is structured to allow use of single point or ADCP current meter data inputs. It can also simulate tidal flows based on site specific tidal characteristics and can utilize advanced 3D hydrodynamic model output. AquaModel is one of several “plug in” models developed for use within Geographic Information System software known as Environmental Analysis System (EASy) which has multiple functions and purposes. At present the model is a consulting tool of Science Systems Applications (SSA) which is owned by Dr. Dale Kiefer and Mr. Frank O’Brien. Dr. Jack Rensel is a third partner in the team and is an aquaculture effects specialist who works with SSA on model design, testing and application. Dr. Katsuyuki Abo of the Japanese Fisheries Research Agency has also contributed in development of the hydrodynamic submodels.

Model Description

Overview

To our knowledge our EASy AquaModel is the only software that provides a complete, dynamic model of farm operation and environmental impact. It is also the only software that fully integrates environmental information with model computations within a user-friendly geographical information system (GIS). More information can be found at www.AquaModel.org and simplified demonstrations of model use can be found at <http://netviewer.usc.edu/projects.htm> (only use Internet Explorer and closely follow browser options). The GIS program EASy is described at <http://www.runeasy.com/>

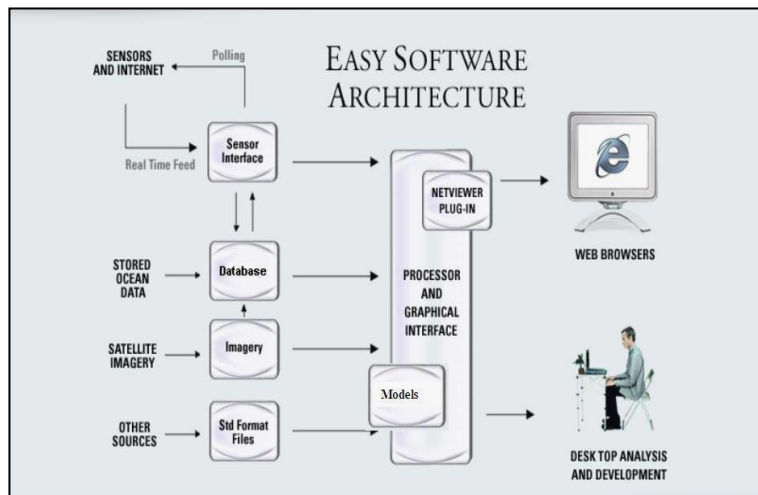


Figure 1. EASy software architecture and data integration processes.

AquaModel and the underlying EASy GIS system have the capability to contain environmental information obtained from satellite-ocean thermal and color sensors and field surveys or remote sensing and reporting of currents, nutrients, oxygen, chlorophyll and other related parameters. It also contains a simulation of virtual fish farms that can be “placed” within given water body and operated according to the conditions found at that location. Most importantly, the information system fully integrates field surveys of conditions in the water body with a dynamic model describing the growth and physiology of penned fish under any operating conditions selected by the user. The GIS software EASy provides a 4 dimensional framework (latitude, longitude, depth, and time) to run simulation models and analyze field measurements as graphical, numerical and statistical outputs. EASy, whose components are summarized in Figure 1, is an advanced, PC-based geographical information system designed for the storage, dissemination integration, analysis and dynamic display, of spatially referenced series of diverse oceanographic data.

AquaModel graphically renders dynamically in time, within their proper geo-spatial context, both field and remotely sensed data and model outputs as diverse types of plots, including vector, contour, false color images and includes a built-in data contouring feature. Vertical structure of data, critical in oceanographic applications, is depicted as vertical contours for transects or depth profiles at selected point locations. Time series for measurements and relationships such as vertical profiles within the database at individual stations can also be visualized interactively as XY-plots. Presently there are over 50 different X-Y plots available for different parameters viewed as vertical profiles or horizontal cross sections that are dynamically updated in real time simulations. The software also provides access to data, integrated visualization products, and analytical tools over the Internet via Netviewer, a client-server, plug-in for EASy.

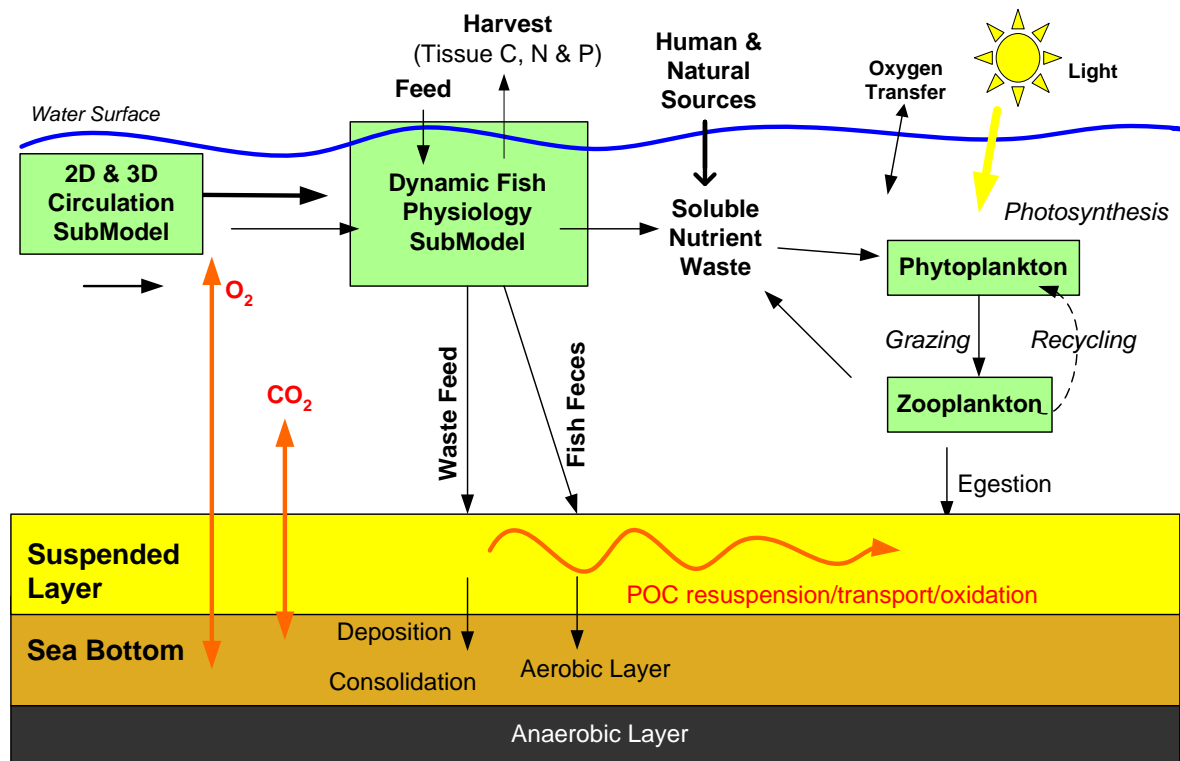


Figure 2. Diagrammatic representation of key processes simulated in AquaModel.

AquaModel consists of 4 components: a 2 or 3 dimensional description of water circulation, a description of the growth and metabolic activity of the cultured fish within the farm, a description of the planktonic community's response to nutrient loading, and a description of benthic effects (Figure 2).

The primary benthic parameter of interest is the loading of total organic carbon, but the model also simulates the status of sulfides, interstitial dissolved oxygen, aerobic and anaerobic bacteria biomass, carbon dioxide and related parameters in the sediments. AquaModel uniquely tracks waste feed and fish fecal matter separately and is pre-equipped with pertinent coefficients and functions to simulate salmon, cobia, striped bass and other species soon to be completed.

Parameters of the model, including pen array center, location in the Cartesian coordinate system, cell (grid) size, farm dimensions, capture cell locations (i.e., vertical profiles from specific locations that is exported to spreadsheets), fish loading and feed rates, etc. Many are set interactively with drop down menu selection. Virtually all parameter settings and coefficients are user adjustable, either in drop down menus (See Figures 3 to 11) or using a text editor in the accessible software files.

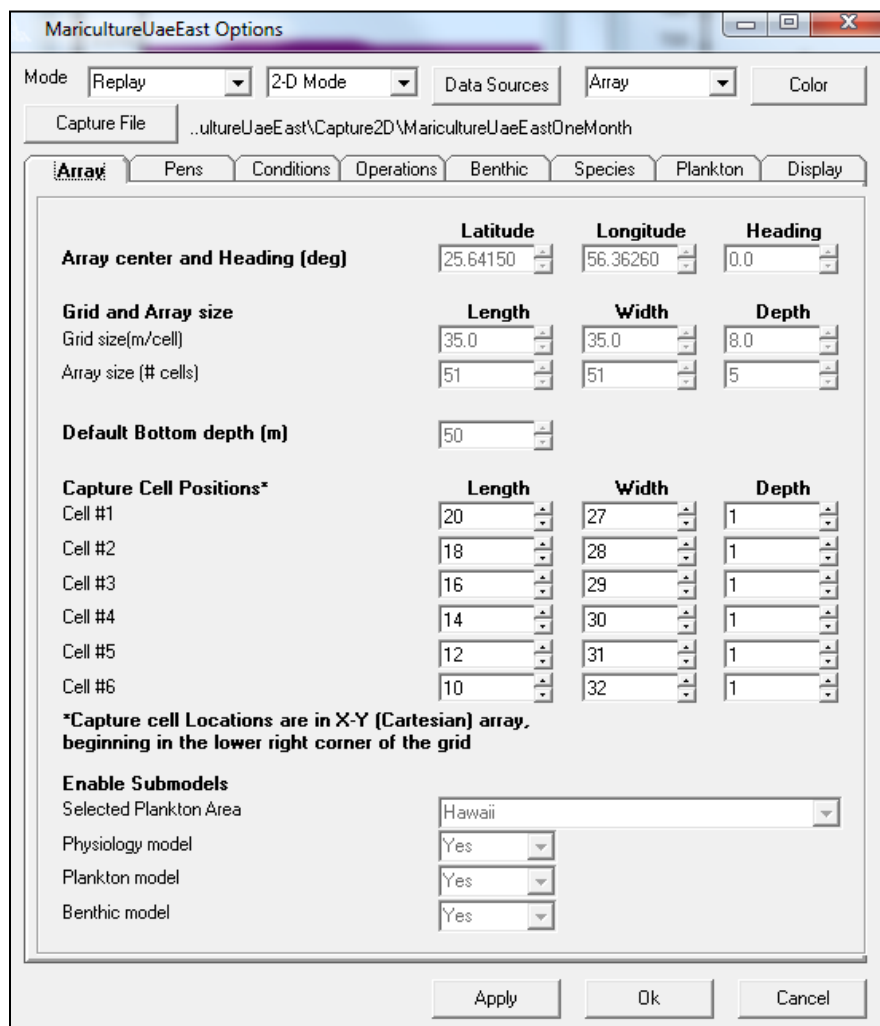


Figure 3. Array settings for AquaModel such as location of center or farm(s), default bottom depth (if detailed bathymetry not available) and capture cell locations to output spreadsheet or database results.

Figure 3 is for the single net pen farm (2-D mode, near field) simulation. The same interface is used for multiple fish farms (3-D mode, far field) applications but the data sources (Figure 11) requirements are more elaborate for the latter.

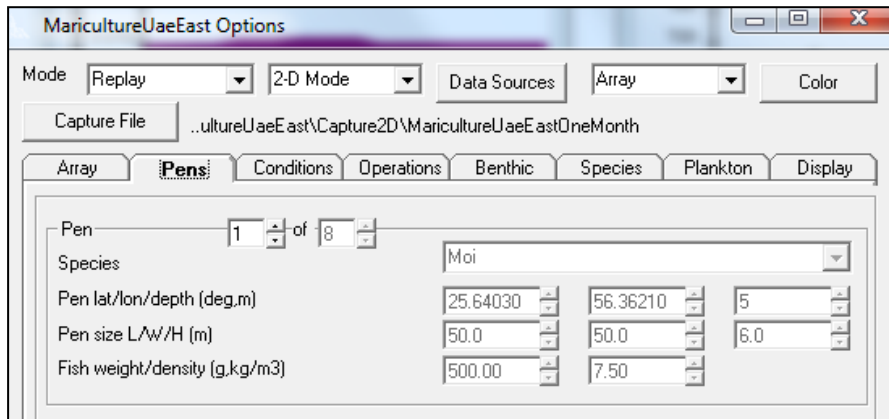


Figure 4. Pen location, size and initial loading settings (for Pen 1 only).

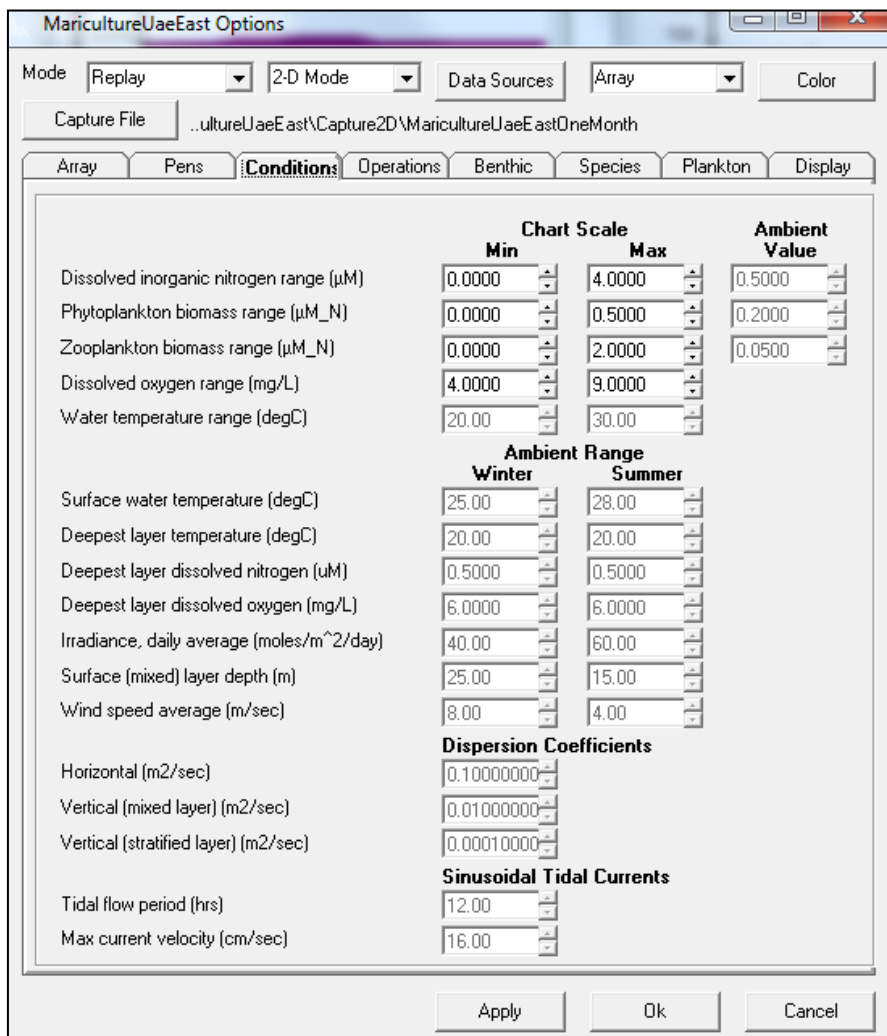


Figure 5. Water column conditions and optional synthetic tidal flow simulation settings¹, the latter not used when current meter or 3D flow field data are available.

¹ A large variety of water, sediment, atmospheric and other input or boundary conditions factors can be input using spreadsheets on any time step desired. See the Recommendations section for more information regarding the need for completing this before use in the UAE if better accuracy is to be achieved.

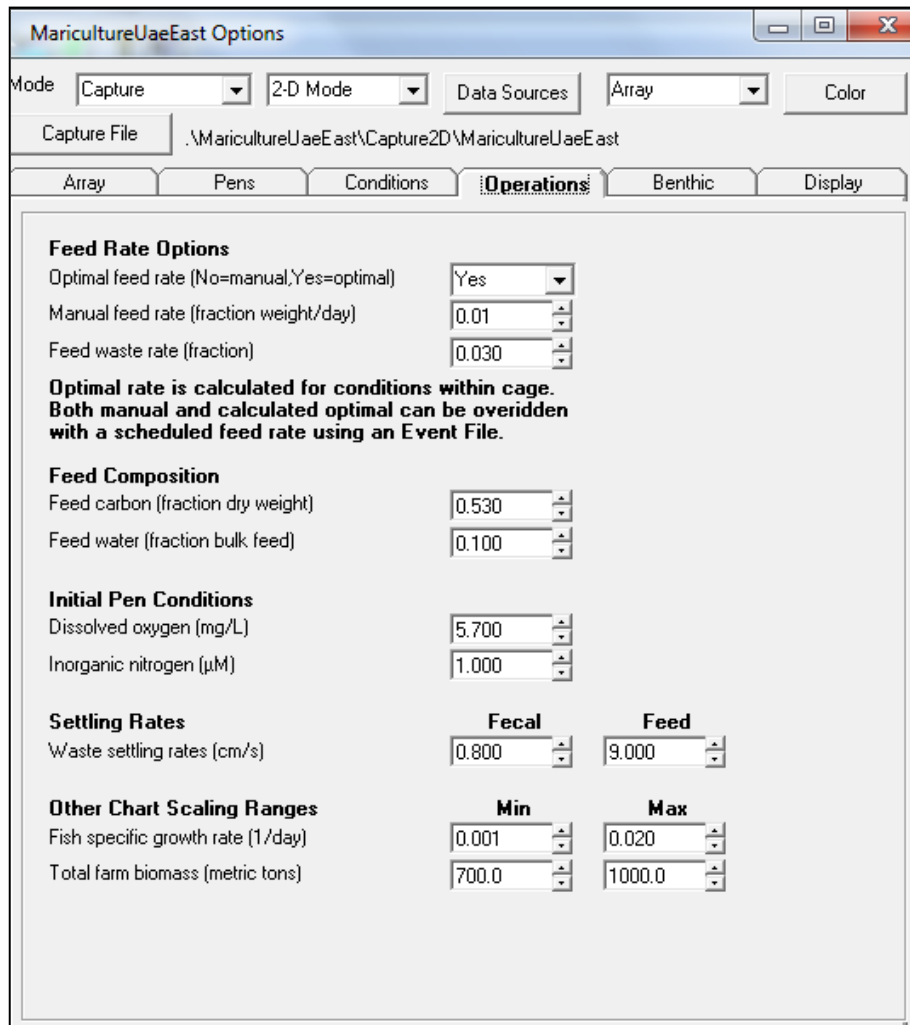


Figure 6 Feed rate override settings, compute optimum feed use settings, percent feed loss level, initial pen oxygen and nitrogen settings, fecal and waste feed sinking rate, fish growth range bounds.

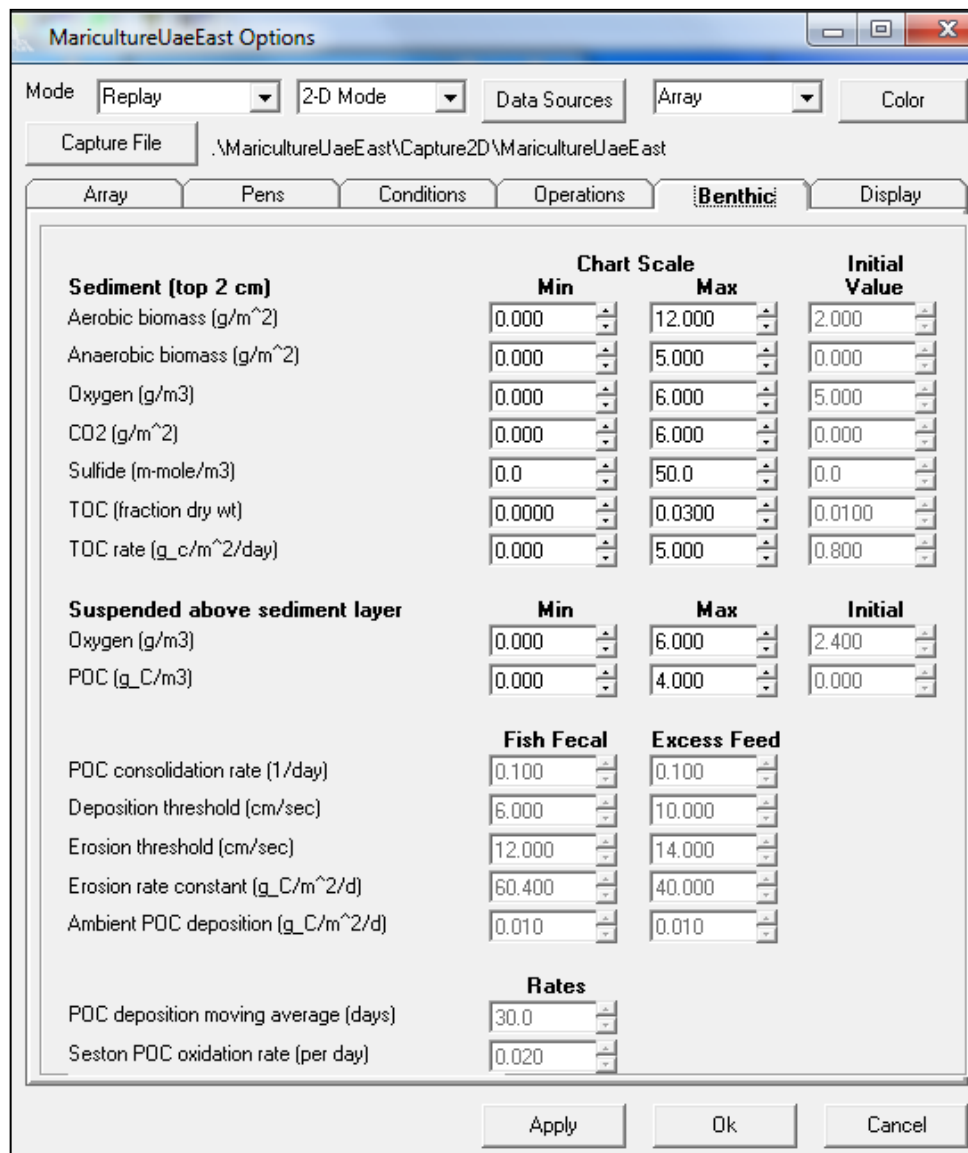


Figure 7. Benthic and sediment properties plot ranges, initial values, settling rates of feed and feces and other related controls.

The values selected for erosion deposition and erosion threshold in Figure 7 are highly conservative for the present application.

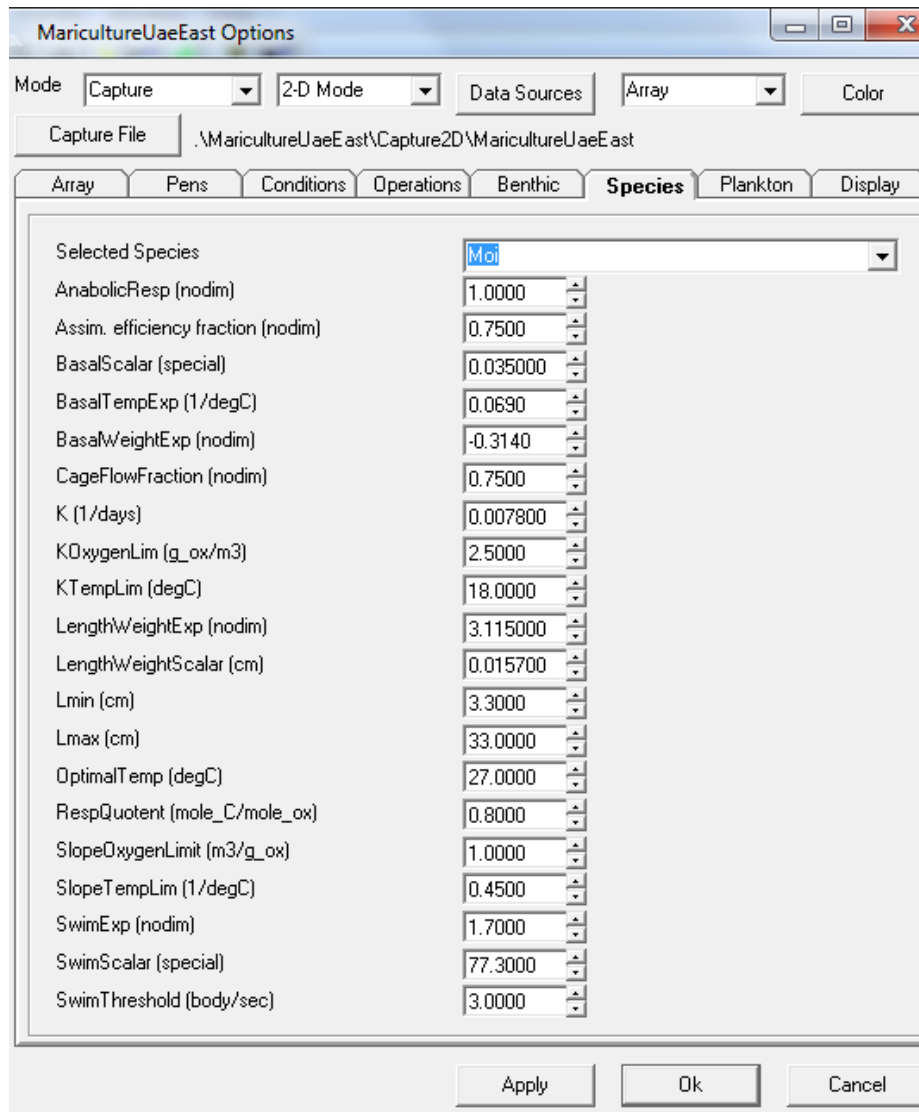


Figure 8. Several of the fish physiological parameters and coefficients obtained from best fit to literature values and our growth experiments (developer’s version only).

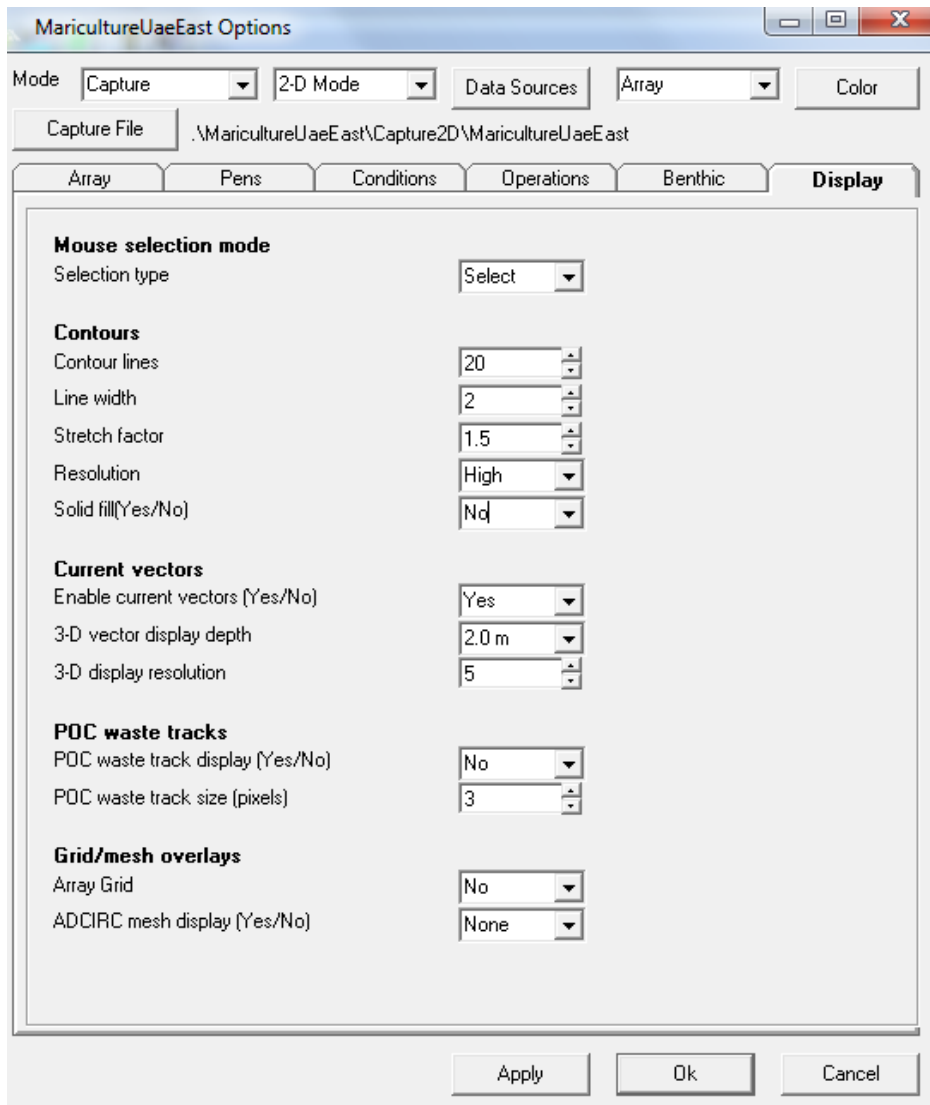


Figure 9. Contouring, current vector display, time stream and other display settings.

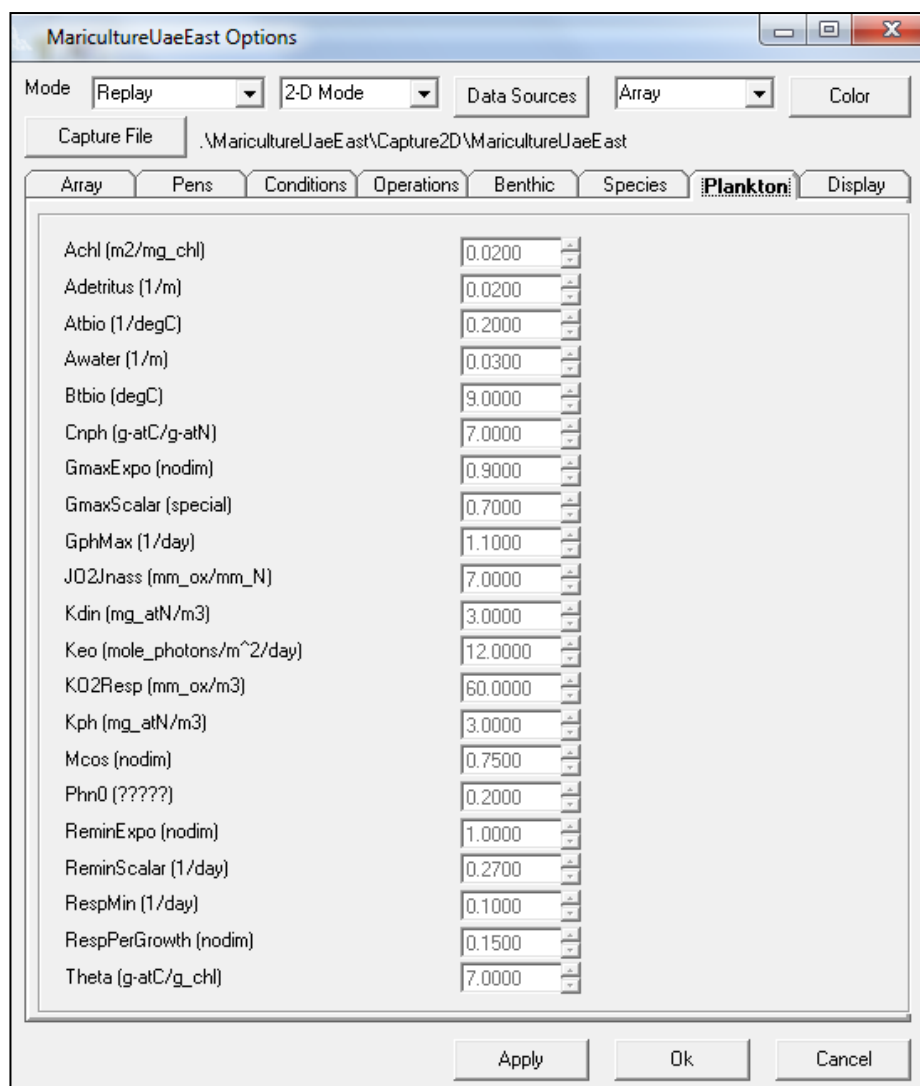


Figure 10. NPZ (plankton) model settings, factors, coefficients and rates (developer's version only).

Circulation Module

AquaModel's circulation routine flushes cages with ambient waters and transports wastes from them. The computations during each step of the simulation occur within each element of a 3-dimensional grid of rectangular cells that populate an array of such cells. The size, orientation, and geospatial location of the array as well as the number and dimension of the cells that populate the array are entered by the users. The array of cells begins at the sea surface and extends to the sea floor. The geometry and flow at the sediment/water interface is described in more detail in the Benthic Routine Section and the farm layout is described in the site description section. The time steps for the simulation vary between 1 and 5 minutes depending upon the speed of the currents.

The system of equations describing circulation is a simple finite element description of advection and dispersion. Each element of the array is treated as a box model in which materials flow

across the 6 interfaces of each element, top, bottom and the four sides. Each element is treated as instantly mixed throughout. These movements are determined by a simple, finite difference calculation that is most simulations of coastal water flow. The maintenance of conservation of mass of conservative a tracer such as water itself is a key constraint upon the calculations. Water and dissolved and suspended materials also move across the side boundaries of the array; however, here the values for the concentrations of dissolved and particulate materials at the boundaries remain constant and equal to the initial, ambient concentrations of tracers entered by the user at the start of the simulation. If the calculations of such a model are to be trusted, the array must be sufficiently large such that the exchange across the boundary does not significantly perturb the results of calculations.

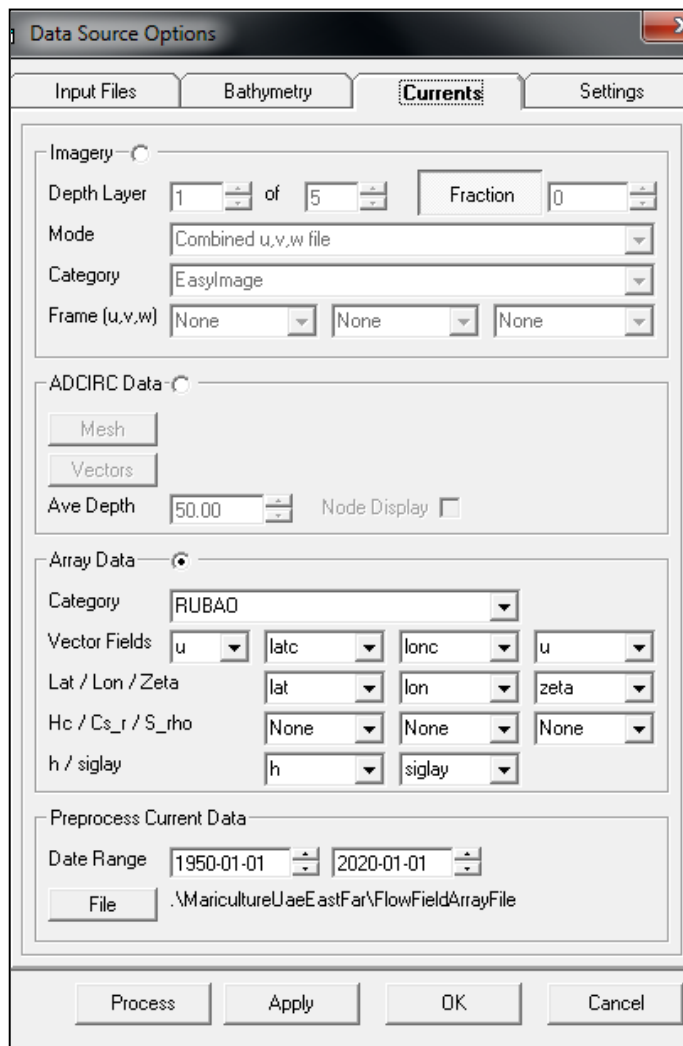


Figure 11. AquaModel current data input menu for inputting ROMS, ADCIRC and FVCOM circulation model data.

“Imagery” box used for ROM, ADCIRC box shown below, “Array Data” refers to FVCOM circulation model data import controls and a large number of other categories of data.

Other menus available for entering bathymetry and 2D flow files from current meters.

The circulation at the sediment-water column interface, where uneaten feed and feces from the farm not only transported but also deposited into the sediments, resuspended from the sediments, or consumed by benthic organisms will be described in the benthic section.

The flow field in AquaModel is either of two modes. As the name suggests the calculated flow field in the “3-dimensional mode” is in 3 dimensions. Exchange of water between adjacent cells

has no constraints other than the requirement of conservation of mass. Convergent and divergent motion can be represented within the array as well as local eddies. In addition the water depth can vary within the array. Unfortunately, such detailed descriptions of motion are difficult to measure at small scales and thus rarely measured in coastal waters. Thus, such types of description come from coastal circulation models which include such drivers of circulation as winds, tides, and local gradients in water density due to thermal exchange as well as evaporation and precipitation. *AquaModel* assimilates output from such coastal circulation models. In the present case, we were provided an FVCOM model prepared by Dr. Rubao Ji of Woods Hole Oceanographic Institution. The model was prepared to examine the initiation of the major red tide bloom in the summer and fall of 2008. As such, we do not have most of winter, spring and early summer time periods to examine and there could be difference in direction or even magnitude of flow.

In the “2-dimensional mode” at any time step of the simulation both horizontal and vertical motions are uniform throughout the array. Unlike the “3-dimensional mode” there is neither divergence nor convergence flow within the array. In the case of horizontal motion both advection and turbulent exchange between adjacent sides of the cells are equal throughout the array. In the case of vertical motion exchange between adjacent sides of cells are also equal throughout the grid, but restricted to turbulent exchange in which flow across the upper and lower sides of adjacent cells is equal. The “2-dimensional flow” mode also consists of two layers, an upper mixed layer and the lower stratified layer. The depth intervals of the mixed layer and the stratified layers vary with season as a sinusoidal oscillation. Finally, in this mode the depth of the water column is uniform throughout the array.

We had no current meter data for any of the sites for this preliminary study, including Site 1, the location assessed in more detail for benthic effects. We were able to generate a record of flow from the 3D model runs, by specifying vector recording in the capture cells for 6 depths throughout the 42 m deep water column at this site. To make the analysis of benthic effects highly conservative, and to better illustrate the nature of graphic results from the model, we reduced bottom flow by 33% that would cause waste particles to be more likely to remain upon the bottom and not be resuspended. As shown below, despite this highly conservative measure, the degree of effects on the seabottom was predicted to be very minimal as water current velocity exceeded thresholds of resuspension on a daily basis. In such a mode as described above, turbulent and advective exchange of water is the same across the 4 lateral sides of all cells and there is no divergence or convergence of water motion. We provide additional recommendations for future data needs if fish farming is to expand on the UAE east coast near the end of this report.

Fish Physiology and Farm Module

In *AquaModel* simulations, a fish farm is characterized by its two main properties, the farm’s physical settings and layout and the farm’s stocking, feeding, and harvesting regime. The physical layout requires entry of the following types of information that are specified later in this report:

- The number of cages

- The location of the cages as described by their geographic co-ordinates (latitude, longitude, depth)
- The size of the cages length, width, height and slight adjustments to approximate fitting into the square grid system
- The fractional difference between the current speed within the cages and ambient current speed

Farms operations require entry of the following information for each cage:

- Species of fish.
- Metabolic model of the fish as described below. Although the system of equations describing growth and metabolism is invariant with species, the coefficients found within the equations likely vary with species
- Mean weight of fish in grams wet weight at initial stocking or a selected time intervals
- Density of fish in number of fish per cubic meter at initial stocking or at selected time intervals
- Feed rate in grams dry weight of feed per day. This rate can be entered manually or calculated automatically by AquaModel as an optimal feed rate
- Estimate percentile of uneaten feed loss from the cages.

System Science Application has developed *AquaModel's* routine describing the metabolism of modeled fish; it is based upon extensive review and parameterization of basic bioenergetics studies as well as some of our own unpublished laboratory experiments (See Rensel, Kiefer and O'Brien 2006 for more background). Its unique feature is its inclusion of equations for oxygen-limited metabolism, a feature necessitated by its importance in farms where fish are cultured at relatively high densities and in waters of moderate or lower dissolved oxygen concentration. Dissolved oxygen is a primary limiting factor to net pen carrying capacity and is therefore of considerable modeling interest. As indicated in figure 12, the routine includes the processes of ingestion, egestion, assimilation, respiration, excretion, and growth. Carbon, nitrogen, and oxygen fluxes are all computed, and of course the rates of these fluxes vary with operational and environmental conditions. The operational independent variables are listed above while the environmental variables that determine metabolism are:

- Water temperature
- Ambient oxygen concentration which is one of the determinants of the concentration of oxygen within a cage
- Ambient current velocity, which is another determinant of oxygen concentration within the cage as well as a determinant of the respiration rate required of the fish to swim at a speed in order maintain their position within the cage.

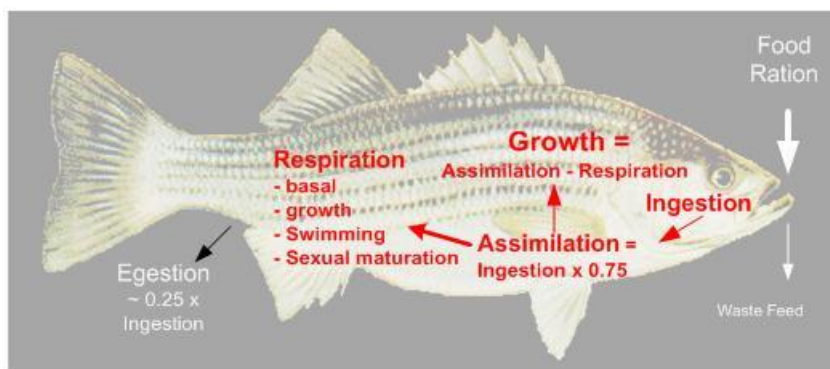


Figure 12. Generalized fish metabolic processes described by the routine for fish metabolism. (Background drawing by Duane Raver, USFWS; assimilation factor is adjustable).

The striped bass routine consists of a series of functions describing the fluxes of carbon, nitrogen, and oxygen as determined by the basic features of metabolism, ingestion, egestion, assimilation, respiration, and growth. Specifically, each element is tracked according to these 5 basic features, which are related to each other by conservation of mass in the following Equations:

1. ingestion rate = egestion rate + assimilation rate
2. assimilation rate = rate of respiration + rate of growth
3. respiration rate = resting rate of respiration (i.e. basal) + respiration rate of activity (i.e. swimming) + respiration rate of anabolic activity (i.e. growth)
4. rate of feces production = egestion rate
5. rate of loss of uneaten feed = feed rate – ingestion rate

The functions for the 5 basic metabolic processes can be summarized as follows. Ingestion rate is determined by both the rate of supply of food and rate at which the fish can assimilate ingested food (Equation 1). If the rate of supply of food exceeds the sum of the rate of egestion and the rate of assimilation, then a fraction of the food will be uneaten and contribute to the particulate waste produced by the cage (Equation 5). As indicated in Figure 12, egestion is assumed to be a fixed fraction of ingestion as determined largely by the nutrient composition of the feed. The rate of egestion is in fact the rate of feces production (Equation 4). The assimilation rate of the fish will be a function of the size (age) of the fish, the temperature of the water, and the concentration of oxygen within the cage. The assimilated nutrients are then either consumed by respiration or contribute to the growth of the fish (Equation 2). (We assume that there are no reproductive demands within the cage.) The rates of respiration, which include both the consumption of oxygen and excretion of nitrogen, are determined by three processes, basal metabolism, swimming metabolism, and anabolic metabolism demanded by growth (Equation 3). Basal metabolism is a function of water temperature and the size of the fish, swimming metabolism is a function of the fish size and its swimming speed, and anabolic metabolism is proportional to growth rate. The growth rate of the fish is simply calculated by subtracting the rate of respiration from the rate of simulation.

We were not informed as to what fish to use in this preliminary report but had intended to use gilthead sea bream (*Sparus aurata*) a very popular fish to culture in the Mediterranean Sea and elsewhere. We made progress on development of this species specific model, but found that growth patterns varied more than expected in areas with different seasonal temperature ranges. As discussed in the recommendations, we can easily complete this growth submodel but need real data from the UAE grow out experiences to tune the model to local conditions. In lieu of having the completed submodel, we used a generalized tropical fish model, in part based on moi (aka, [Pacific threadfish](#), *Polydactylus sexfilis*). We completed a physiological model of this fish previously that included validation with literature and our own laboratory studies (O'Brien, Rensel and Kiefer 2011) and the temperature range of this fish is similar to conditions that may exist along the UAE east coast.

We do this with the knowledge gained from our own experiments and the literature that most all marine teleost fishes of this size have fecal settling rates in the 0.5 to 1.2 cm/s range and because the commercial feed tends to have a similar proximate analysis, the fecal waste should be similar in composition and settling characteristics. Moreover, moi have relatively high rates of respiration so the choice of this fish is conservative (i.e., biased toward more effect) compared to many other marine fish. Some examples of the predictions of the moi bioenergetic routine are available on line at our website (see O'Brien et al. 2011 at the [AquaModel publications page](#)). The next section more explicitly describes the fish physiology model used in AquaModel.

Many native species of fish may be suitable for culture in the subject area of the Sea of Oman, but as noted by others, water temperature minima in the Sea of Oman preclude at least one candidate species growth (cobia, *Rachycentron canadum*). This is not necessarily a matter of fish mortality, but rather an issue about optimizing growth and the expense of fish feed, that is usually the most expensive cost involved in commercial net pen operation. For example, although not lethal to desirable species such as gilthead sea bream (*Sparus aurata*), water temperature at or above 30 C may result in reduced growth rate and food conversion ratios resulting in less competitive business results if competing with others from areas with more ideal conditions.

Outline of AquaModel Fish Physiology Structure

The structure of our fish physiology model is illustrated here as designed by Dr. Kiefer and shown for rainbow trout (*Oncorhynchus mykiss*) as an example. Figure 13 shows the logic of the system of functions used to calculate the physiological rates for an individual fish at each time step of the AquaModel simulation. Table 1 contains the functions of the model, numbered in the order in which they will be executed during a single time step of the simulation. Table 2 contains short descriptions of these functions, and Table 3 contains the coefficients and conversion factors found in the system of functions. Both Tables 1 and 3 also contain the scientific units of the independent variable on the left hand side of the function or the coefficient or conversion factor. The independent variables of the model are fish weight, water temperature, current velocity, feed rate, and oxygen concentration. The key output of the model are the time series of values for the specific rates of growth, respiration, ingestion, egestion and excretion of fish growing under a given times series of feeding rates and environmental conditions.

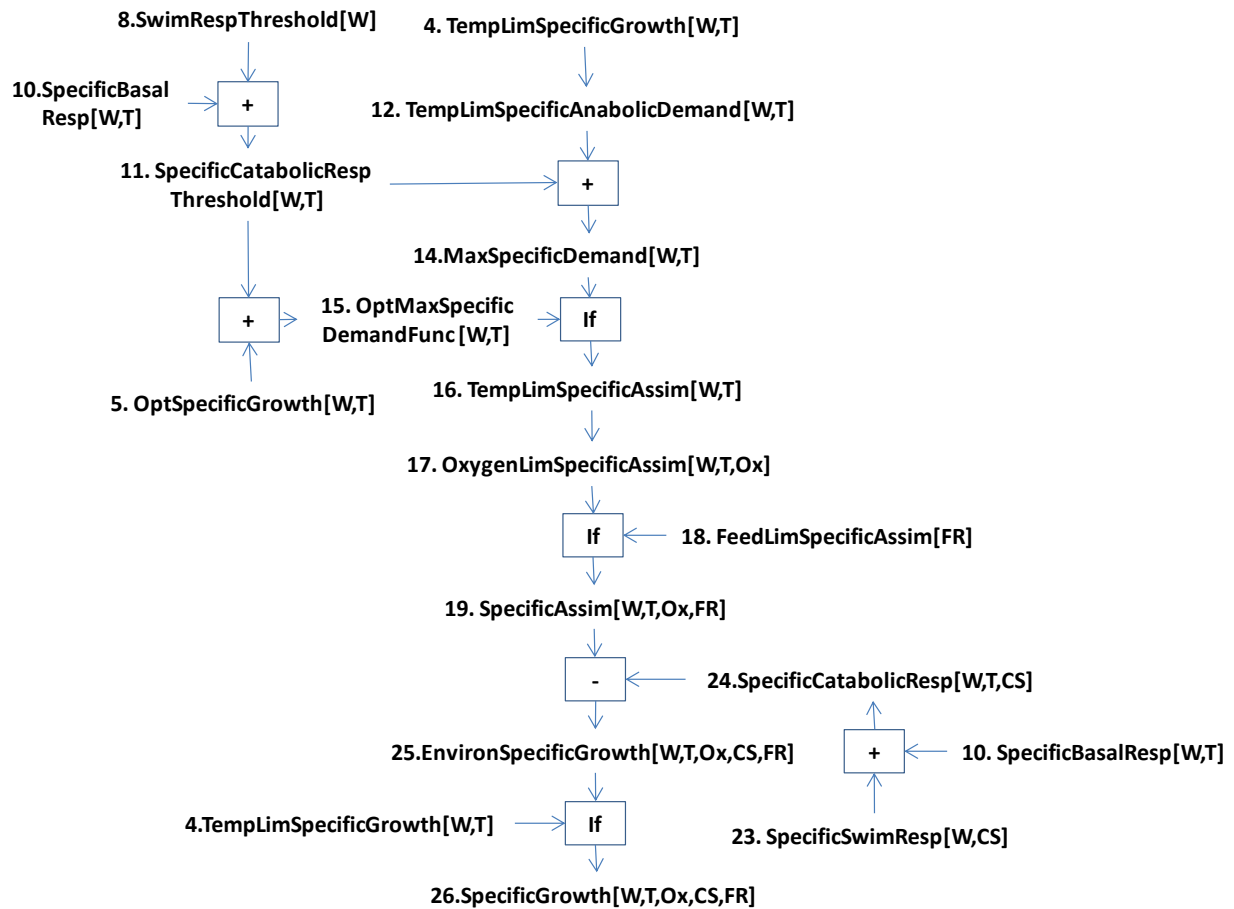


Figure 13. Logic of Fish Physiological Model.

Names and numbers refer to the functions in Tables 1 and 2 and line numbers in Table 2. The symbols W, T, Ox, CS, and FR refer to fish weight, water temperature, oxygen concentration, current speed, and specific feed rate. The text boxes refer to mathematical transformations that involve a conditional statement “If”, the summation of the inputs “+”, and the difference between inputs “-”. If there is no text box associated with an arrow connecting two functions the transformation is a scaling of variable value by either a division or multiplication.

Table 1. Example AquaModel fish physiology submodel functions (*O. mykiss*).

Maximum Growth Rate

$$1. \text{LengthFunc} = \frac{\text{Weight}}{\text{LengthWeightScalar}}^{\frac{1}{\text{LengthWeightExpo}}} \quad (*\text{cm}*) ;$$

$$2. \text{AgeFunc} = \frac{\text{Log} \left[-\frac{\text{Lmax} - \text{Lmin}}{-\text{Lmax} + \left(\frac{\text{Weight}}{\text{LengthWeightScalar}} \right)^{\frac{1}{\text{LengthWeightExpo}}}} \right]}{k} \quad (*\text{g}*) ;$$

$$3. \text{WeightLimSpecificGrowthFunc} = \frac{1}{\text{Weight}} e^{-\text{WeightAgeFunc} * k} * k * \text{LengthWeightExpo} * \text{LengthWeightScalar} * (\text{Lmax} - e^{-\text{WeightAgeFunc}[\text{Weight}] * k} * (\text{Lmax} - \text{Lmin}))^{-1 * \text{LengthWeightExpo}} * (\text{Lmax} - \text{Lmin}) \quad (*1/\text{day}*) ;$$

$$4. \text{TempLimSpecificGrowthFunc} = \frac{\text{WeightLimSpecificGrowthFunc}[\text{Weight}]}{1 + \text{Exp}[\text{SlopeTempLim} * (\text{KTempLim} - \text{Temperature})]} \quad (* 1/\text{day}*) ;$$

$$5. \text{OptSpecificGrowthFunc} = \frac{\text{WeightLimSpecificGrowthFunc}[\text{Weight}]}{1 + \text{Exp}[\text{SlopeTempLim} * (\text{KTempLim} - \text{OptimalTemperature})]} \quad (* 1/\text{day}*) ;$$

Upper Limit of Catabolic Respiration

$$6. \text{CurrentSpeedThresholdFunc} = \frac{\text{VBodyLimitToMaxGrowth} * \text{LengthFun}[\text{Weight}]}{\text{CageFlowFraction}} ;$$

$$7. \text{SwimSpeedThresholdFunc} = \text{VBodyLimitToMaxGrowth} * \text{CurrentSpeedThresholdFunc} \quad (*\text{cm/s} *) ;$$

$$8. \text{SwimRespThresholdFunc} = \text{SwimScalar} * \text{VBodyLimitToMaxGrowth}^{\text{SwimExpo}} \quad (*\text{mg oxygen}/(\text{m}^3 * \text{day}) *) ;$$

$$9. \text{SpecificSwimRespThresholdFunc} = \frac{\text{HrToDay} * \text{CarbonToOxygen} * \text{CurrentSpeedThresholdFunc}}{\text{CarbonToWet} * \text{KgToGram} * \text{GramToMGram}} \quad (*1/\text{day}*) ;$$

$$10. \text{SpecificBasalRespFunc} = \text{BasalScalar} * \text{Exp}[\text{BasalTempExpo} * (\text{Temperature} - \text{BasalTempNominal})] * \text{Weight}^{\text{BasalWeightExpo}} \quad (*1/\text{day}*) ;$$

$$11. \text{SpecificCatabolicRespThresholdFunc} = \text{SpecificSwimRespThresholdFunc} + \text{SpecificBasalRespFunc} \quad (*1/\text{day}*) ;$$

Assimilation Rate

$$12. \text{TempLimSpecificAnabolicDemandFunc} = \text{TempLimSpecificGrowthFunc} * (1 + \text{SpecificAnabolicResp}) \quad (*1/\text{day}*) ;$$

$$13. \text{OptSpecificAnabolicDemandFunc} = \text{OptSpecificGrowthFunc} * (1 + \text{SpecificAnabolicResp}) \quad (*1/\text{day}*) ;$$

$$14. \text{MaxSpecificDemandFunc} = \text{SpecificCatabolicRespThresholdFunc} + \text{TempLimSpecificAnabolicDemandFunc} \quad (*1/\text{day}*) ;$$

$$15. \text{OptMaxSpecificDemandFunc} = \text{SpecificCatabolicRespThresholdFunc} + \text{OptSpecificAnabolicDemandFunc} \quad (*1/\text{day}*) ;$$

$$16. \text{TempLimSpecificAssimFunc} = \text{If}[\text{Temperature} > \text{OptimalTemperature}, \text{OptMaxSpecificDemandFunc}, \text{MaximumSpecificDemandFunc}] \quad (*1/\text{day}*) ;$$

$$17. \text{OxygenLimSpecificAssimFunc} = \left(\frac{1}{1 + \text{Exp}[\text{SlopeOxygenLim} * (\text{KOxygenLim} - \text{Oxygen})]} \right) * \text{TempLimSpecificAssimFunc} \quad (*1/\text{day}*) ;$$

$$18. \text{FeedLimSpecificAssimFunc} = \text{FeedRate} * \text{AssimilationEfficiency} \quad (*1/\text{day}*) ;$$

$$19. \text{SpecificAssimFunc} = \text{Min}[\text{FeedLimSpecificAssimFunc}, \text{OxygenLimSpecificAssimFunc}] \quad (*1/\text{day}*) ;$$

Specific Catabolic Respiration

20. $\text{SwimSpeedFunc} = \text{CageFlowFraction} * \text{CurrentSpeed} (*\text{cm/s}*)$;
 21. $\text{VBodyFunc} = \text{SwimSpeedFunc} / \text{LengthFunc} (*\text{bodylengths/s}*)$;
 22. $\text{SwimRespFunc} = \text{SwimScalar} * \text{VBodyFunc}^{\text{SwimExpo}} (*\text{mg oxygen/m}^3*\text{day}*)$;
 23. $\text{SpecificSwimRespFunc} = \frac{\text{HrToDay} * \text{CarbonToOxygen} * \text{SwimRespFunc}}{\text{CarbonToWet} * \text{KgToGram} * \text{GramToMGram}} (*1/\text{day}*)$;
 24. $\text{SpecificCatabolicRespFunc} = \text{SpecificSwimRespFunc} + \text{SpecificBasalRespFunc} (*1/\text{day}*)$;

Growth Rate

25. $\text{EnvironSpecificGrowthFunc} = \frac{1}{1 + \text{SpecificAnabolicResp}} (\text{SpecificAssimFunc} - \text{SpecificCatabolicRespFunc}) (*1/\text{day}*)$;
 26. $\text{SpecificGrowthFunc} = \text{Min}[\text{WeightLimSpecificGrowthFunc}, \text{EnvironSpecificGrowthFunc}] (*1/\text{day}*)$;

Rates of Ingestion, Egestion, Respiration, and Optimal Feeding

27. $\text{SpecificAnabolicRespFunc} = \text{SpecificAnabolicResp} * \text{SpecificGrowthFunc} (*1/\text{day}*)$;
 28. $\text{SpecificRespFunc} = \text{SpecificAnabolicRespFunc} + \text{SpecificCatabolicRespFunc} (*1/\text{day}*)$;
 31. $\text{FeedSatSpecificAssimFunc} = \text{Min}[\text{OxygenLimSpecificAssimFunc}, \text{TempLimSpecificAssimFunc}] (*1/\text{day}*)$;
 32. $\text{FeedSatSpecificIngestionFunc} = \frac{\text{SpecificAssimAtSatFeedRateFunc}}{\text{AssimilationEfficiency}} (*1/\text{day}*)$;
 33. $\text{OptimalFeedRateFunc} = \text{SpecificIngestionAtSatFeedRateFunc} (*1/\text{day}*)$;

Carbon, Nitrogen, and Oxygen Fluxes in Cage

34. $\text{CageCarbonRespFunc} = \frac{\text{FishNumDensity} * \text{Weight} * \text{CarbonToWet}}{\text{gCToMoleC}} * \text{SpecificRespFunc} (*\text{moleCarbon}/(\text{m}^3*\text{day})*)$;
 35. $\text{CageOxygenRespFunc} = \frac{\text{gOxygenToMolesOxygen}}{\text{RespiratoryQuotient}} * \text{CageCarbonRespirationFunc} (*\text{gOxygen}/(\text{m}^3*\text{day}) (\text{FishDensity in } \#/\text{m}^3)*)$;
 36. $\text{CageNitrogenExcretionFunc} = \left(\frac{1}{\text{CToN}} \right) * \text{CageCarbonRespirationFunc} (*\text{molesN}/(\text{m}^3*\text{day})*)$;
 37. $\text{CageEgestionFunc} = \text{FishNumDensity} * \text{Weight} * \text{CarbonToWet} * \text{SpecificEgestionFunc} (*\text{gCarbon}/(\text{m}^3*\text{day})*)$;

Functions 29-30 omitted intentionally.

Table 2. Description of functions for AquaModel fish physiology model

Name of Function	Description
1. LengthFunc	length as a function of fish weight
2. AgeFunc	age as a function of fish weight
3. WeightLimSpecificGrowthFunc	specific growth rate as a function of fish weight
4. TempLimSpecificGrowthFunc	specific growth rate as a function of fish weight and water temperature
5. OptSpecificGrowthFunc	specific growth rate growing at fish optimal temperature and limited only by its weight
6. CurrentSpeedThresholdFunc	maximum current speed at which the fish can still achieve its maximum growth rate
7. SwimSpeedThresholdFunc	maximum swimming speed at which the fish can still achieve its maximum growth rate
8. SwimRespThresholdFunc	respiration rate (mg O ₂ /*kg*hr) when the fish swimming speed = SwimSpeedThresholdFunc
9. SpecificSwimRespThresholdFunc	specific respiration rate (1/day) when the fish swimming speed = SwimSpeedThresholdFunc
10. SpecificBasalRespFunc	specific basal respiration rate as a function of fish weight and water temperature
11. SpecificCatabolicRespThresholdFunc	specific catabolic respiration rate when the fish swimming speed = SwimSpeedThresholdFunc
12. TempLimSpecificAnabolicDemandFunc	Specific anabolic demand as a function of as a function of fish weight and water temperature
13. OptSpecificAnabolicDemandFunc	specific anabolic demand as a function of fish weight and when water temperature = OptimalTemperature
14. MaxSpecificDemandFunc	specific anabolic and catabolic demand as a function of fish weight, water temperature, and its swimming speed = SwimSpeedThresholdFunc
15. OptMaxSpecificDemandFunc	specific anabolic and catabolic demand as a function of fish weight, water temperature = OptimalTemperature, and its swimming speed = SwimSpeedThresholdFunc
16. TempLimSpecificAssim	temperature limited specific assimilation rate
17. OxygenLimSpecificAssimFunc	oxygen limited specific assimilation rate
18. FeedLimSpecificAssimFunc	Feed rate limited specific assimilation rate
19. SpecificAssimFunc	specific assimilation rate limited by either oxygen, temperature, or feed rate
20. SwimSpeedFunc	speed (cm/s) at which a fish must swim to maintain its position in the cage
21. VBodyFunc	speed (bodylengths/s) at which a fish must swim to maintain its position in the cage
22. SwimRespFunc	respiration rate (mg O ₂ /kg wet Weight*hr) as a function of fish swimming speed
23. SpecificSwimRespFunc	specific respiration rate (1/day) as a function of fish swimming speed
24. SpecificCatabolicRespFunc	specific catabolic respiration rate = SpecificSwimRespFunc + SpecificBasalRespFunc
25. EnvironSpecificGrowthFunc	specific growth rate limited by either temperature, oxygen, current speed, or feed rate
26. SpecificGrowthFunc	realized specific growth rate = the lesser of EnvironLimSpecificGrowthFunc or BioLimSpecificGrowthFunc

27. SpecificAnabolicRespFunc	realized specific anabolic respiration rate
28. SpecificRespFunc	realized specific respiration rate
29. SpecificEgestionFunc	realized specific egestion rate
30. SpecificIngestionFunc	realized specific ingestion rate
31. FeedSatSpecificAssimFunc	specific assimilation rate when assimilation is limited by either temperature or oxygen
32. FeedSatSpecificSpecificIngestionFunc	specific ingestion rate when assimilation is limited by either temperature or oxygen
33. OptimalFeedRateFunc	specific feed rate when assimilation is limited by either temperature or oxygen
34. CageCarbonRespFunc	rate of carbon respired by all fish in a cage in moles carbon/(m3*day)
35. CageOxygenRespFunc	rate of oxygen respired by all fish in a cage in g oxygen/(m3*day)
36. CageNitrogenExcretionFunc	rate of nitrogen excreted by all fish in a cage in moles nitrogen/(m3*day)
37. CageEgestionFunc	rate of fecal carbon egested by all fish in a cage in g carbon/(m3*day)

Table 3. Example fish physiology coefficients and conversion factors (from *O. mykiss*)

Coefficients of *Oncorhynchus mykiss*

```

LengthWeightScalar = 0.0118
LengthWeightExpo = 3.006
Lmin = LengthFunc[10]
Lmax = 90
k = 1.3 / 365
BasalScalar = 0.119
BasalWeightExpo = -0.314
BasalTempNominal = 17
BasalTempExpo = 0.069
SwimScalar = 77.3
SwimExpo = 1.7
SpecificAnabolicResp = 0.8
OptimalTemperature = 17
AssimilationEfficiency = 0.75
ThresholdSwimSpeed = 3
SlopeTempLim = 0.7
KTempLim = 11
SlopeOxygenLim = 2
KOxygenLim = 4
CageFlowFraction = 0.75

```

Conversion Factors

```

gCToMoleC = 12 (*gCarbon:moleCarbon*);
gOxygenToMolesOxygen = 32;
CToN = 6 (*molesCarbon:molesNitrogen*);

MoleNTogC =  $\frac{1}{gCToMoleC * CToN}$  (*moleNitrogen/gCarbon*);
CarbonToDry = 0.5 (*gCarbon/gdryweight*);
HrToDay = 24;
CarbonToOxygen = (12 / 32) * RespiratoryQuotient (*gCarbon*moleC-1)/(gOxygen*moleO2-1 *);
RespiratoryQuotient = 0.807 (*molesCarbon/molesOxygen*);
CarbonToWet = 0.15 (* gCarbon/gwetweight CarbonToDry * DryToWet *);
DryToWet = 0.3 (*gdryweight/gwetweight*);
GramToMGram = 1000 (*mg/g*);
FeedDryToWet = 0.9 (*g/g*);

```

The concept of specific rates, which are in units of 1/day, are most easily understood in terms of a carbon budget for the fish metabolism; in this case the units of the specific rate can be described in units of the daily metabolic flux of carbon divided by the carbon mass of the fish, i.e. grams carbon (as growth, respired, or egested)/(grams carbon in fish mass*day). In order to calculate the daily increase in carbon biomass, the daily release of carbon dioxide by respiration, or the daily loss of carbon as feces within a cage, one simply multiplies the specific rate by the number of fish in the cage, and the average carbon content of the fish. Thus, one calculates the daily increase in carbon biomass within a cage:

$$\text{Daily Fish Carbon Increase in Cage} = \text{Specific Growth Rate} * \text{Number of fish in cage} * \text{Average Fish Carbon Content}$$

Since we assume in the model that the elemental composition of the feed and fish are constant, we can similarly calculate the metabolic fluxes of other elements such as oxygen and nitrogen.

Figure 13 shows how the system of functions in the model are linked to each other. The figure describes how the specific growth rate of a single fish is calculated as a function of the independent variables of a calculation at a given time step. These variables are represented by the symbols W, T, Ox, CS, and FR that refer to fish weight, water temperature, oxygen concentration, current speed, and specific feed rate, respectively. The text boxes refer to mathematical transformations that involve a conditional statement "If", the summation of the inputs "+", and the difference between inputs "-". If there is no text box associated with an arrow connecting two functions the transformation is a scaling of variable value by either a division or multiplication.

The names and numbers refer to those found in Tables 1 and 2. Starting at the bottom of the figure we see that the specific growth rate of the fish, *SpecificGrowth*, is calculated by a conditional function, *If*. Here the conditional statement is that *SpecificGrowth* is the lesser of the value of either the *TempLimSpecifcGrowth* or the *EnvironSpecifcGrowth*. The *TempLimSpecifcGrowth* is the maximum rate at which the fish can grow given its weight and water temperature. We derived the *TempLimSpecifcGrowth* function from the Bertalanffy

equation for growth, and morphometric equations that relate the length of a species of fish to its weight. *EnvironSpecificGrowth* is the growth rate of the fish as determined by the functions that describe the full array of environmental factors that influence growth rate and that are listed in the second sentence of this paragraph. We see in the figure that the *EnvironSpecificGrowth* Function is simply the difference between the specific assimilation function, *SpecificAsim*, and the specific catabolic respiration function, *SpecificCatabolicResp*. The specific assimilation function is the rate at which ingested food is assimilated given the fish weight, food supply, water temperature, and oxygen concentration. As shown in the figure, the specific catabolic respiration function is the sum of basal respiration, *SpecificBasalResp*, and swimming respiration, *SpecificSwimResp*. The anabolic respiration of growth is not included here. If the assimilation rate exceeds the catabolic respiration rate, the fish will gain weight and if the the assimilation rate is less than the catabolic respiration rate, the fish will lose weight.

We see that the specific assimilation function is also calculated by a conditional function such that the rate of assimilation is equal to the least value calculated for either limited food supply, *FeedLimSpecificAssim*, or weight, water temperature, and oxygen concentration, *OxygenLimSpecificAssim*. It is clear from the diagram that the logic required to calculate *OxygenLimSpecificAssim* consists of many steps. As indicated the *TempLimSpecificAssim*, which is only a function of fish weight and water temperature, is calculated with a conditional statement. If water temperature is greater than the temperature for optimal growth, *TempLimSpecificAssim* is equal to *OptMaxSpecificDemand* function and if less than the optimal temperature, it is equal to the *MaxSpecificDemand* function. The *OptMaxSpecificDemand* function is the sum of the *OptSpecificGrowth* and the *SpecificCatabolicRespThreshold* functions. The *OptSpecificGrowth* function is the maximum specific growth rate of the fish under optimal temperature, while the *SpecificCatabolicRespThreshold* is the specific catabolic respiration rate of the fish when it is swimming at threshold speed that still provides the fish with a sufficient specific assimilation to support a maximum growth rate. As indicated, this function is the sum of the specific basal respiration rate *SpecificBasalResp* and the specific swimming respiration rate at threshold speed, *SwimRespThreshold*.

The *MaxSpecificDemand* function is the sum of the *SpecificCatabolicRespThreshold* function, which is described in the previous paragraph, and the *TempLimSpecificAnabolicDemand* function... In other words it is the specific rate of supply of substrates to meet the demand of a fish growing at its maximal specific growth rate when it is swimming at a maximum speed (the threshold speed) that still allows the fish to achieve its when it is swimming at threshold speed that still provides the fish with a sufficient specific assimilation to support a maximum growth rate. As its name suggest the later function is the temperature-limited specific rate to support the daily increase in fish biomass and the associated anabolic respiration. This function is calculated from the *TempLimSpecificGrowth* function that has been described earlier.

Plankton Module

The plankton module describes the cycling by plankton of nitrogen and oxygen within each element of the array, both within the farm and the surrounding waters. This model is similar to the PZN models that have been published by Kiefer and Atkinson (1984) and Wroblewski, Sarmiento, and Flierl (1988). The “master” cycle describes the transforms of nitrogen between three compartments, inorganic nitrogen, organic nitrogen in phytoplankton, and organic nitrogen in zooplankton. The three biological transforms are:

- Photosynthetic assimilation of inorganic nitrogen by phytoplankton which is a function of temperature, light level, DIN (dissolved inorganic nitrogen consisting of ammonia, nitrite and nitrate) concentration
- Grazing by zooplankton on phytoplankton which is a function of temperature and concentrations of zooplankton, and phytoplankton
- Excretion of DIN by zooplankton, which is a function of temperature and the concentration of zooplankton.

All three components are transported by advective and turbulent flow as described above. The model displays predator-prey oscillations, which dampen over time and reach a steady state. The default simulations for DIN, phytoplankton, and zooplankton stabilize at roughly 1 mg-at N m^{-3} , for all 3 components respectively. In order to calculate the concentrations and rates of loss by respiration and production by photosynthesis, we have assumed a constant flux ratio of oxygen to nitrogen of 6 moles $\text{O}_2 \text{ gm-at N}$, consistent with the Redfield ratio. The inputs to this model consist of the time series of exchange coefficients produced by the hydrodynamic model, surface irradiance, and water temperature as well as concentrations of dissolved oxygen, dissolved inorganic nitrogen, cellular nitrogen in phytoplankton and zooplankton. Outputs of this model consist of a time series of the concentrations of dissolved inorganic nitrogen and oxygen, phytoplankton (traced as chlorophyll), and zooplankton. See prior publications or reports at <http://www.aquamodel.net/Publications.html> for more details about this module.

Benthic Module

The benthic loading component of our model is based upon several literature citations and functions found in the existing, previously-verified DEPOMOD model (Cromey et al. 2002a, 2002b) that in turn was based on the G-model of carbon degradation (Westrich and Bernier 1984 and subsequent papers). Despite some limitations involving lack of user control and flexibility, DEPOMOD is presently the international standard for assessing the impact of loading of organic carbon in sediments underlying fish farms and in some countries calculations with the code are a requirement for obtaining fish farm permits. Since the DEPOMOD model is proprietary and only addresses benthic processes, we have written our own code to describe the fate of farm wastes that are deposited in sediments. Two processes, the physical dynamics of waste transport through the water column and deposition into the sediments and the biological dynamics of waste assimilation and remineralization by the benthic community, most conveniently describe our benthic routine.

As uneaten feed and feces produced by fish in each cage sink through the water column, they are transported downstream of the cage. Since uneaten feed is larger and denser than feces it must be treated separately. Not only will these different classes of particles sink at different rates and be transported at different distances from the farm, but when they reach the bottom boundary layer their shear thresholds for deposition and resuspension will also differ, leading to further separation. Eventually, both uneaten feed and feces will either be consumed by the benthos or consolidated into the sediments and no longer subject to resuspension. Thus, AquaModel has three categories of particulate waste: uneaten feed, feces, and consolidated waste contributed by both the uneaten feed and feces that have been deposited for a sufficient length of time on the bottom that are no longer erodible.

As illustrated in the figure 14, we have simplified the formulation of physical processes. This was required because simulations running on a PC became too time-consuming or mathematically unstable with a more detailed formulation. Waste particles produced in the farm are “collected” over a specified time interval as “capsules” that sink through the water column at a rate determined from measurements in the laboratory. These capsules are shown as brown dots in the figure. As these capsules sink, the ambient currents transport them through the 3-dimensional array of cells. This is somewhat analogous to water moving through an unsecured garden hose that is in continual motion but in this case is driven by variations in current velocity and direction. The waste particles are however not subject to turbulent dispersion as is the case for the dissolved wastes. As the capsules near the bottom the waste particles are “released” and evenly distributed into an underlying cell that is part of the grid of the suspension layer of the water column. The length and width of these cells are the same dimensions as the cells within the overlying water column, but their depth is user selectable. In the case of the demonstration farm, we have chosen a depth of 1 meter. Once released into the suspension layer the particles are now treated as suspended particles and subject to both advection and turbulent dispersion.

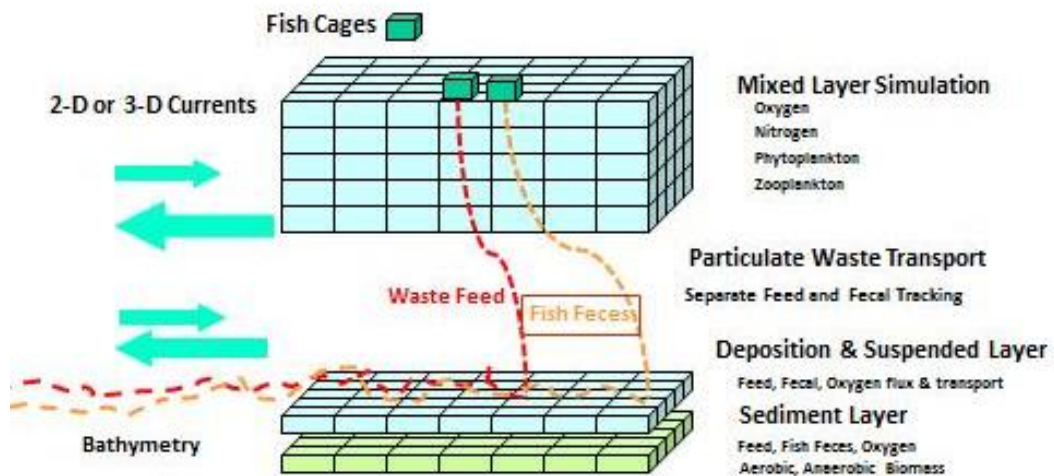


Figure 14. Conceptual diagram of waste transporting model components.

Following the logic and formulations of DEPOMOD (Cromey et al. 2002a, 2002b), when shear between the sediment and the bottom water falls below a threshold value, waste particles in the suspension layer are deposited into the sediment layer. Furthermore, the rate of deposition not only increases with the concentration of particles in the layer but will also increase with decreases in shear. When shear at the interface exceeds a threshold value, waste particles in the sediment layer will be resuspended into the suspension layer and thus subject to additional transport (and dispersion) from the site. The thresholds for deposition and resuspension differ with the size, density, and stickiness of the particles and thus will differ between feed and feces. When shear at the bottom falls between the threshold for deposition and the threshold for resuspension, the particles in the suspension layer will be remain in suspension and thus dispersed.

The wastes deposited in the sediment undergo aggregation and compaction, and will consolidate into organic particles that are no longer subject to resuspension. Cromey and his co-workers have derived a function for this process in which compaction begins at a given rate after a 4 day delay. We have on the other hand chosen a simple first order rate function in which a fixed fraction of the mass of feed and feces in the sediments consolidates each day. We have selected for our simulations the same values found in reference above for shear thresholds and the rate constant for resuspension of wastes.

Dynamics of the Benthos

The 3 types of fish farm waste found in the sediments, uneaten feed, feces, and consolidated waste (from feed and feces) are energy and nutrient sources for the benthic community, which consist of both macroscopic and microscopic organisms. Thus, at any given time, the concentration of waste in the vicinity of a farm will depend upon the previous history of deposition and resuspension, but also upon the previous history of growth and remineralization by the benthos. As shown in Figure 14 above, we treat the sediment layer as a single layer; this is despite the fact vertical profiles within sediments indicate sharp, predictable biological and chemical gradients within. In our simulations we have chosen a depth interval of 2 cm for each cell of our sediment array. This depth was chosen because it is the standard depth for sediment monitoring (core collection) in and around fish cages in many jurisdictions worldwide and is the most important venue for most of benthic infauna except the large-bodied organisms such as large clams and tubicolous polychaete worms. The length and width of these cells are selected by the model user and the same as those within the water column and suspension layers. Our functions are based upon the assumption that they provide a prediction of average biological and chemical conditions within the layer. Describing the complexity and biochemical processes within the sediment layer has challenged marine scientists, and the models that have been developed (including ours) are relatively crude and lacking in comprehensive testing. Despite these limitations, field data describing benthic responses to variations in organic loading of the sediments show clear understandable patterns, and that when tuned to local conditions models such as the pioneering G-Model of Westrich and Bernier (1984), can provide good quantitative estimates of the response. Testing of our submodule components is completed in Mathematica software before assembly into AquaModel code, when additional testing occurs.

Figure 15 below shows the components and process that are described by our benthic routine. The processes described here are all formulated in the series of equations found in the routine. As shown the components of the routine consist of four dissolved compounds species, oxygen, sulfate, hydrogen sulfide, carbon dioxide, which flow between the suspension and sediment layer by diffusion. It also consists of particulate organic carbon (POC) produced in overlying waters from farm waste or the planktonic community, and the benthos, which consists of two groups of macro and microscopic organisms that mediate the chemical transformations.

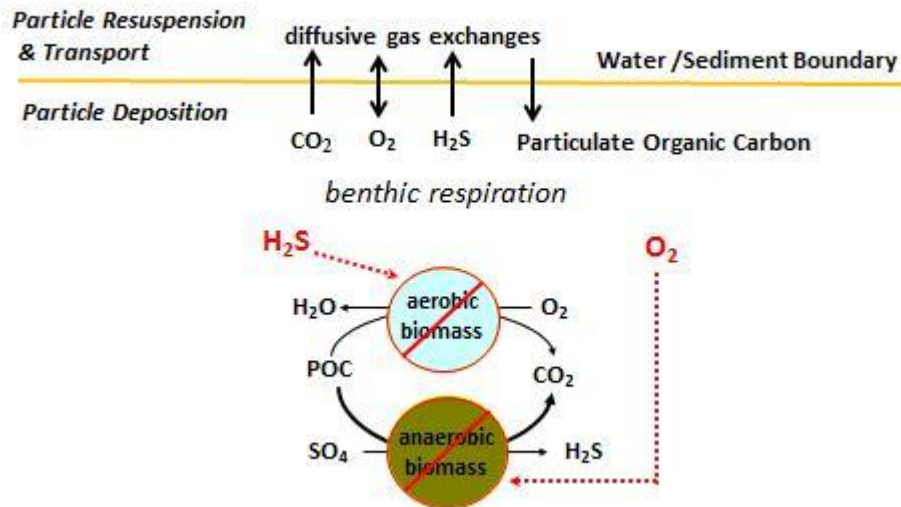


Figure 15. Conceptual model of benthic dynamics processes and respiration. Sulfide inhibits aerobes, oxygen inhibits anaerobic organisms and vice versa. Increased carbon loading leads to domination by anaerobes when the oxygen supply is inadequate for the aerobes.

The aerobes respire particulate organic material (POC in the diagram) and oxygen in order to grow and meet other metabolic needs. The main by-products of their metabolism are carbon dioxide and water. If either the concentration of oxygen or POC decreases below saturating concentrations, rates of growth and respiration will decrease. Furthermore, at the lower extremes of oxygen or POC availability, aerobe growth will stop and respiration will be reduced to a basal level. The anaerobes, which here consist only of the sulfate reducing micro-organisms, respire POC and sulfate in order to grow and meet other metabolic needs. The main by-products of their metabolism are carbon dioxide and hydrogen sulfide (or other reduced sulfur compounds). If either the concentration of sulfate or POC decreases below saturating concentrations, rates of growth and respiration will decrease. Additionally, at the lower extremes of oxygen or POC growth will stop and respiration will be reduced to a basal level. If produced at a sufficient rate the hydrogen sulfide produced by anaerobes will inhibit the growth of the aerobes. On the other hand, oxygen inhibits the growth of the anaerobes.

Figure 15 indicates that the size and growth rate of the aerobes can be limited by the supply of oxygen from the overlying water column. In our routine the rate of supply of oxygen to the sediments is determined by the diffusion of oxygen from the suspension layer into the sediment

layer, and the rate of diffusion will be determined by the difference in the concentration of oxygen in the suspension layer and the sediment layer, the thickness of the diffusion boundary layer at the interface:

$$JO_2 = \frac{O_2\text{DiffCoef [temperature]} * (O_2 \text{ suspended} - O_2\text{sediment})}{Z \text{ [velocity]}}$$

Where JO_2 is the flux of oxygen into the sediment layer, $O_2\text{DiffCoef}$ is the diffusion coefficient of oxygen, which varies with temperature, $O_2\text{suspended}$ is the concentration of oxygen in the suspended layer, $O_2\text{sediment}$ is the concentration of oxygen in the sediment layer, and Z is the thickness of the diffusion boundary layer, which is less than a millimeter in most open waters, and as indicated varies with the velocity of flow in the suspended layer. If the current speed in the suspension layer increases the thickness of the boundary layer will decrease and the rate of diffusion will increase. The concentration of oxygen in the sediments is assumed to be in quasi-steady state such that the rate of oxygen consumption by the aerobes, which varies with the concentration of oxygen and the concentration of particulate organic carbon within the layer, is equal to the rate of oxygen supplied by diffusion.

Figure 16 below, which is an example of a calculation by the routine, illustrates relationship between organic loading of the sediments and the oxygen concentration within the sediments. In the figure we see straight line, which is calculated from the equation above, describes the flux of oxygen into the sediment layer as determined by the concentration of oxygen in the sediment layer. In this example the concentration of oxygen in the suspension layer is 10 g m^{-3} (= mg/L). The curved lines show the rate of respiration by the aerobic members of the benthic community as determined by the concentration of oxygen in the sediment layer. The lower curve shows the respiration rate of the aerobes when the deposition rate of POC is $1 \text{ g carbon m}^{-2} \text{ d}^{-1}$, and the upper curve shows the respiration rate of the aerobes when the deposition rate of POC is $5 \text{ g carbon m}^{-2} \text{ d}^{-1}$. Both curves represent steady state conditions for the aerobes at which growth rate of the community is zero and the respiration rate is basal. This condition occurs when the concentration of POC has been reduced to a concentration at which it cannot support growth. Thus, the upper curve is the consequence of catabolic metabolism by a high concentration of aerobes in the sediment layer, and the lower curves the upper curve is a consequence of catabolic metabolism by a low concentration of aerobes.

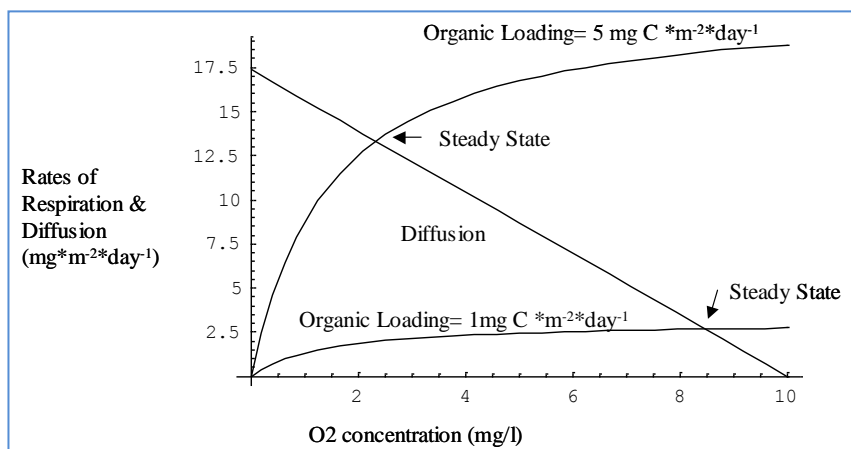


Figure 16. Organic loading to sediments and interstitial oxygen concentration relationship.

A similar diagram and similar arguments can be presented for regulation by POC deposition and sulfate diffusion for the anaerobes. However, because of the high concentrations of sulfate in seawater, the rates of diffusion of sulfate into the sediments layer are sufficiently high to rarely constraint the growth rate and biomass of the anaerobic community in the upper sediments.

It is clear from this diagram that increases in organic loading decreases the concentration of oxygen in the sediments, thereby releasing anaerobic organisms from their oxygen limitation of growth. As a consequence, the biomass of anaerobes will increase and possibly competing for POC with the aerobes and producing hydrogen sulfide. The latter may inhibit the metabolism and growth of the aerobes. Consequentially, if the gross metabolism of the aerobic community declines, oxygen concentrations will increase inhibiting the gross metabolism of the anaerobes. Such interactions will tend to drive the system toward a well defined steady state determined by the rate of organic loading, as well as the temperature, concentration of oxygen, and current velocity in the suspended layer above the bottom.

The importance of these dynamics to the management of fish farms is that provided the organic loading rate of the sediments is not too large, the respiratory activity of the benthic community will remineralize much if not all of the particulate organic material thereby releasing carbon dioxide into the sediments and water column. These predictions from our benthic routine have been confirmed by field studies such as those of Findlay and Watling (1997) and modeling work of Chamberlin and Stucchi (2007). In fact we have conducted a general tuning of the benthic routine to match the data of Findley and Watling's measurements of benthic dynamics under a salmon farm at Toothacre Cove in Maine and Chamberlin and Stucchi (2007) modeling of salmon farms in British Columbia.

After this initial work we then conducted a more detailed tuning of our routine to observations of waste loading by salmon farms in Puget Sound, described in the next section. We will see in our concluding section on impact assessment that the rate of waste deposition under the HSWRI demonstration farm is so low because of large dispersion over a broad area that the perturbation to sediment chemistry or the benthic community will be exceedingly small and likely undetectable. Our benthic routine indicates that the major response of the sediment under the farm will be a slight increase in the density of aerobic organisms and a corresponding increase in benthic respiration that will prevent the accumulation of farm waste and actually embellish food supply for the benthic food web.

Physical Circulation Module

AquaModel operates with a variety of inputs to drive physical circulation from simple built-in sinusoidal tidal amplitude models, to current meter data and several types of leading circulation model outputs. Current meter outputs are best for single net pen fish farm sites with relatively homogeneous flows over small areas in coastal areas (e.g., $< 1 \text{ km}^2$) that have recurring, mostly tidal-origin flow processes. As often this is not possible, AquaModel also accepts output from far field 3D circulation models such as ROMS, FVCOM and ADCIRC. Open ocean and more exposed coastal areas are subject to other forcing physical factors in addition to tides that are simulated in these models, notably the effects of winds and sometimes bordering ocean currents.

AquaModel pre-processes these data from gridded (normal mesh) or un-gridded (uneven mesh) models and calculates the depths and vectors necessary to produce an accurate conversion to

the Cartesian coordinate system that is necessary to operate with the limited computation power of standard desktop and laptop personal computers.

AquaModel's circulation routine flushes net pen fish farm cages with ambient waters and transports wastes from them. The computations during each step of the simulation occur within each element of a 3-dimensional grid of rectangular cells that populate an array of such cells. The size, orientation, and geospatial location of the array as well as the number and dimension of the cells that populate the array are entered by the users. The array of cells begins at the sea surface and extends to the sea floor. The geometry and flow at the sediment/water interface was previously described. The time steps for the simulation vary between 1 and 5 minutes depending upon the speed of the currents but the user can choose to view the movie-like visual output on any time step from minutes, to hours, to days.

The system of equations describing circulation is a simple finite element description of advection and dispersion. Each element of the array is treated as a box model in which materials flow across the 6 interfaces of each element, top, bottom and the four sides. Each element is treated as instantly mixed throughout. These movements are tracked using a simple, finite difference calculation. Conservative tracers such as water and elements are conserved within the computational array.

Water and dissolved and suspended materials also move across the boundary of the array; however, here the values for the concentrations of dissolved and particulate materials at the boundaries are determined by the boundary conditions of the computational array. During the course of our NMAI project we added the capability to vary the values of current velocities and the concentration of tracers at the boundary to vary at a time step specified by the user. If the calculations of such a model are to be trusted, the array must be sufficiently large such that the exchange across the boundary does not significantly perturb the results of calculations. At the sediment-water interface uneaten feed and feces from the farm are transported, deposited into the sediments, resuspended from the sediments, or consumed by benthic organisms. These processes will be described in the next section.

The flow field in AquaModel can be either 2- or 3-dimensional. In 2-dimensional simulations advection only occurs horizontally; neither divergence nor convergence flow occurs within the array. In 3-dimensional simulations the movement of water between adjacent cells has no constraints other than the requirement of conservation of mass. Convergent and divergent motion can be represented within the array as well as local eddies. In addition the water depth can vary within the array. Since 3-dimensional flow on small spatial and temporal scales is rarely measured in the field, our 3-dimensional simulations draw upon 3-D coastal circulation models. The spatial scale of these models is generally no smaller than 1 km and thus small scale turbulence is not included in the output. However, AquaModel provides the user the option to add specified levels of horizontal and vertical eddy diffusivity. While rates of horizontal dispersion are constant throughout the computational array, the rates of vertical dispersion can be specified for two layers, the upper mixed layer and the underlying stratified waters. The depth intervals of the mixed layer and the stratified layers vary with season as a sinusoidal oscillation. The system is designed to limit mixing between the mixed layer and stratified layer, and if the user specifies depth ranges of cells in the grid that overlap the boundary condition input for

mixed layer depth, the system automatically alters the mixed layer depth slightly to insure that rapid mixing from one layer to the other is avoided.

Prior Validation

The intent of the model calibration process is to refine the model “to achieve a desired degree of correspondence between the model output and actual observations of the environmental system that the model is intended to represent” (EPA 2002). As in any simulation model, testing and validation is necessary (Cromey and Black 2005, Rensel et al. 2006, O’Brien et al. 2011, Kiefer et al. 2011). Testing and validation of AquaModel has been done in several stages over many years and continues at present. This is necessary as the model is being applied to different ecoregions and fish species, in many cases where no aquaculture modeling has been done before.

First, it is conducted upon initial equation development when we create mathematical formulas to characterize known physical and biological processes. These outputs are compared to field or laboratory measurements from the literature or that we have personally conducted. Then it is tested when linked to other interdependent functions and processes. Curves are fitted to natural processes such as growth rates and the best possible equations are derived to describe them.

Our first work was with salmon as so much is known about their physiology that we did not need to conduct any additional laboratory work. The comparison of predictions of growth and metabolic activity for fish growing over a broad range of environmental conditions with published data displayed good agreement (Rensel, Kiefer and O’Brien 2007). Subsequently, we have closely compared our growth estimates with data from the U.S. Pacific Northwest and British Columbia and from Chile where conditions are somewhat similar. The results have indicated a very close final fish size after 18 to 20 months for Atlantic salmon (*Salmo salar*).

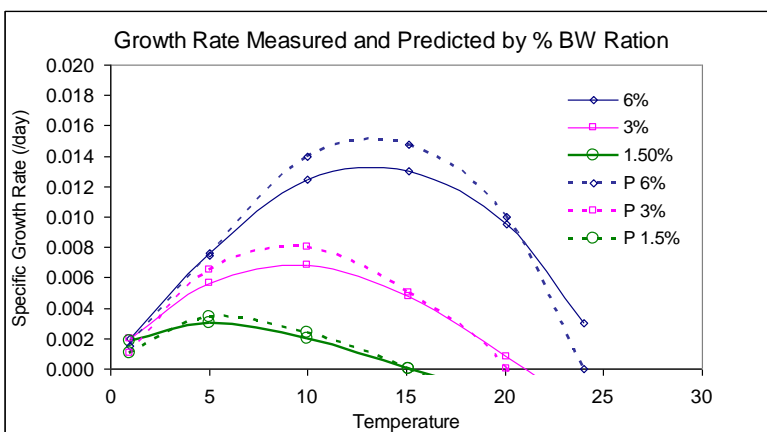


Figure 17. Growth rate measured in culture versus predicted (P) by model for initial calibration runs.

Figures 17 and 18 show two comparisons of model predictions with laboratory measurements. Figure 17 shows predicted (dashed lines) and measured (solid lines) growth rates for young sockeye salmon grown at different temperatures (abscissa) and different feed rates (legend). The growth rates are in units of the fractional change in body weight per day, and the feed rates of 0.06, 0.03 and 0.015 are in units of fractional body weights of food per day. Note that the

model accurately predicts the decreases in the temperature of optimal growth with decreases in feed temperature.

Figure 18 shows predicted (dashed lines) and measured (solid lines) respiration rates for young sockeye salmon swimming at different speeds (see legend) and at different temperatures (abscissa). The swimming speeds found in the legend are in units of body lengths per second. The upper graph shows respiration rates for maximum swimming speed record for a given temperature. Although our model describes steady state conditions as opposed to the short time interval during which the measurements was made, the fit is still good except at maximal swimming speeds.

These types of analyses were made for striped bass from literature and laboratory data, as described elsewhere in this report.

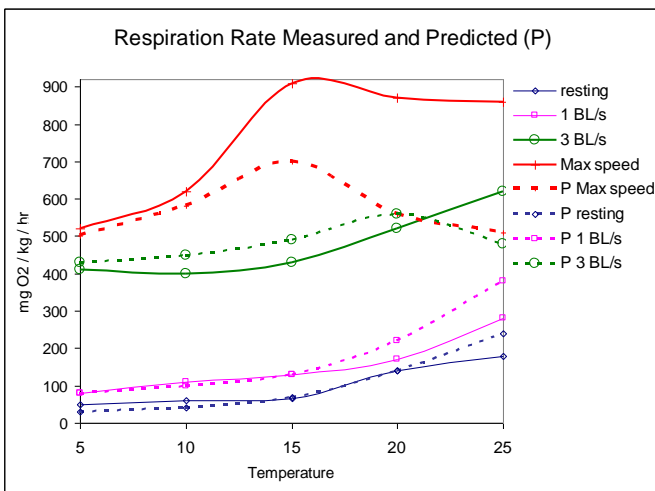


Figure 18. Laboratory measured vs. model predicted (P) respiration rate for initial calibration runs.

With respect to water column effects, Rensel (in WDF 1991 appendices and subsequently collected unpublished but reported NPDES monitoring data) has examined nutrient and dissolved oxygen deficit plumes around commercial net pen farms. In both cases the extent to which the plume can be detected is typically less than 30m for these large farms with 1,000 MT (2.2 million pounds) or more of fish biomass as shown in Figures 19 and 20, respectively. For dissolved oxygen, thousands of measurements have been collected in Maine by C. Heinig, yielding similar results (Normandeau Associates and Battelle 2003).

Previously we have conducted sensitivity analyses of key factors used in AquaModel simulations (Rensel, Keifer and O'Brien 2006). The sensitivity analysis we performed demonstrated the importance of resuspension as a factor that limits carbon deposition and allows for broad transport of waste particulates. This effect has previously been demonstrated with a benthic model (DEPOMOD) using a fluorescent tracer in a situation where current velocity was significantly less than the OHA site (Cromey et al. 2002b, mean velocity 4.9 cm s^{-1} , maximum velocity 23 cm s^{-1}). In our prior studies, the largest factor controlling water column and benthic effects was fish biomass (a function of fish density and size) and at the highest levels tested would produce significant and undoubtedly adverse effects if current velocity (primarily) and depth (secondarily) were minimal.

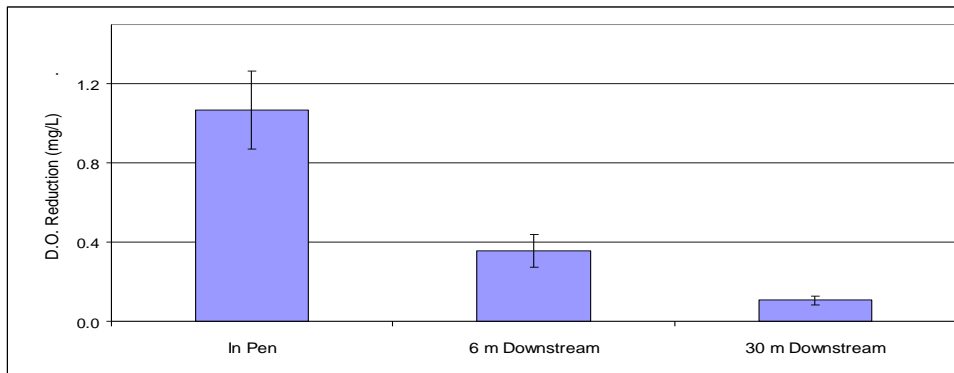


Figure 19 Summary of dissolved oxygen deficit compared to background (upstream) conditions for commercial net pens in prior studies. N = 12.

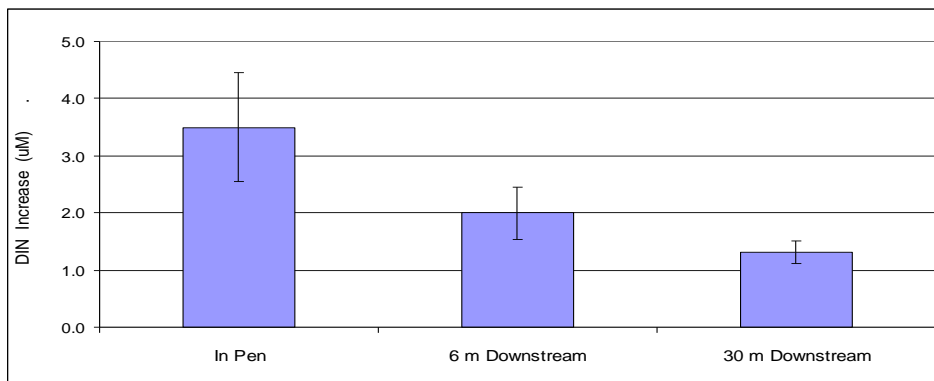


Figure 20. Summary of dissolved inorganic nitrogen increases inside commercial net pens and immediately downstream relative to ambient conditions as described in text. N = 12.

Beginning in 2012, we began testing all other aspects of AquaModel’s performance including the correspondence between boundary conditions and the simulation domain when no fish are being reared. In the past we had observed perturbation of deepwater conditions that were related to shallow bathymetry or shoreline interactions of the water current, vertical mixing and diffusion. We resolved and corrected these minor variations by creating a deepest layer system that allows the user to enter boundary conditions at the bottom of the modeling array as well as the sides for oxygen, nitrogen and water temperature. Additionally, a new mixed (surface) versus stratified (deep) layer separation system is used to more closely control vertical diffusion through the boundary between these layers. As with all AquaModel controls, they can be set seasonally in a drop down menu or entered as more frequent entries via a spreadsheet input system.

Primary AquaModel Coefficients for UAE Simulation

The following coefficients were evaluated for this specific application and used in the model. Several have been previously evaluated for proper range through a sensitivity analysis (Rensel,

Kiefer and O'Brien 2007) and more or less continuously since then as reported on the [AquaModel Publications page](#).

Fish Species Selection and fecal Settling Rates

Fecal settling rates for salmonids dominate the literature but these are necessarily representative of other fishes including striped bass. Findlay and Watling (1994), Elberizon and Kelly (1998), Panchang et al. (1997), Chen et al. (1999) all examined settling rates of salmon feces, from small (25g) to relatively large (1kg) fish. Reid et al. 2009 recently reviewed the literature and found considerable variability because of differences in diet, water viscosity, fish size and methodologies. Rates cannot be estimated from physical science calculations but despite all this salmonid settling rates are fairly well characterized over a range of fish size. The mean settling rates varied from 2 to 6 cm s⁻¹ and rate was related to fish size as expected. Cromey et al. (2002a) examined fecal pellets from even larger fish (*Salmo salar*) of 3.4 kg mean weight, and found settling rates averaging 3.2 cm s⁻¹. Determination of fecal setting rates is not easy, one of us has considerable experimental experience in this work and note that it is known that that fecal pellet sinking rates for marine species are often multi-modally distributed (i.e., there are differing size and density fractions that settle at different rates but the mean rates can still be determined).

Marine fish fecal settling rates are scarcer, but perhaps of higher quality. With the exception of Japanese *Seriola quinqueradiata* (Japanese yellowtail, Iikura 1974, 5 cm s⁻¹ but likely large fish) marine species had diffuse, slowly sinking fecal matter. Magill et al. (2006) reported rates for gilthead sea bream, *Sparus aurata*, and sea bass *Dicentrarchus labrax*, that are raised in pens in the Mediterranean Sea and elsewhere. They collected fecal matter from sediment traps suspended below net pens for 2.5 to 6.75 hours and transferred the contents to the laboratory for resuspension in 2 m high Plexiglas cylinders. Using advanced but laborious video tracking methods applied to over 1000 particles for each species, they found mean settling rates of 0.70 and 0.48 cm s⁻¹ for sea bass and sea bream fecal matter respectively. These authors carefully documented that the settling rates were not unimodal, as discussed above. As gilthead sea bream are presently the only fish species reared in marine cages, we could have used the rate of 0.48 cm s⁻¹ in our simulations for this project. However, to be conservative, we increased the rate to 0.8 cm s⁻¹ so that there would be more concentrated effect in case other species were used too.

Waste fish feed settling rates

In comparison to fish feces, waste feed particles are easily studied and quantified within columns or containers. A small range of values have been obtained but we chose to use 9.0 cm s⁻¹ for our evaluation with larger fish that will require a larger and therefore slightly faster sinking pellet than those used with smaller fish.

Waste fish feed loss rates

It should be noted that waste fish feed loss rates for large, corporate-owned fish farms were once considered to be relatively high (5 to 20%) but are now thought by most authorities and scholars in this field as averaging about 3%. Other modelers have recently used this rate and we believe it is appropriate for the relatively clear waters of offshore of the UAE where the fish can

see the feed easily. Some countries such as the U.S. requires some kind of feed loss prevention feedback mechanism for all U.S. marine fish farms, so 3% loss can easily be achieved. Most commonly submerged video cameras are used and when this rule was invoked most of the fish farmers in the U.S. already had adopted the technique, ostensibly for economic reasons².

Waste feed loss rates have fallen dramatically in the past decade for several reasons. First, feed is the single largest cost of marine fish farming and no fish farmer could stay in business long if loss rates were consistently high. Waste feed is much richer in carbon and nitrogen than waste feces and it sinks much faster, therefore the adverse effects of oxygen demand on and in the seabottom will be most pronounced from waste feed compared to fish feces (dry wt. basis). Waste feed can be eaten by wild fish and invertebrates and this has been demonstrated as a significant mitigating factor in semitropical and tropical environments in particular. Use of chemical therapeutants or antibiotics in the feed is increasingly rare with modern fish mariculture due to use of effective vaccines and best management practices.

Resuspension threshold

In recent years several studies have indicated that resuspension and transport of fish farm wastes are among the key factors to understand in modeling the effects of fish farms on sediments (Panchang et al. 1997, Cromey et al. 2002a, 2002b, Riedel and Bridger 2003).

At less than a given, species-specific current velocity, fish fecal and food wastes will settle to the bottom and remain in the same location, which is termed a “depositional “ condition.

At higher rates of flow, wastes are resuspended and hop, skip and move across the bottom in a process termed “saltation” until current velocity decreases again. This often occurs in “erosional” conditions and of course there is a continuum between the two extremes that we term “transitional” conditions. Most modern fish farms are located in these transitional conditions and as long as the sediments do not remain on the bottom for extended periods (i.e., days), the recently deposited sediments are subject to being resuspended and transported in the process of saltation. In this process, particles are eroded into smaller sized particles and more easily moved and are of course available to the food web for assimilation. Some fraction of the deposited materials will remain behind under all but the most erosive conditions, a process known as “consolidation” that is discussed below.

AquaModel allows for separate particle tracking of feces and feed fate, unlike any other available models that only track all solids at one rate. A prior estimate of threshold for resuspension rates for salmon wastes (feed and feces combined) is 9.5 cm s^{-1} as measured or modeled 2 m above the bottom (Cromey et al. 2002a, 2002b, Cromey and Black 2005). But the model they used does not differentiate between rates of waste fish feed and fecal matter and obviously the latter settle much slower than the former. Very little guidance is available for marine fish species waste fecal matter resuspension rates, but in lieu of definite values, we pro rate the resuspension rates similar to the slower settling rates of marine fish fecal waste.

² Dr. Rensel was the co-chair of the U.S. Dept. of Agriculture, Joint Subcommittee for Aquaculture Net Pen Committee charged with helping develop environmental performance standards for the U.S for four years.

As shown in Figure 7, we selected rates of 12 and 14 cm sec⁻¹ for resuspension rates of waste fish feces and fish feed, respectively, for this project. We would be justified in using lower rates, but as there are other uncertainties about the subject area, we elected to choose these conservatively high rates. These rates are uncertain and change with the hydration of these particles and amount of time on the bottom, so they are typically the focus of sensitivity analysis in our model validation studies.

Once the threshold of resuspension is exceeded, we quantify the rate of erosion for feces of 60.4 g C m² d⁻¹ and 40.0 g C m² d⁻¹ for waste feed, but these rates are indexed to water flow rates above the threshold rate similar to what other modelers have done with particle resuspension models.

Deposition threshold

A contrasting calibration parameter to the erosion threshold is the deposition threshold, the near bottom water velocity at which fish fecal and waste food particles settle out. We selected 3.0 cm s⁻¹ for fish feces and 4.5 cm s⁻¹ for waste feed. The literature combined values for salmonids are not well defined, but Cromey et al. (2002a, 2002b) used 4.5 cm s⁻¹ for the combined value and since the fecal matter of striped bass is likely less dense than salmon fecal matter, we scaled its threshold rate down commensurately. Both erosion and deposition thresholds are indexed to 2 m above the bottom, which allows the use of bottom mount ADCP current meter data.

Consolidation rate

For long-term modeling of the effects of fish farming on the sea bottom chemistry and infauna, an important consideration is the degree of consolidation of waste particle. As described by Cromey et al. (2002a, 2002b) this is the stickiness of materials that may remain consolidated upon the bottom despite elevated rates of flow over the bottom. There is evidence that the rate increases with elapsed time of slow velocities, but it has not specifically been studied for fish wastes. Since this factor is poorly known or described we opted to consider this the primary variable to vary in our calibration runs. The values selected ranged two orders of magnitude from 0.1% d⁻¹ to 10% d⁻¹ and we found that values near the lowest end of the range produces results that were most realistic. We are comfortable with this approach as we essentially have only one unknown in this analysis and the factor has both time of flow below the deposition threshold and near bottom current velocity as primary components so we need not change the calibration for differing conditions. We found that consolidation rates are important for fish farms in more quiescent waters, but for the HSWRI offshore aquaculture demonstration site the effects of varying consolidation are muted. This is because there simply are not prolonged periods of minimal flows. Any drop in near bottom current velocity is short-lived and does not allow an extensive accumulation of organic carbon containing wastes.

Organic carbon oxidation rates

Another important factor in modeling fish farm effects is the rate at which carbon deposited on, or moving along the bottom is oxidized by bacteria or assimilated by the food web. The rate of organic matter degradation by microorganisms is often estimated using a first order kinetics or a Michaelis-Menton kinetics approach with similar result in cases where substrate, instead of

microbial biomass, is limiting. When a fish farm begins operating at a new site, the biomass of microorganisms on and in the sediments beneath and immediately adjacent to it will increase in abundance commensurate with the increase in organic matter provided by the farm. Within reasonable bounds, after the farm operates for some period of time the microbial biomass (and macrofauna too) approximate a steady state to process the wastes. Beyond reasonable bounds, if too much carbon is deposited, sediment bacterial communities shift to anaerobic (sulfide reducing) which tends to extirpate many sensitive invertebrate macroinvertebrates, infauna or epifauna. Generally, up to 1 to 1.5 percent total organic carbon added to the top 2 cm will not result in the shift to anaerobic conditions, depending on sediment grain size and water temperature. Here we deal with the carbon to be added by the fish culture operation, keeping in mind background levels of TOC that are relatively low, approximately 0.6 percent. Total carbon levels are much higher but most of this carbon is locked up as biogenic, refractive carbonates from shell.

Thlusty et al. (2000) demonstrated that fish fecal matter had a very high solubility potential, losing approximately 50% of its organic matter in 12 day exposures to water flow. Fish feces are thus “non-refractile” forms of carbon, unlike carbon more tightly locked up in refractile forms such as tree trunks or bark or carbonate carbon such as shell.

Prior modelers of fish farm carbon oxidation rates (Fox 1991, Pachang et al. 1993) in Washington State and Maine have often used the value of 1 percent per day, which stems from an EPA (1982) document dealing with sewage sludge oxidation. Hendrichs and Doyle (1986) found carbon in phytoplankton cells (*Cyclotella sp.* diatom) decomposed at rates $> 0.14 \text{ d}^{-1}$ (1.4% per day), but that was for a mean temperature of 7°C. This low compared to summer bottom water temperatures but just about similar to winter bottom water temperatures at the subject site.

Fujii et al. 2003 found carbon decomposition rates for *Skeletonema* of $1.4\% \text{ day}^{-1}$ and semi-refractory carbon in the form of POC at $0.08\% \text{ d}^{-1}$, both at 20°C. From the literature it is clear that most fish farm waste carbon is highly labile (i.e., not refractory) so the former rate would apply for the present analysis.

Given the above, we conservatively choose to use $1.0\% \text{ d}^{-1}$ carbon oxidation rate in sediments and during the interval that particles are in the water column. A higher rate may have been justified, but without more experimental and observational data regarding fish farm wastes, we selected a lower rate. Water temperatures of bottom waters at the proposed site are approximately equal to or less than in most of the studies above which is one factor in our choice.

Description of Study Sites and Virtual Fish Pens

Here we describe the modeled fish farm sites, dimensions, configuration and other attributes and factors used in our simulation modeling. Again, these are theoretical sites only, we are not advocating any of them without further study. Figures 21 and 22 are vicinity maps and Table 4 includes location of the center of the simulated clusters of fish farm pens in the eight locations shown in the figures.



Figure 21. Landsat image of part of UAE with eight virtual fish farm sites for demonstration purposes only. The authors of this document are not suggesting that fish farms should be placed at these locations as indicated in this document.



Figure 22. Vicinity map of sites 1 (near field site) and 2 near the shoreline bight of Fujairah.

Positioning of Site 1 with respect to the bathymetric drop off at 40 m depth is shown in Figure 23. Figure 24 is the same site but viewed close up and with a bathymetric transect line showing in the XY plot, image profile. Figure 25 is of GEBCO bathymetry throughout the entire region, and Figure 26 shows all eight study sites along the UAE east coast within the green line rectangular box indicating the modeling domain.

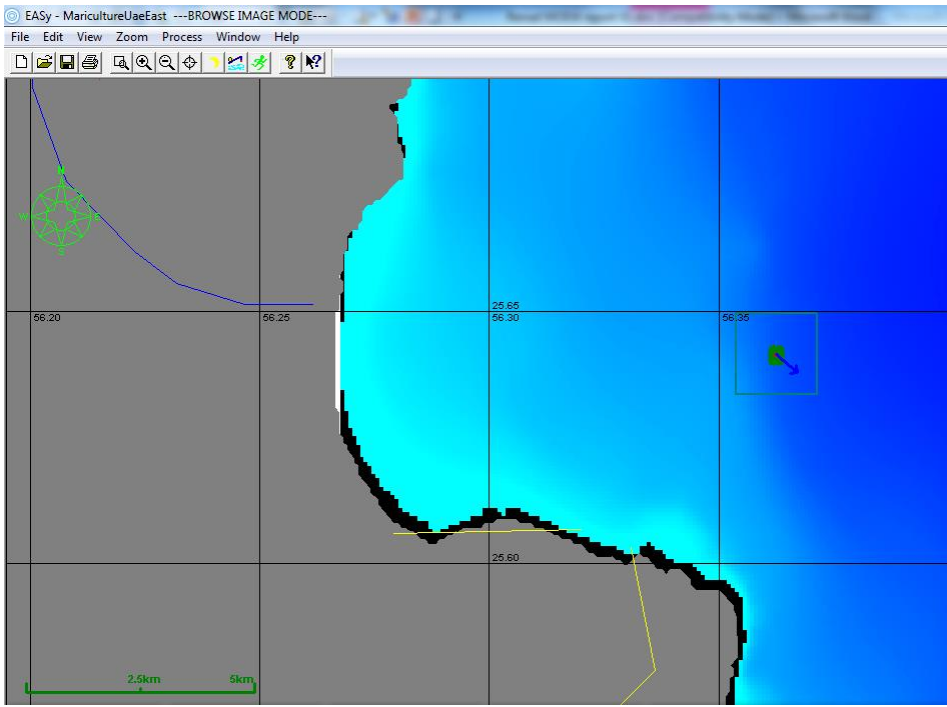


Figure 23. AquaModel bathymetry and modeling domain (small box to the left) with green net pens in center for Site 1, the near field site that was examined with regard to sediment effects on a fine scale.

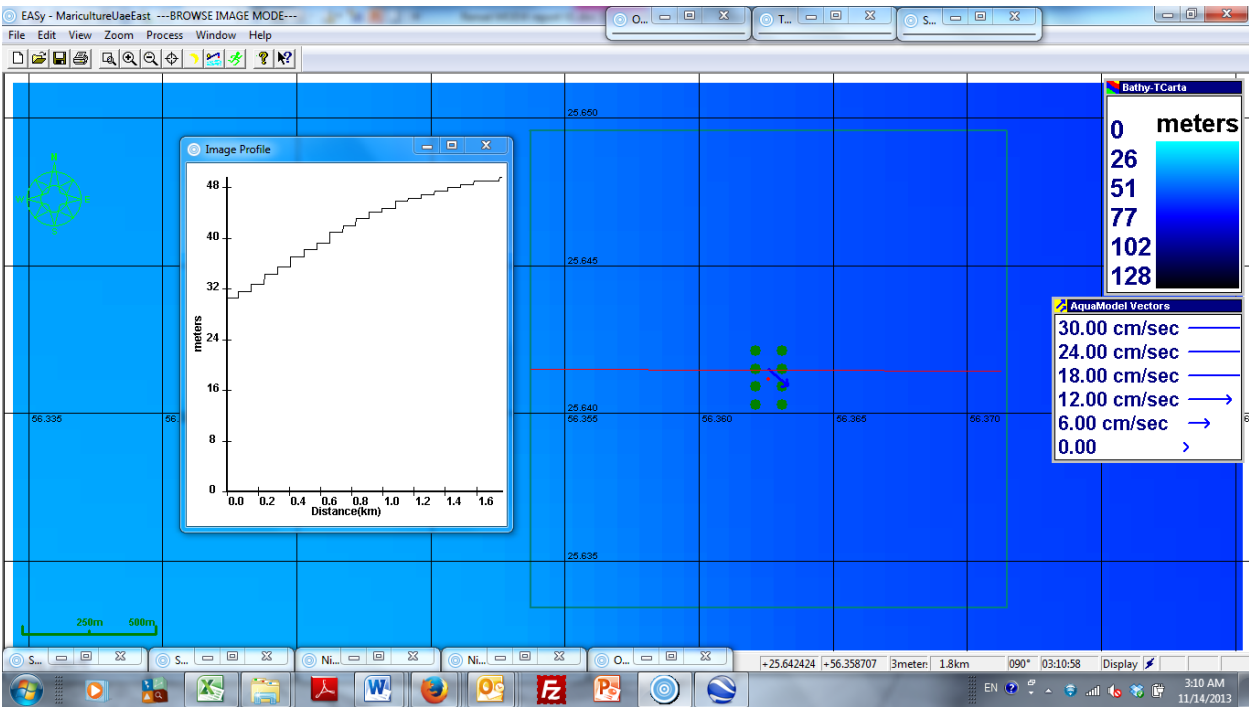


Figure 24. Site 1 net pen fish farm with the eight net pen cages shown within the 1.8 km square modeling domain and with a red transect line drawn across the middle to illustrate the gradually sloping depth profile with the cages at about 42m depth.

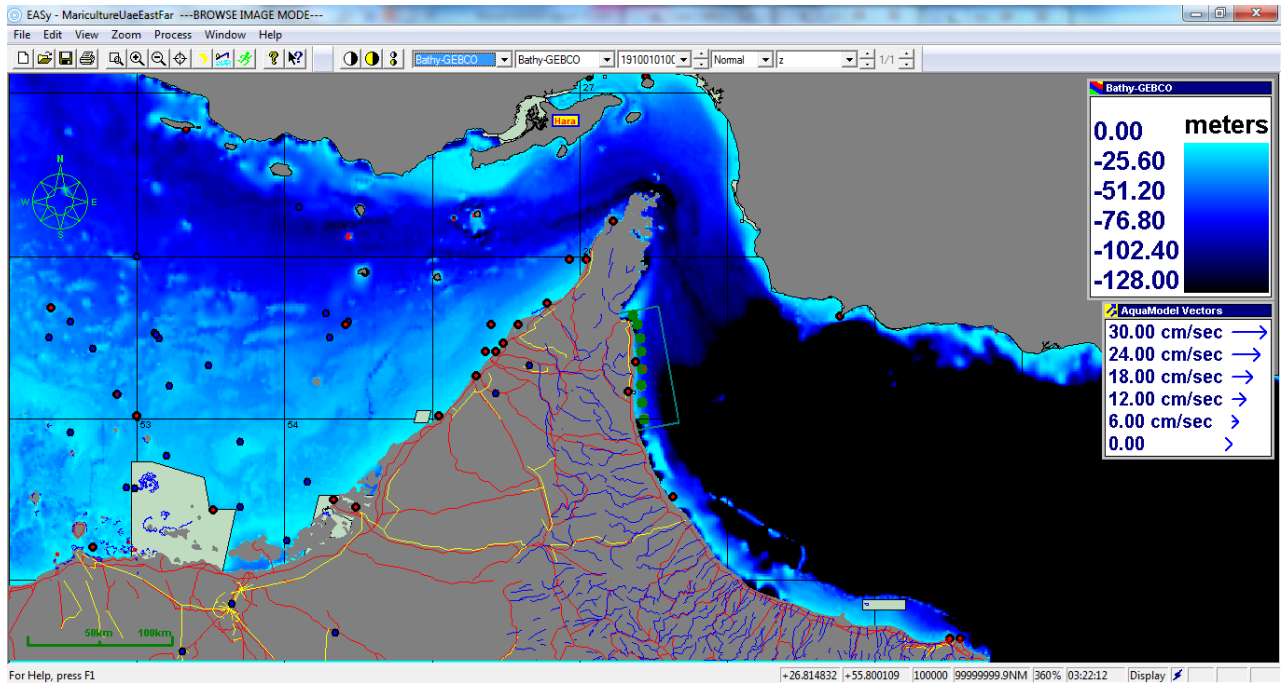


Figure 25. AquaModel view of Arabian Gulf (left) and Sea of Oman/Arabian Sea (right) with part of the Arabian Peninsula. United Arab Emirates east coast modeling domain indicated by the rectangular green box and some of the GIS shapefiles turned on to illustrate the GIS functions of the program.

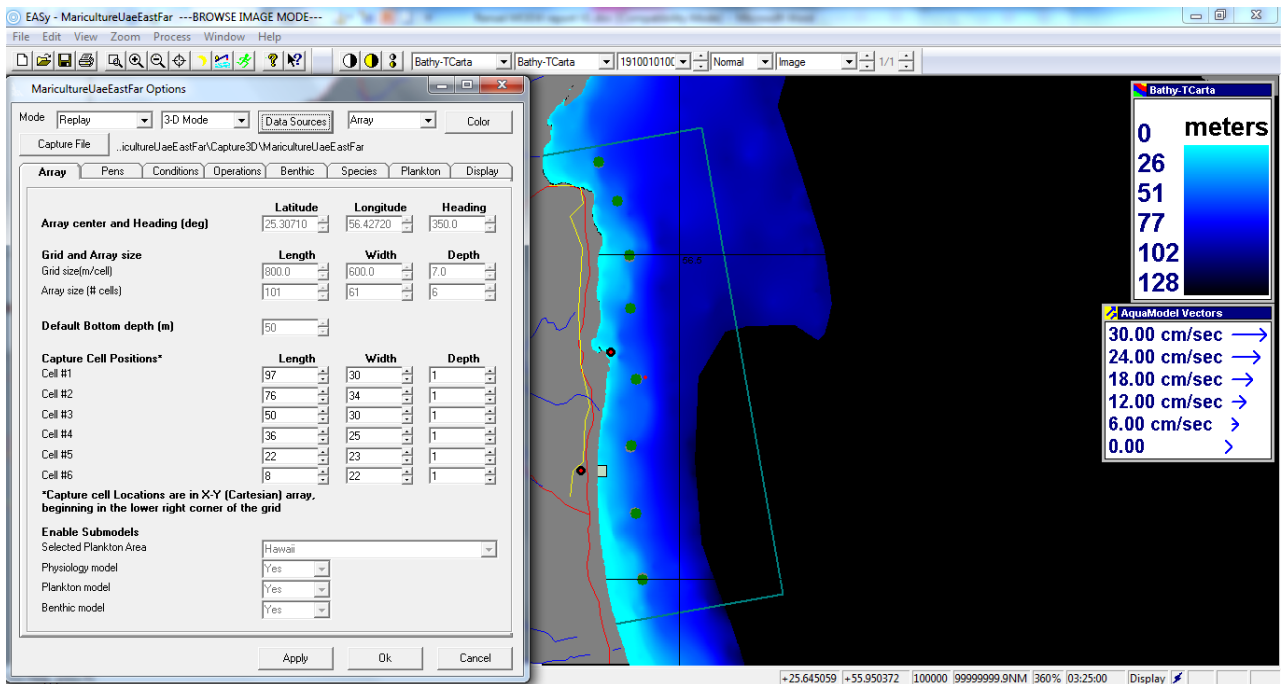


Figure 26. Closer view of the modeling domain for the far field examination of 8 locations along the UAE east coast with mariculture options showing the basic layout of the array.

Table 4 provides layout of the study sites utilized for this site. The primary consideration was to assay sites in about 40m depth of water, including one site near the bight near Fujairah and

several more distributed approximately equidistant along the UAE east coast. Note again, we do not represent these locations as suitable for net pen aquaculture until other studies are done that look at a variety of factors besides fish farm optimization or water column and benthic effects discussed in this report.

Table 4. Study location sites, cage volume, fish density, weight and biomass at the beginning of the final month of culture for fish farm No. 1 near Fujairah only (above) and eight fish farms spread along the entire east coast UAE (below). All sites were about 40 m deep.

Net Pen Number	Latitude	Longitude	Pen Volume m³	Last month Fish Density kg/m³	Last month beginning fish weight g	Last Month Beginning Fish Biomass MT
1	25.6403	56.3621	15,000	7.5	500	112.5
2	25.6409	56.3621	15,000	7.5	500	112.5
3	25.6415	56.3621	15,000	7.5	500	112.5
4	25.6421	56.3621	15,000	7.5	500	112.5
5	25.6403	56.3631	15,000	7.5	500	112.5
6	25.6409	56.3631	15,000	7.5	500	112.5
7	25.6415	56.3631	15,000	7.5	500	112.5
8	25.6421	56.3631	15,000	7.5	500	112.5
Total per one single farm:			120,000 m³			900 MT

Fish Farm Number	Latitude	Longitude	Total Volume m³	Last month Fish Density kg/m³	Last month begin fish weight g	Last Month Beginning Fish Biomass MT
1	25.6415	56.3626	120,000	7.5	500	900
2	25.5816	56.3943	120,000	7.5	500	900
3	25.4981	56.4152	120,000	7.5	500	900
4	25.4162	56.4175	120,000	7.5	500	900
5	25.3071	56.4272	120,000	7.5	500	900
6	25.2056	56.4182	120,000	7.5	500	900
7	25.1001	56.4264	120,000	7.5	500	900
8	24.9979	56.4380	120,000	7.5	500	900
Total for all eight farms:			960,000 m³			7,200 MT
						Ending biomass for all eight farms: 8,160 MT

Figure 27 is an AquaModel generated view of the UAE coast showing the actual bathymetry used to 140 m deep and offshore. The image statistics model provides area and volume estimates of bathymetry and image statistics summary for all the 50+ different categories that AquaModel utilizes. This perspective highlights the relatively smooth profile of the eastern coastline of the United Arab Emirates. Figure 28 is a slice of the Arabian Peninsula including the west and east coasts of the UAE that illustrate the profound differences between them.

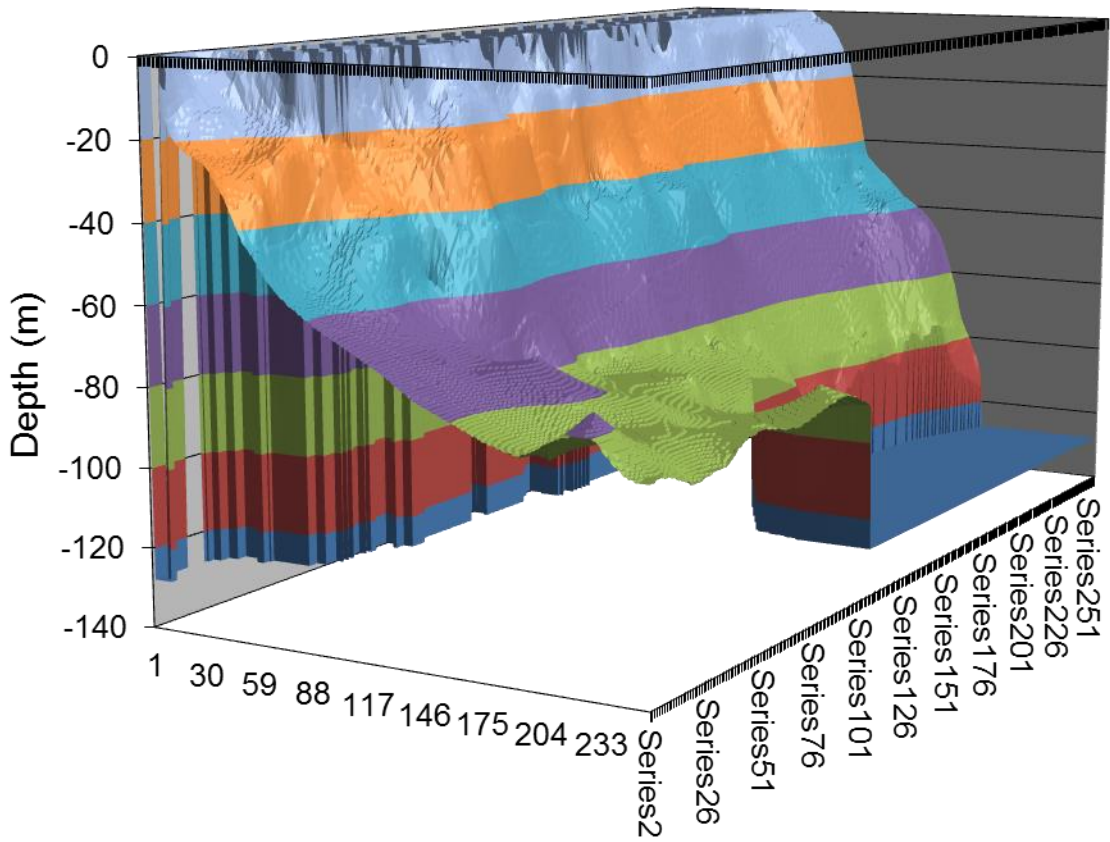


Figure 27. 3D view of the UAE east coast AquaModel bathymetry from using the AquaModel Image Statistics tool.

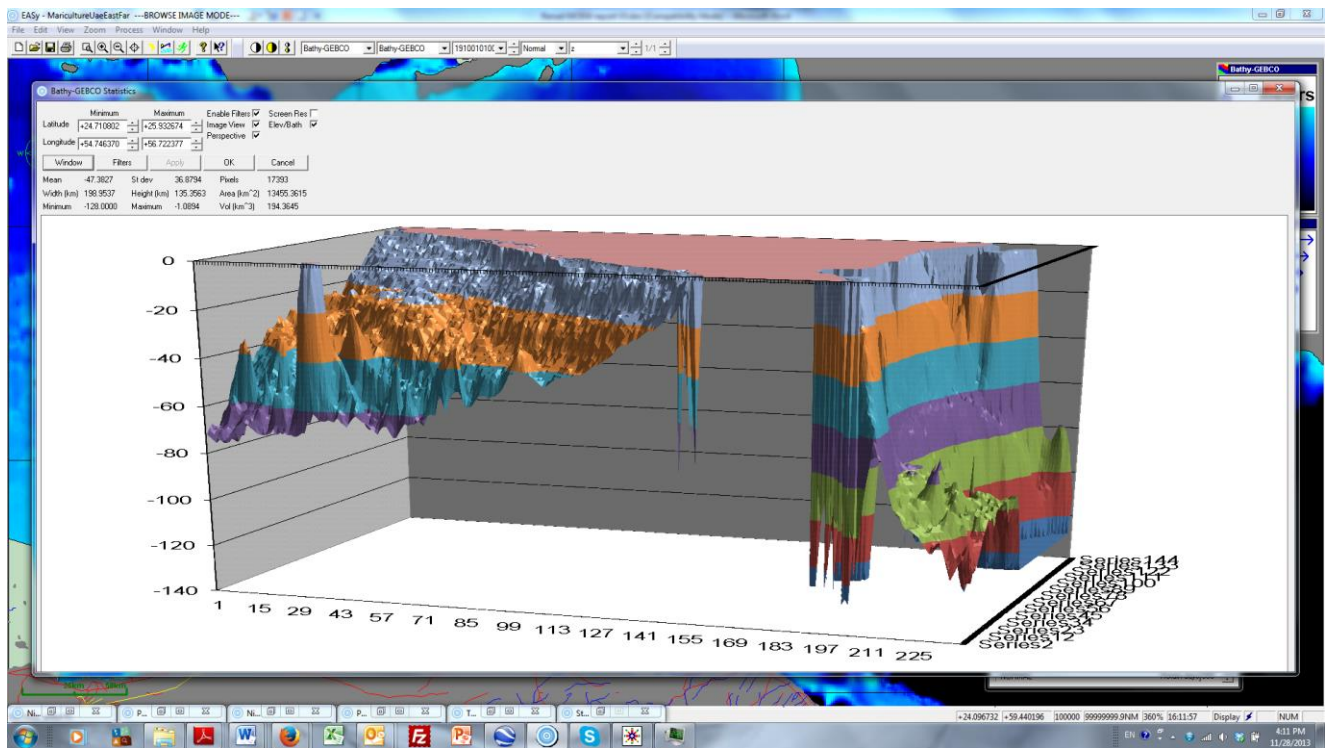


Figure 28. 3D view of UAE west coast (left side) and east coast (right side) showing profound differences in depth structure.

Near Field, Single Fish Farm AquaModel Analysis Results

Current Velocity

Water current velocity, and to a lesser degree total depth, are among the most important factors for the optimum siting of fish net pens to produce profitable results and protect the environment. The ideal fish farm site is relatively deep and has moderately strong current velocity. Literature ranges are quite broad (e.g., 10 to 60 cm s⁻¹ range considered ideal by Beveridge, 1987) but the higher values cited by this author often cause problems with cage structures and may result in reduced fish growth. Smaller fish may be unable to deal with sustained velocities beyond 2 to 3 body lengths s⁻¹ and fish farm net and anchor system maintenance is more difficult in strong current situations exceeding about 25 cm s⁻¹. Curiously, slow velocities are not conducive to better growth of teleost fish, based on research with salmon and a few other species in North America (e.g., Davidson 1997). This is fortuitous as progressive fish growers realize that moderately strong velocity of flow benefits their fish as well as reduced environmental impacts on the sea bottom.

Stronger currents not only disperse waste feces or feed further to initial point of bottom contact, but will allow for resuspension and further transport. Cumulatively, these properties of a suitable net pen aquaculture site allow the waste materials to be aerobically assimilated by the surficial bottom sediments. Without such currents, the wastes from larger fish farms would fall and be maintained in a smaller area and may exceed the carrying capacity of the sea floor organism to process them. This may result in a rise of the redox potential discontinuity layer (i.e., the RPD or “black layer”) towards the surface of the bottom with the associated increased sediment sulfides and concomitant shift to anaerobic bacteria decomposition of the wastes. This process involves the use of sulfate rather than oxygen as a primary substrate for reduction and may result in hydrogen sulfide production which may be undesirable for marine life or the cultured fish above. AquaModel simulates these processes continuously during a model run.

Optimum water currents are also desirable for maintenance of healthy levels of dissolved oxygen within the fish cages and removal of ammonia and urea. In tidal channels, currents often drop to nil during slack tide and it is at this point that fish may become stressed due to these factors. This may happen repeatedly and during naturally occurring low dissolved oxygen periods; such stress may contribute to less than optimum growth and survival. By contrast, open ocean areas that are subject to prevailing oceanic currents typically have much more sustained and continuous periods of current motion.

In our 40 year experience with net pen, we have found that an average current velocity of 15 to 20 cm s⁻¹ with maximum current velocity (e.g., 1 percentile exceedence) of 35 cm s⁻¹ at the net pen depths affords the best fish cultural results for large commercial-sized net pen farms with many cages. Additionally, near bottom current velocities that regularly (at least several times a week) exceed > 10 to 12 cm s⁻¹ result in minimal amount of seabottom-benthic impact, or even positive benthic effects of increased diversity and abundance of organisms. Average current velocity is just one metric, however, as it is both the frequency and strength of stronger currents that affect sediment transport and aeration. AquaModel’s benthic submodel has a variety of

settings for differing types of environments that are sensitive not only to average rates of transport, but the distribution of current velocities. For example, a feature known as “sediment consolidation” includes rate functions to simulate how fish farm wastes are more likely to be “consolidated” (i.e., cemented) to the bottom depending on how long a low flow period lasts. AquaModel is the only fish farm model available that separately tracks waste fish feed and feces, with differing parameter of deposition and erosion rates.

Table 7 indicates that the distribution of water currents for the month long survey were quite good compared to the ideal net pen conditions discussed above. Currents at net pen depth averaged 14.6 cm sec^{-1} , just slightly less than ideal with a 95th percentile and maximum result that were reasonable if appropriate anchoring and pen technology is used. Mean sea bottom current velocity was, as normally is, much less at 8.5 cm sec^{-1} but still well above the 5 cm sec^{-1} velocity that some countries have assigned as a minimal mean rate for all depths.

Table 5. Summary of single fish farm current velocity, biomass, feed use, growth rate, pen oxygen and dissolved inorganic nitrogen in cages during a final month of growout of sea bream.

Single Fish Farm	Velocity in Pen cm/sec	Velocity at Sea Bottom below Pen cm/sec	Each Pen Biomass MT	Each Pen Feed Used MT	Specific Growth Rate d^{-1}	Pen Oxygen mg/L	Pen Nitrogen (DIN) μM
Sum	--	--	--	1483.3	--	--	--
Mean	14.6	8.5	121.8	2.0	0.49	6.60	1.3
SD	7.7	3.7	0.04	0.04	0.04	0.38	0.6
Min	1.1	1.13	112.5	1.9	0.42	5.89	0.5
Max	27.6	15.2	130.7	2.1	0.57	7.11	4.3
5th Percentile	2.5	2.3	--	--	0.42	5.92	0.7
95th Percentile	26.0	14.1	--	--	0.56	7.05	2.4

Dissolved Oxygen and Nitrogen

Estimated dissolved oxygen in the net pens did not decline below 5.89 mg/L , averaged 6.6 mg/L and was therefore more than sufficient for the selected fish species given that these estimates were made at maximum annual loading and size of fish.

Dissolved inorganic nitrogen produced by the fish and added to the background load averaged $1.3 \mu\text{M}$ with a 95th percentile value of $2.4 \mu\text{M}$ and maximum of $4.3 \mu\text{M}$. Because boundary (ambient) conditions were set at $0.5 \mu\text{M}$ nitrate, this results in a 95th percentile and maximum value from the fish of 1.9 and $3.8 \mu\text{M}$ total ammonia, respectively. Assuming a pH of 8.1 to 8.3 of the subject seawater, with salinity of 35 psu and a water temperature of 25C, the fraction of toxic ammonia fraction would be about 4% to 6% of the above stated value, or a maximum of $0.11 \mu\text{M}$ and $0.23 \mu\text{M}$ for each of the above stated measures. Converted to ug L^{-1} values, this is equivalent to 1.6 and 3.3 ug/L (or parts per million). This is far below the threshold for marine fish chronic and certainly acute toxicity. For example for sea bass *Dicentrarchus labrax* the safe long term exposure limit was judged to be 0.26 mg/L (i.e., 260 ug/L , Lemarié et al. 2004) about 100x higher than the anticipated values for the pens simulated here. AquaModel is programmed

to spread the ammonia production out over an entire day but we know from many studies that a few hours after first meal consumption that rate of ammonia production peaks at about 3x the normal rate. So in the present case there is a more than comfortable difference between the highest probable values and the safe level as determined by the above cited study.

Nitrogen is also a factor in phytoplankton and other algal growth as well as coastal sea eutrophication and this is discussed in the next section with regard to multiple fish farm modeling results.

Figures 29 through 35 are snapshots frames of the hourly results that play in AquaModel like video output, one frame per second to see patterns. In these images the primary image is of water column dissolved nitrogen concentrations with a mixture of water column and benthic parameter XY plots.

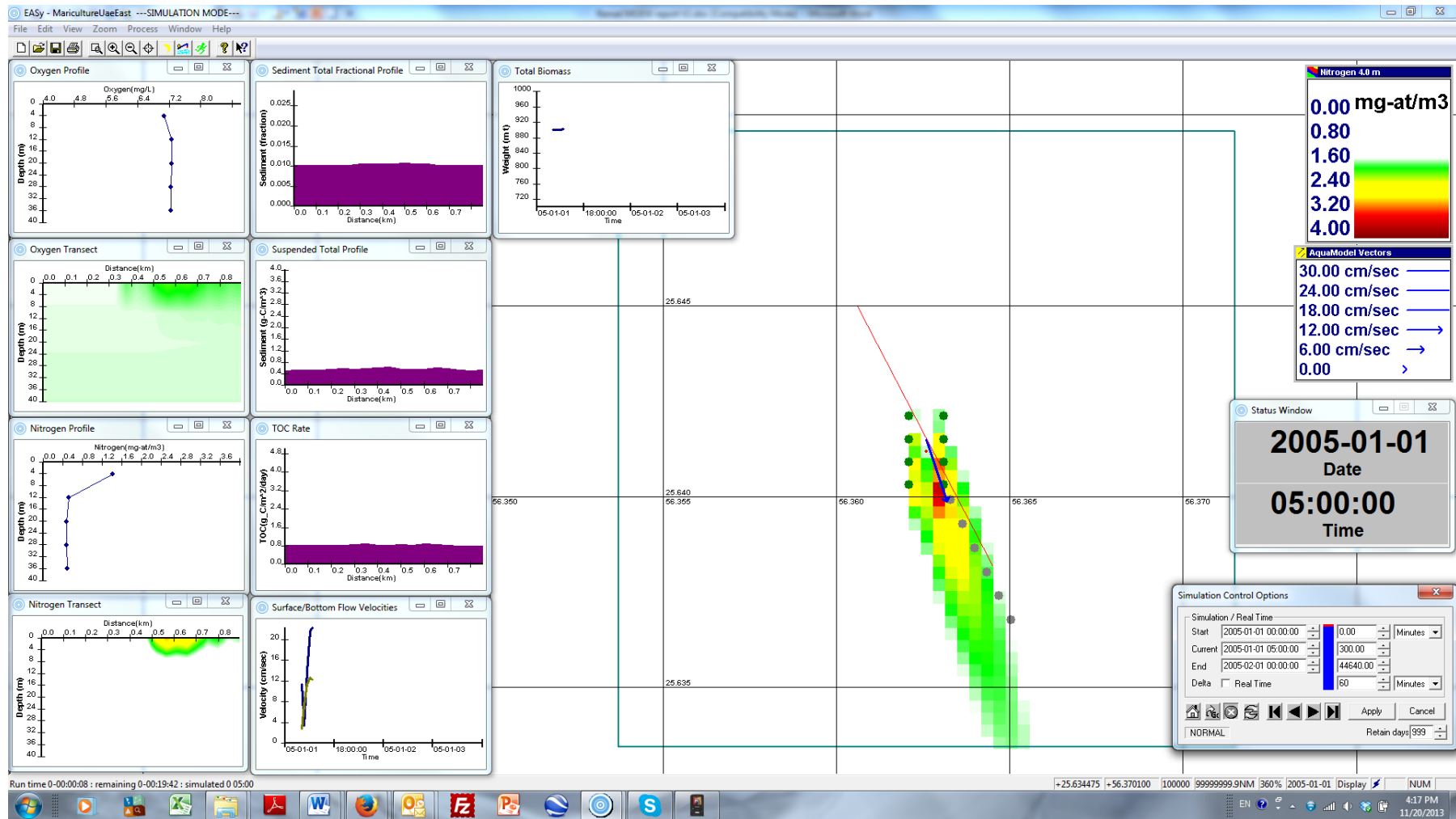


Figure 29. Beginning of last month of fish culture cycle showing water column and benthic parameters X-Y plots with dissolved nitrogen as the primary image.

This series of figures illustrating “snapshots” of the AquaModel single farm output show X-Y plots from left to right, top to bottom as: dissolved oxygen vertical profile at center of farm, oxygen transect along the moveable red transect line, vertical nitrogen profile, nitrogen transect along red transect line, Sediment total fractional organic carbon profile along red transect line, suspended carbon content of area just above seabottom along red transect line, Rate of total organic carbon profile along red transect line, surface and bottom velocities, total fish biomass. Legends, elapsed time and simulation control shown along the right border.

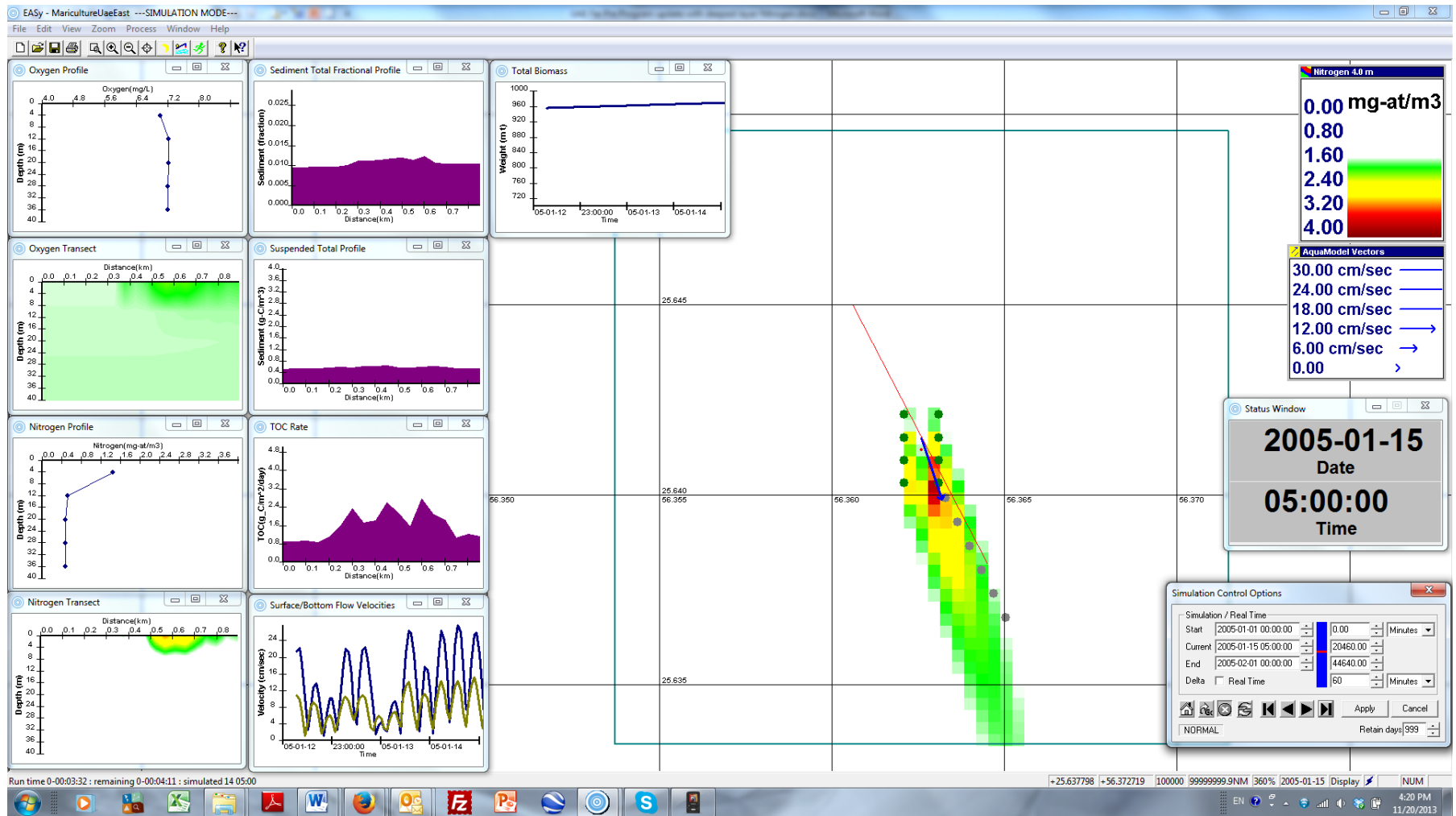


Figure 30. Midway through month 5AM showing a mixture of water column and benthic parameters X-Y plots with dissolved nitrogen as the primary image.

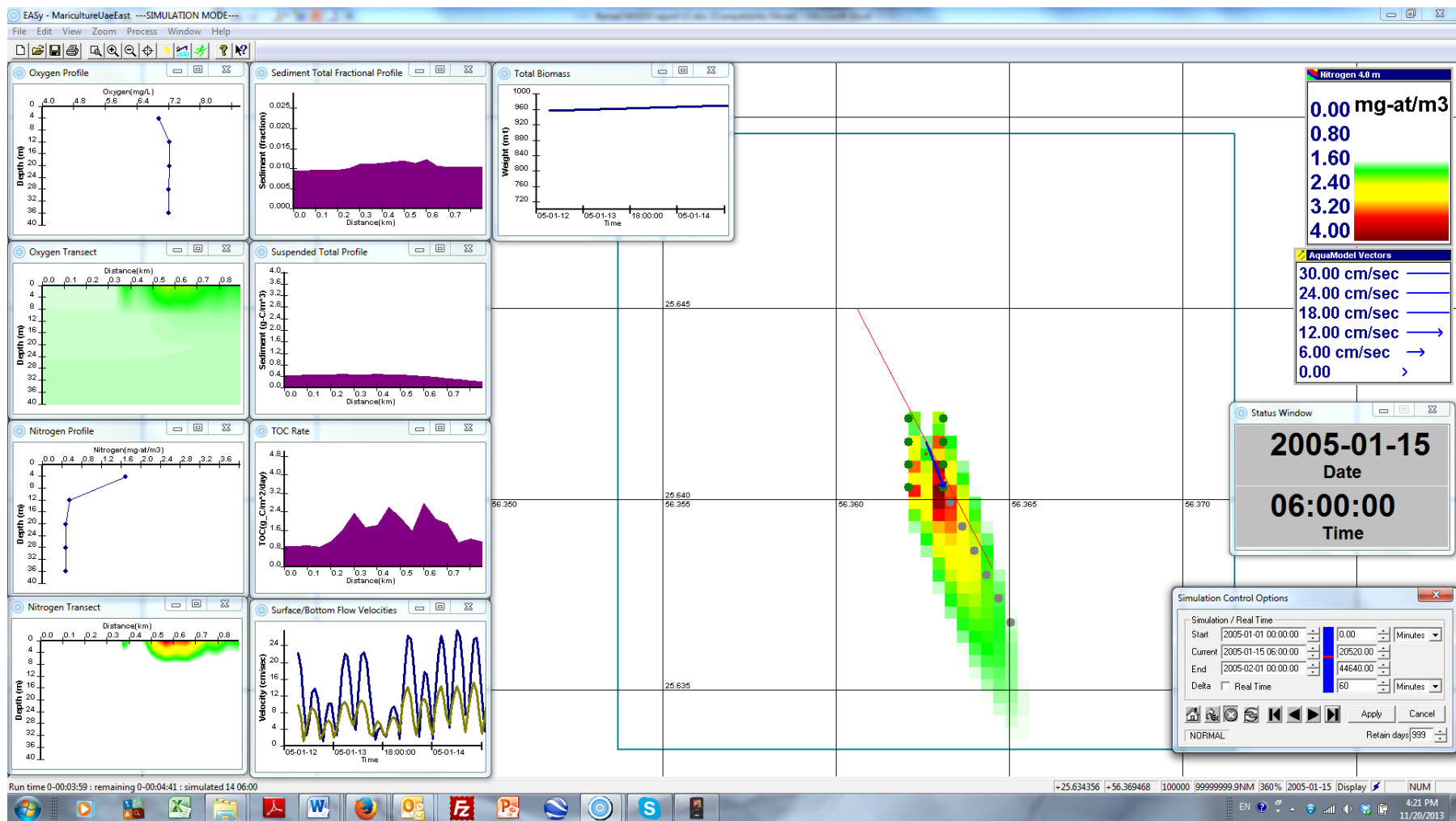


Figure 31. Mid way through month 6AM showing a mixture of water column and benthic parameters X-Y plots with dissolved nitrogen as the primary image.

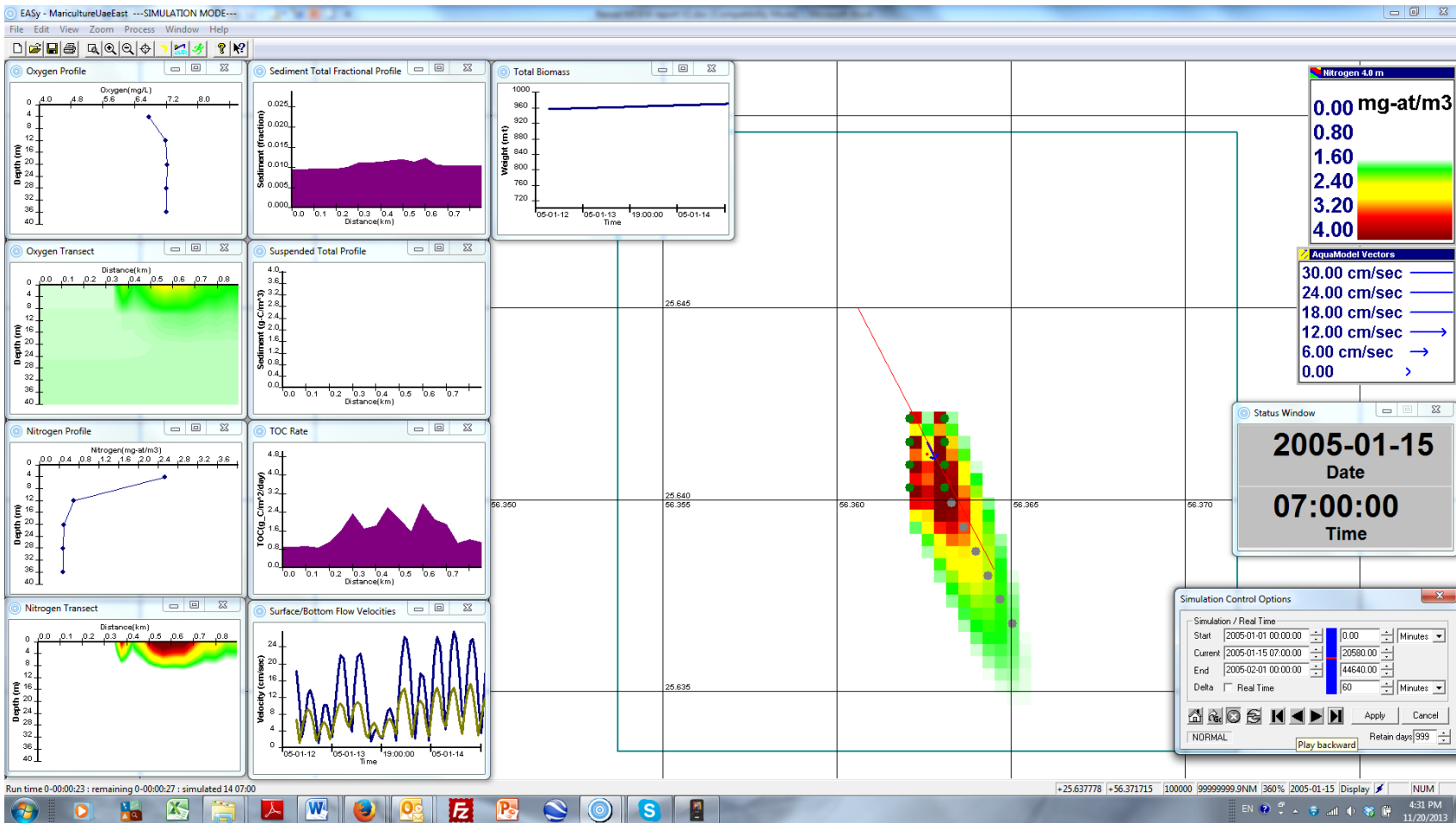


Figure 32. Mid way through month 7AM showing a mixture of water column and benthic parameters X-Y plots with dissolved nitrogen as the primary image.

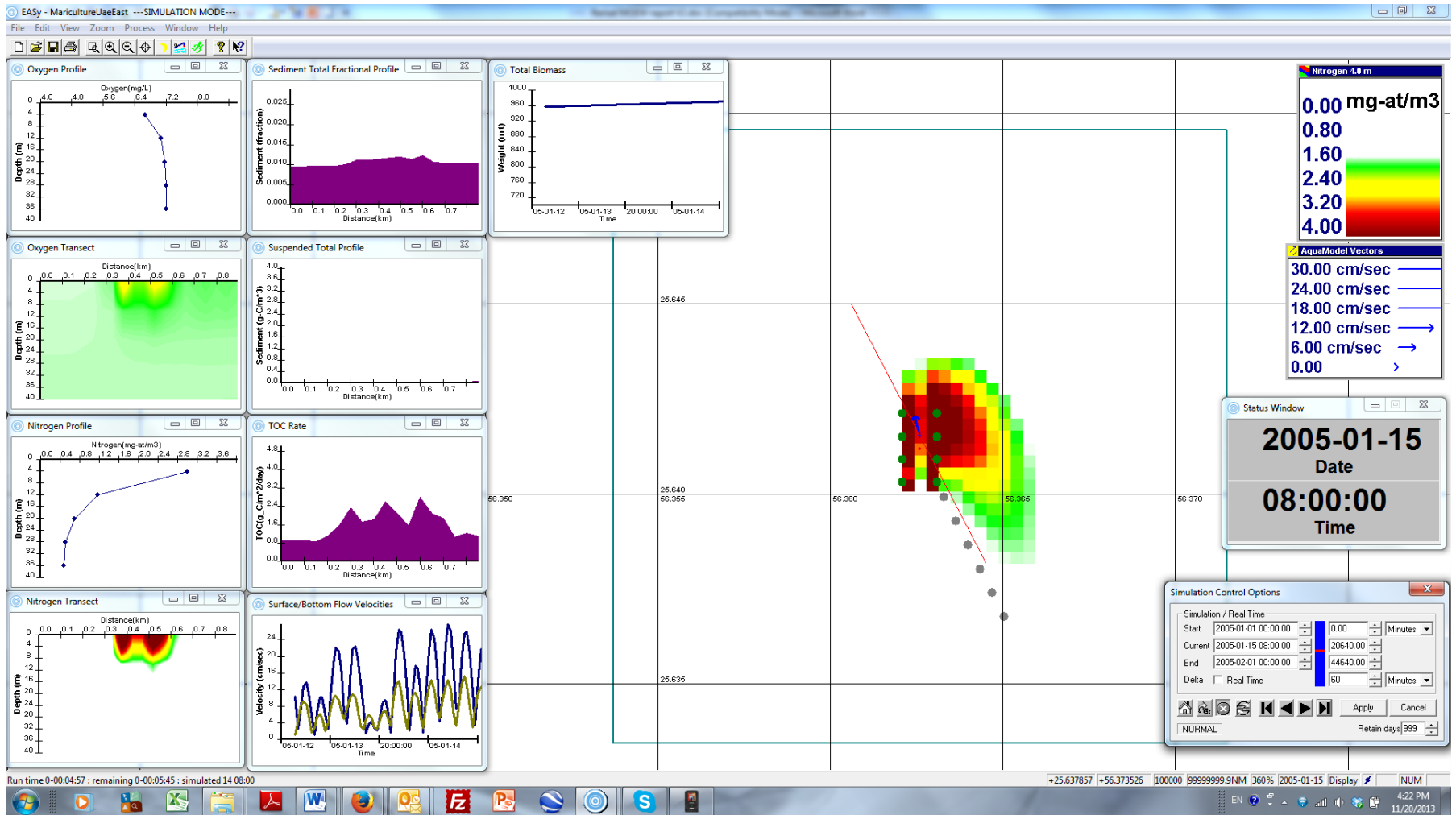


Figure 33. Mid way through month 8AM showing a mixture of water column and benthic parameters X-Y plots with dissolved nitrogen as the primary image.

Mid way through month 9PM showing a mixture of water column and benthic parameters X-Y plots with dissolved nitrogen as the primary image.

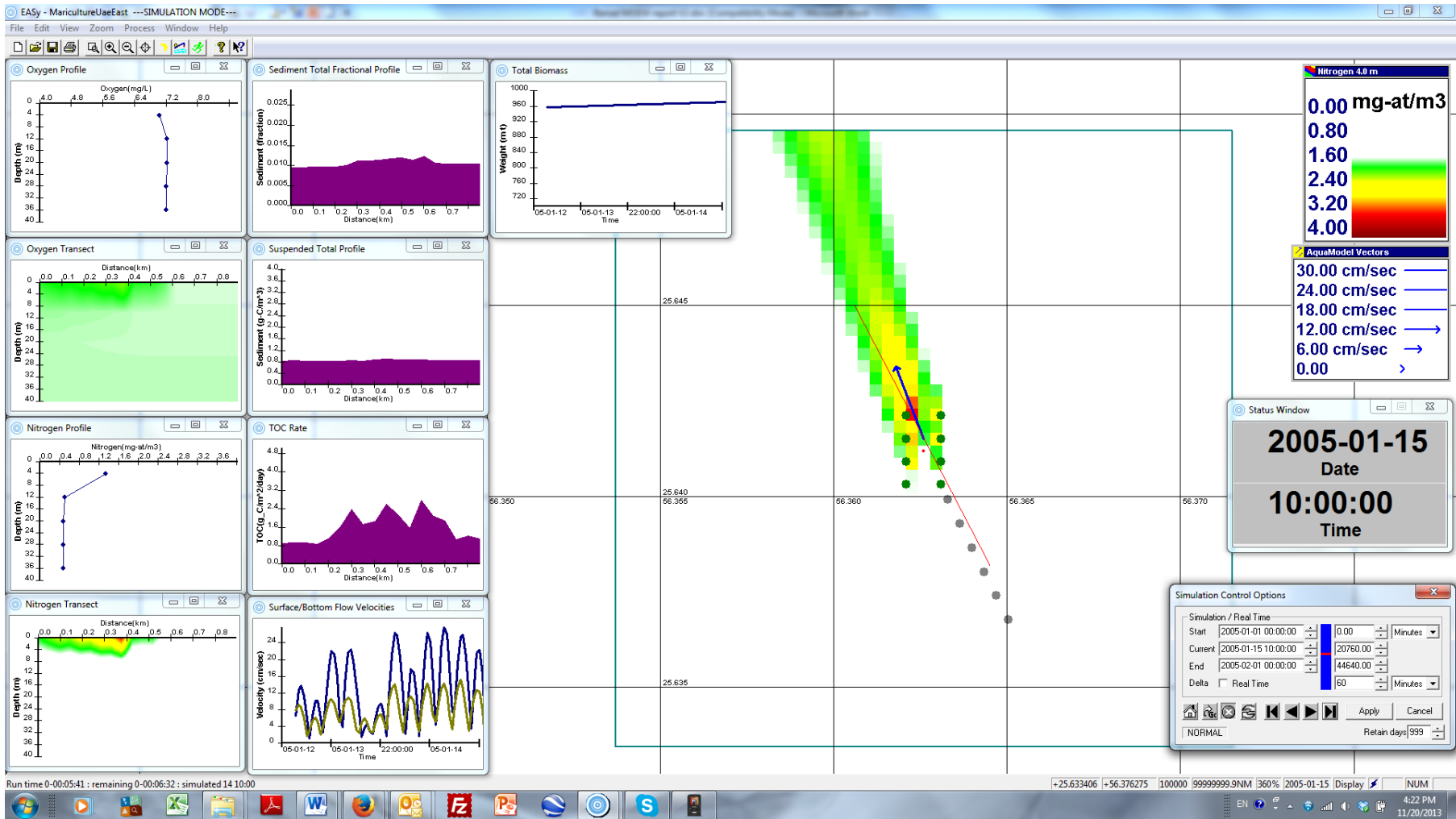


Figure 34. Midway through Month 10AM showing a mixture of water column and benthic parameters X-Y plots with dissolved nitrogen as the primary image.

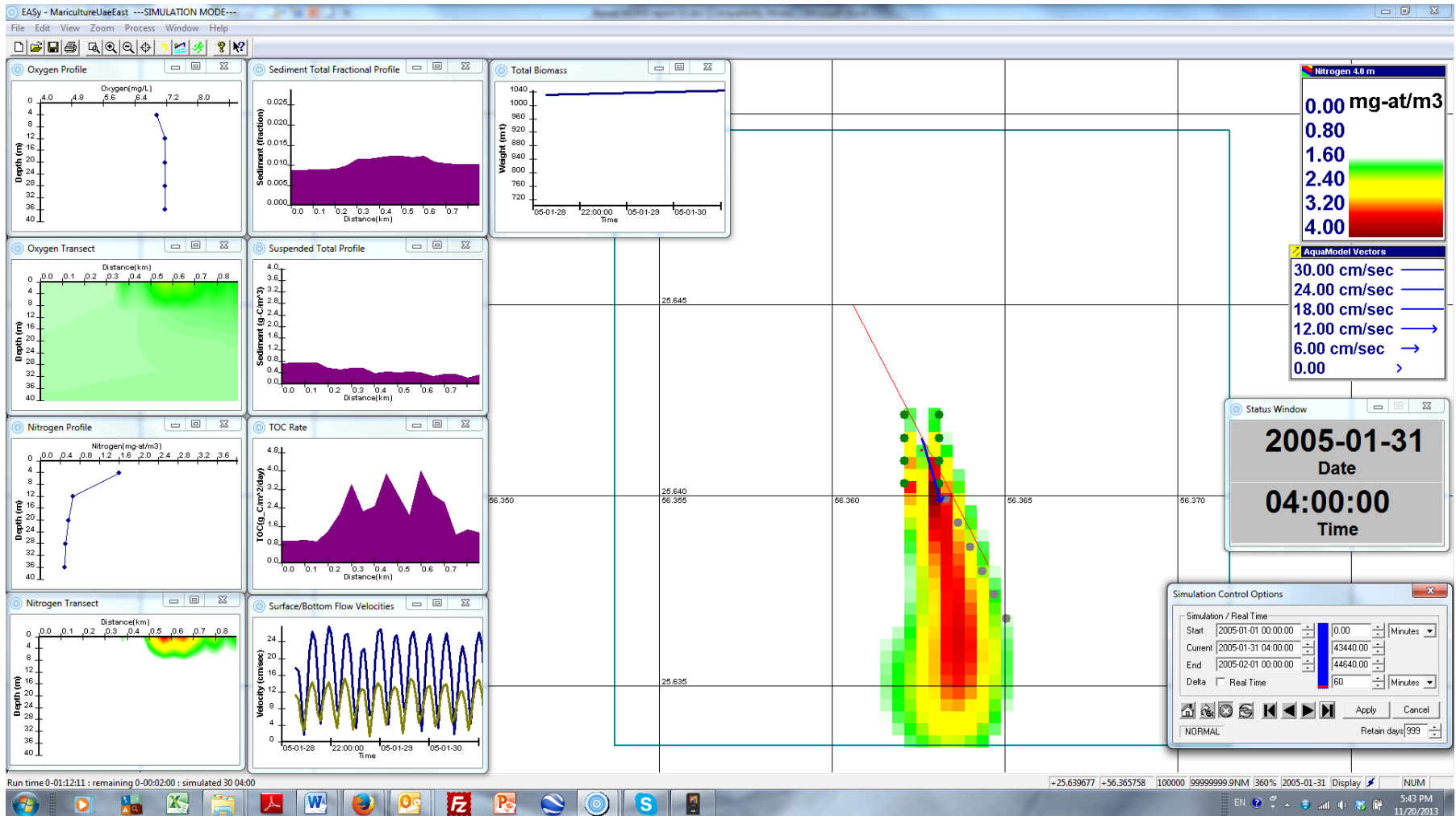


Figure 35. End of Month 4AM showing a mixture of water column and benthic parameters X-Y plots with dissolved nitrogen as the primary image.

Note significant increase in total biomass above 1000 MT.

Net pens in other countries with large commercial net pens have variable amounts of TOC under and near the cages. In the U.S., net pens are allotted a “sediment impact zone” where elevated levels of deposition may occur and perturbation of the benthic invertebrate community may accompany the carbon loading. The level of TOC flux and resulting concentration vary, but it is not uncommon to see a 100% increase in TOC concentration under or adjacent to net pens but by 50 to 100 m distance, levels approximate background conditions.

This simulation for the UAE east coast shows very small increases (< 0.3% maximum) and suggests that benthic loading may not be a limiting issue for the subject sediments with the study site layout and operation.

At present the background concentrations of TOC in sediments in 30 to 40 m deep waters of this region and at these sites are unknown. So this exercise can be viewed more appropriately as showing the degree of possible perturbation of net pen operation when the pens are stocked at their maximum biomass of fish. Table 6 presents this same data in tabular form. Not shown here is the fact that these results vary slightly and inversely with increased current velocity.

Figures 37 through 39 illustrate another set of images from this same AquaModel simulation but with the primary image being total fractional amount of total organic carbon in the surficial sea bottom sediments (i.e., the top 2 cm). Accompanying XY plots show some of the many benthic parameter plots and outputs. Commentary is given below each snapshot to explain further. Again, these slide represent the worst case analysis of the last month of fish culture with maximum fish biomass, peak daily feed use and fish wastes production. In Figure 37, plots from left to right, top to bottom are: total biomass, sediment aerobic profile, sediment anaerobic profile, sediment CO₂ profile, sediment sulfide profile, sediment total fraction profile of organic carbon, total organic carbon rate of (temporary or otherwise) deposition, surface and bottom current flow time series and simulation control panel.

Figure 38 illustrates the extremely minor increase of TOC is within the range where beneficial effects on benthic diversity and biomass would be expected without a major change in community composition. TOC rate to the bottom has increased but the net TOC concentrations are little affected, compare to the prior figure. Suspended total profile changes rapidly on an hourly time basis depending upon the strength of the current velocity at any given time, this shows the movement of particulate wastes across the sea bottom while aeration and assimilation of these wastes occur.

Figure 39 is from the final day of the simulation. Rates of TOC deposition, anaerobic and aerobic bacterial biomass and the concentration of sediment sulfides have increased, but the total fractional profile of organic carbon remains the same as 2 weeks prior. This indicates that the increased rate of organic enrichment is being assimilated with no resulting change of sediment TOC. Compare the total fraction organic carbon plots in Figure 38 and 39 to see this effect. However, if the fish culture continued at this point, the levels of sulfides would have increased from the modestly low levels to concentrations that, together with reduced dissolved oxygen, would have perturbed the benthic community measurably. Not shown here, we conducted simulations of larger fish farms prior to those reported herein, and found this to be the case. This is an illustration of the use of AquaModel to set a reasonable carrying capacity limit.

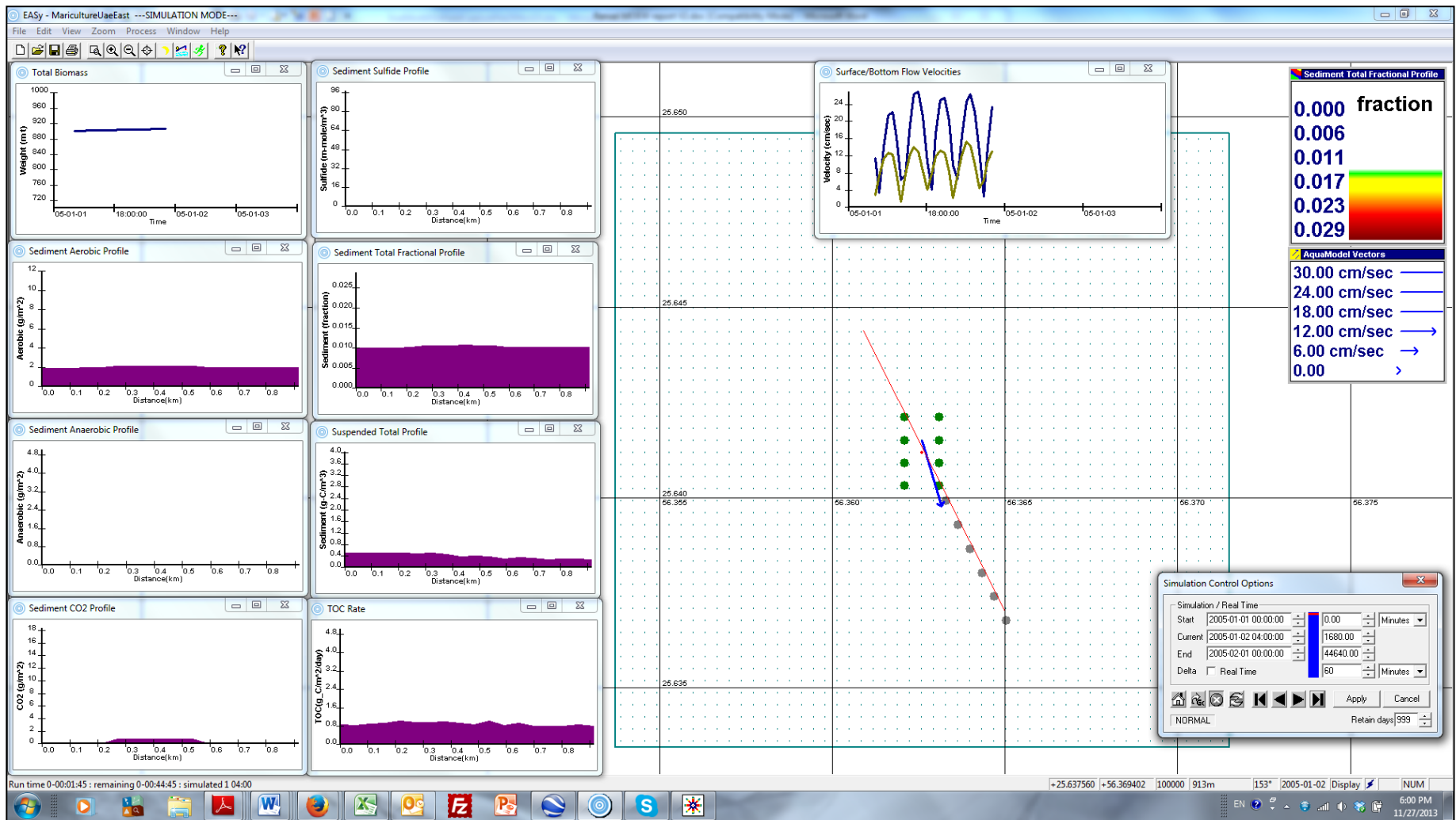


Figure 37. Beginning of last month of fish culture cycle showing benthic parameters X-Y plots with fractional amount of total organic carbon as the primary image.

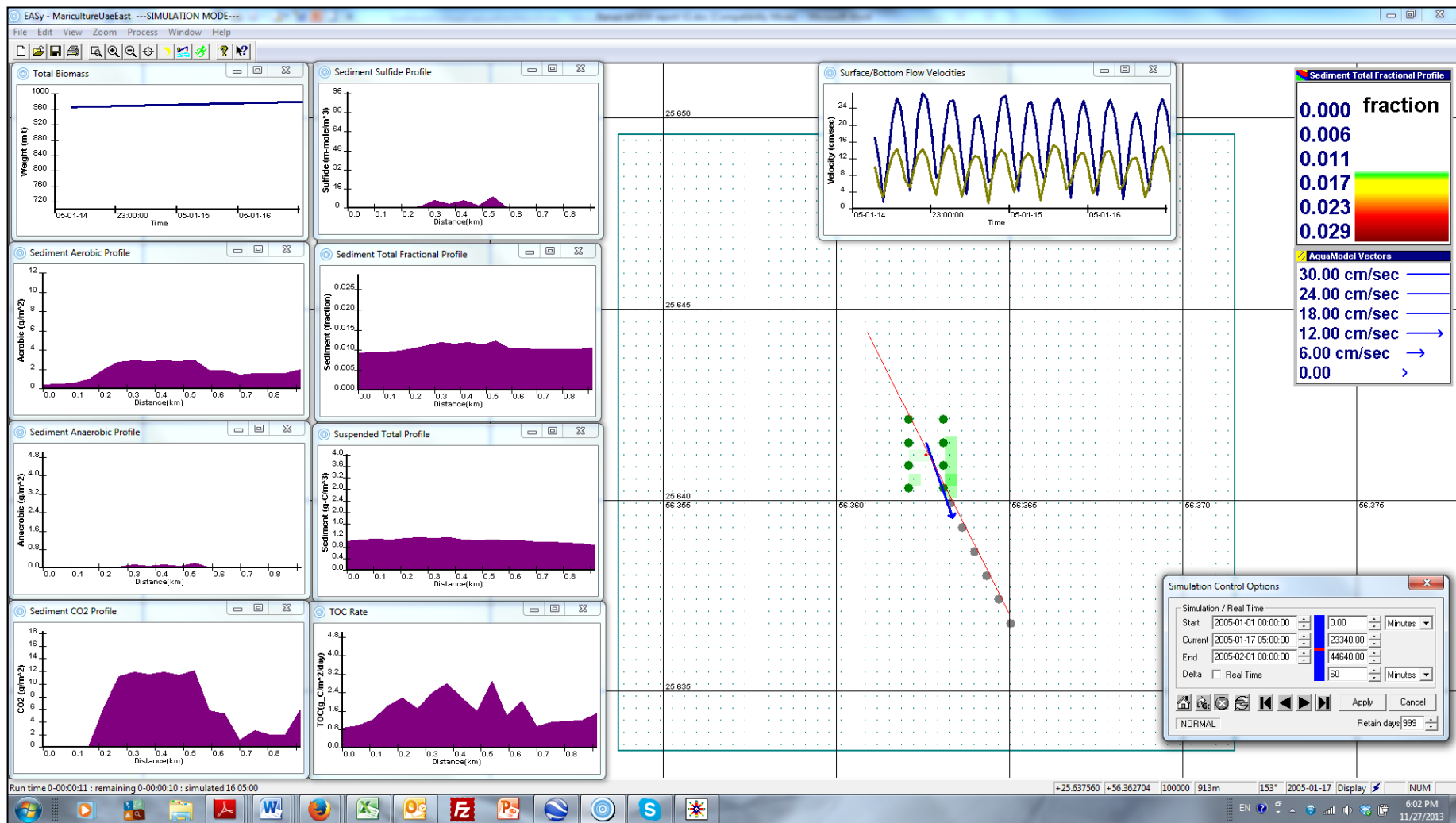


Figure 38. Midway through final month of fish culture with very limited benthic effects occurring only below and immediately adjacent to net pens.

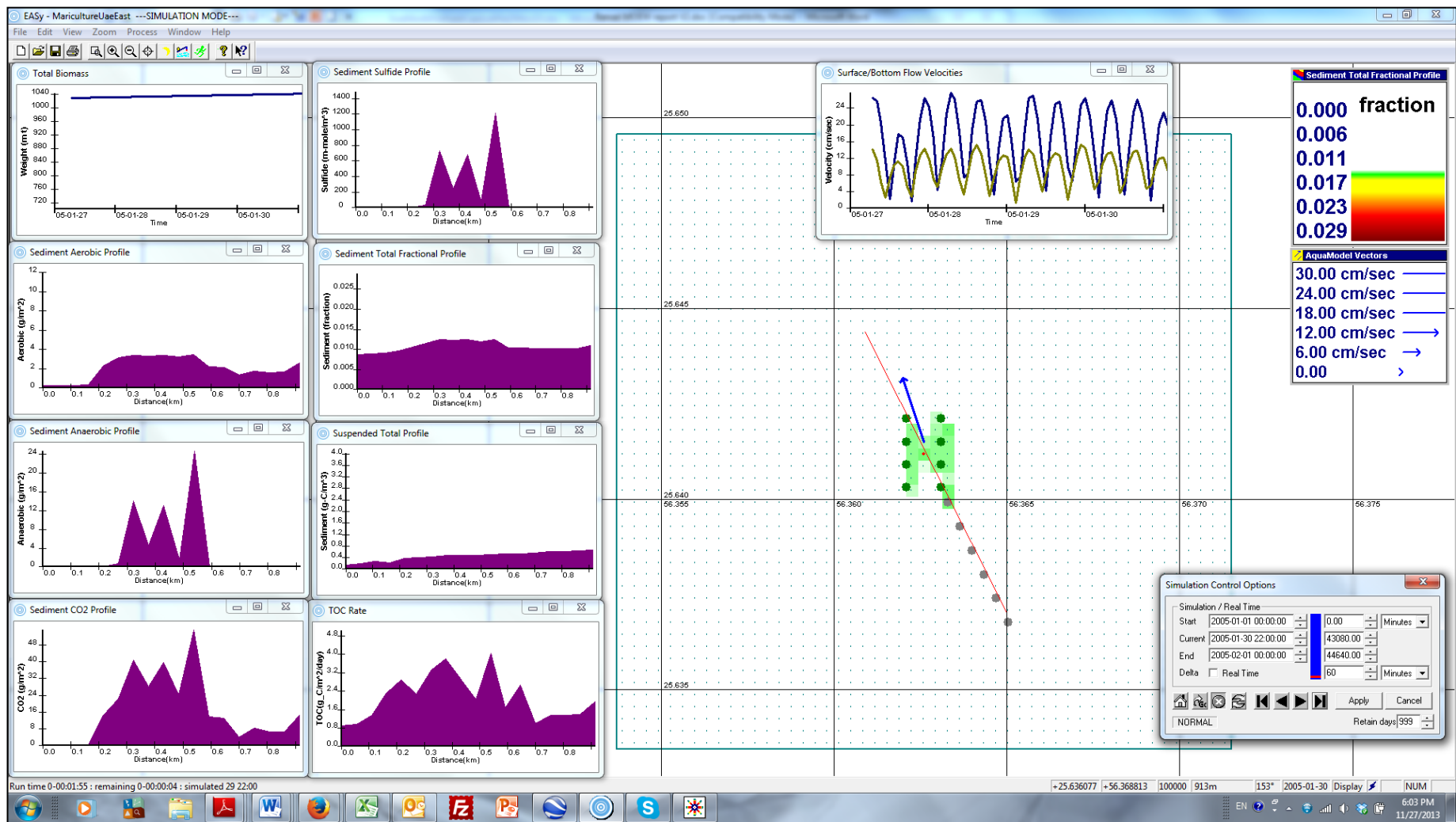


Figure 39. End of last month of fish culture showing increased rates of processing wastes (i.e., in the aerobic and anaerobic bacterial profiles as well as the sediment CO₂ and sulfides profiles) but these and other rates and results indicate that benthic carrying capacity has not been exceeded.

Far Field, Eight Fish Farm AquaModel Analysis Results

Current velocity

An introduction to this the importance of current velocity was given in the prior section: *Near Field Single Fish Farm AquaModel Analysis Results*. Table 7 far field results indicates approximate flow rates using the FVCOM circulation model for the eight study sites along the UAE east coast and Figure 4o shows some of this information in chart format. Individual site current velocity frequency profiles are given in Figure 41.

Table 7. Current velocity average, standard deviation, 5th and 95th percentile for all eight study locations both at net pen depth and seabottom from far field AquaModel analysis of the FVCOM circulation model results.

	Site One		Site Two		Site Three		Site Four	
	Mid Pen	Bottom	Mid Pen	Bottom	Mid Pen	Bottom	Mid Pen	Bottom
Mean Velocity cm/s	14.1	10.4	14.0	9.5	13.3	9.0	13.9	8.6
Standard Deviation	7.6	5.1	8.1	4.7	7.7	4.7	7.9	4.5
5 th percentile	3.0	2.3	3.4	2.1	3.6	1.8	4.5	2.4
95 th percentile	31.0	19.1	32.7	17.9	31.3	17.2	31.5	16.6
	Site Five		Site Six		Site Seven		Site Eight	
	Mid Pen	Bottom	Mid Pen	Bottom	Mid Pen	Bottom	Mid Pen	Bottom
Mean Velocity cm/s	15.2	8.1	12.5	7.6	13.2	8.4	11.4	8.0
Standard Deviation	8.3	4.4	7.2	4.1	7.5	4.5	6.0	4.2
5 th percentile	4.2	1.8	3.5	1.5	3.5	1.6	2.7	1.5
95 th percentile	33.4	15.8	28.2	14.8	29.3	16.1	24.7	15.1

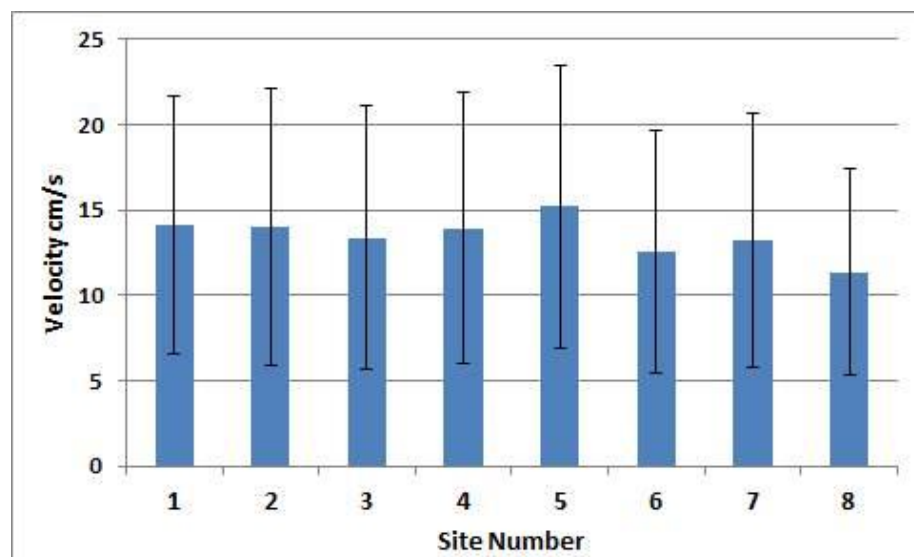


Figure 40. Average and standard deviation of current velocity for net pen depth from all eight study locations from far field AquaModel analysis of the FVCOM circulation model results.

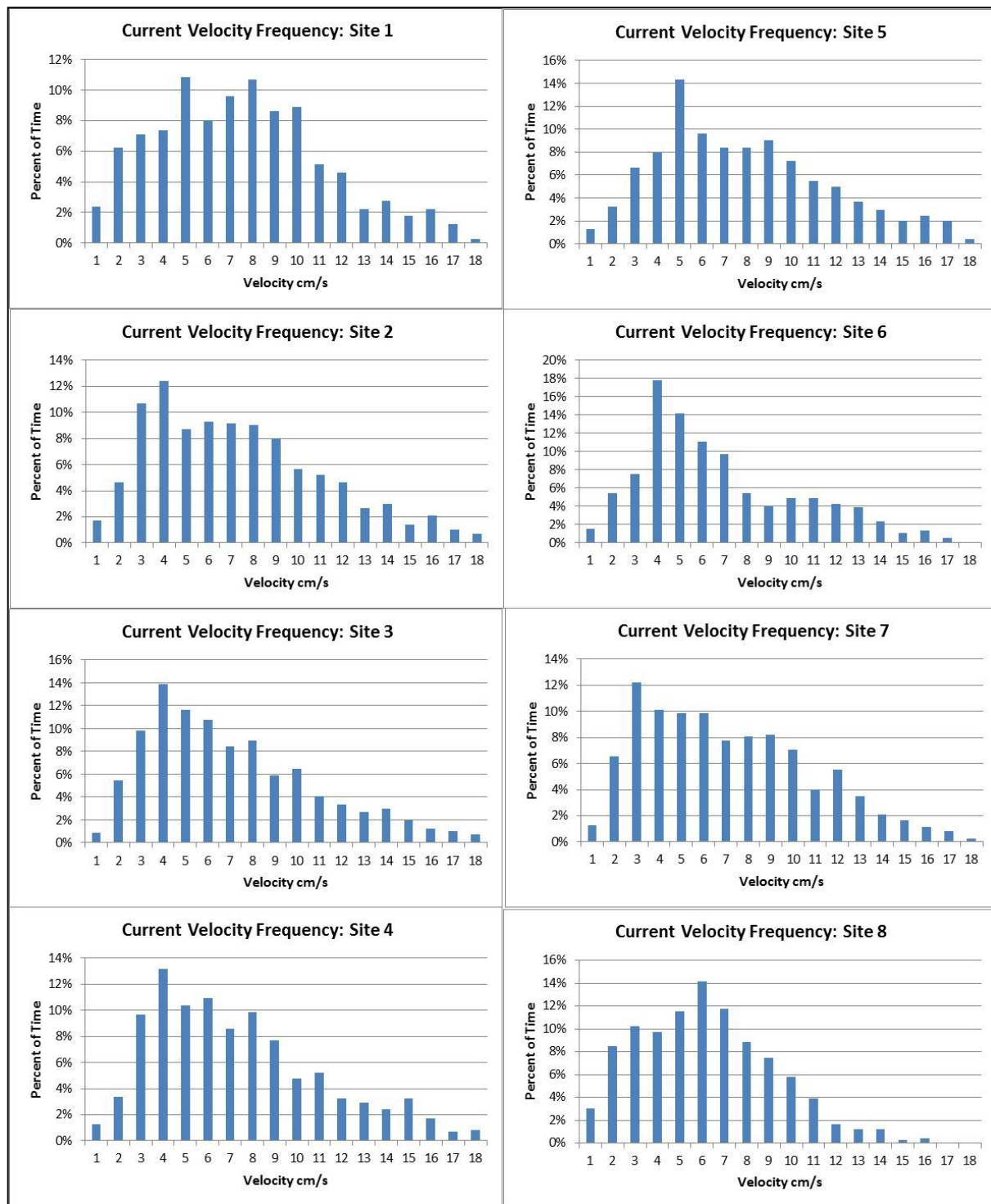


Figure 41. Current velocity frequency diagrams for all eight study sites along the UAE east coast derived from AquaModel tools applied to an FVCOM circulation model prepared by Dr. Rubao Ji, Woods Hole Oceanographic Institution.

Generally, near-surface current velocity estimates were similar among the eight study sites, although slightly stronger at Sites 1 through 5 and slightly less at Site 6 through 8. By inspecting Table 7 and figure 41 you can see that maximum flow rates were considerably less at only site 8. In part this may have been due to the siting in about 10 m less depth than all the other study sites (i.e., 30 m versus 40 m at other sites).

The 95th percentile current velocity at pen depth ranged from ~ 29 to 33 cm sec⁻¹ for all sites except Site 8. Such flows are strong relative to the needs of the fish and existing net pen tolerances, but because they are infrequent and net pen facility design and construction has improved in recent years they are certainly tolerable. And surface flow is often positively correlated with near bottom flow velocity where strong flows are desirable for food web assimilation of organic wastes and to maintain aerobic surficial sediments. This was previously mentioned for study site 1 and in comparison to optimum flow rates in the previous section.

Current Direction

Next we examine a subsample of the current direction results for Sites 1, 4 and 8 that represent the north, middle and southern sections of the UAE coast. Current direction has several important effects. More variable current direction equates to better waste dispersion, if current velocity is the same, but flow toward the shoreline and shallow habitats like coral reefs and sea grass meadows are to be avoided as increased nitrogen or particulate organic carbon can result in undesirable food web effects such as noxious or excessive epiphytic algal growth. For Site 1 (Figure 42), current direction was predominantly south to south-southeast(offshore) and to a lesser fraction of time towards the northeast. Extreme low or high flow rates were distributed approximately equal between these two general directions.

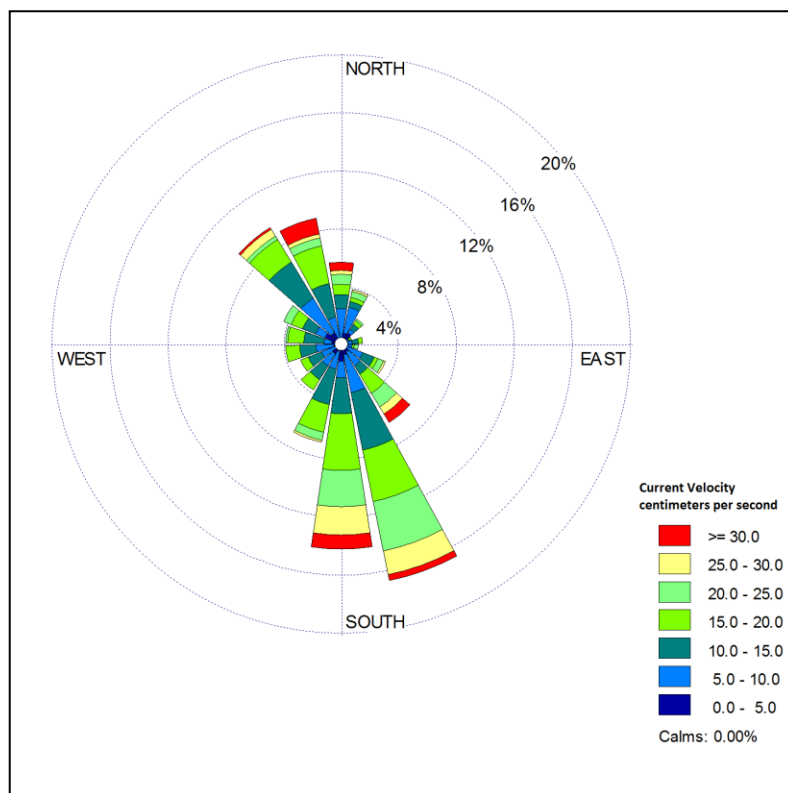


Figure 42. Frequency of occurrence of water currents in each of the specified direction sectors and velocity classes for a month long period at the simulated Site 1 location, using current velocity data extracted from the FVCOM model by AquaModel utilities with vectors showing the towards direction (not the from direction).

Sites 4 and 8 (Figures 43 and 44, respectively) also indicate a general north and south flow rate although the latter was mostly to the north-northwest. The primary result here is a lack of towards shore flow with any significant strength, that helps protect shallow habitats from any unanticipated nitrogen loading and resulting epiphytic algal growth.

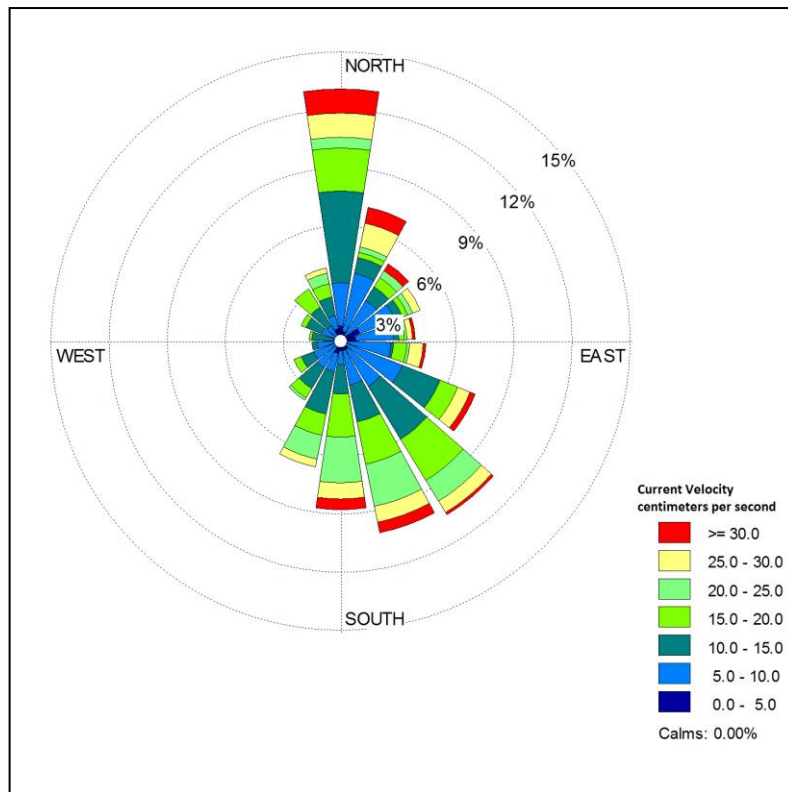
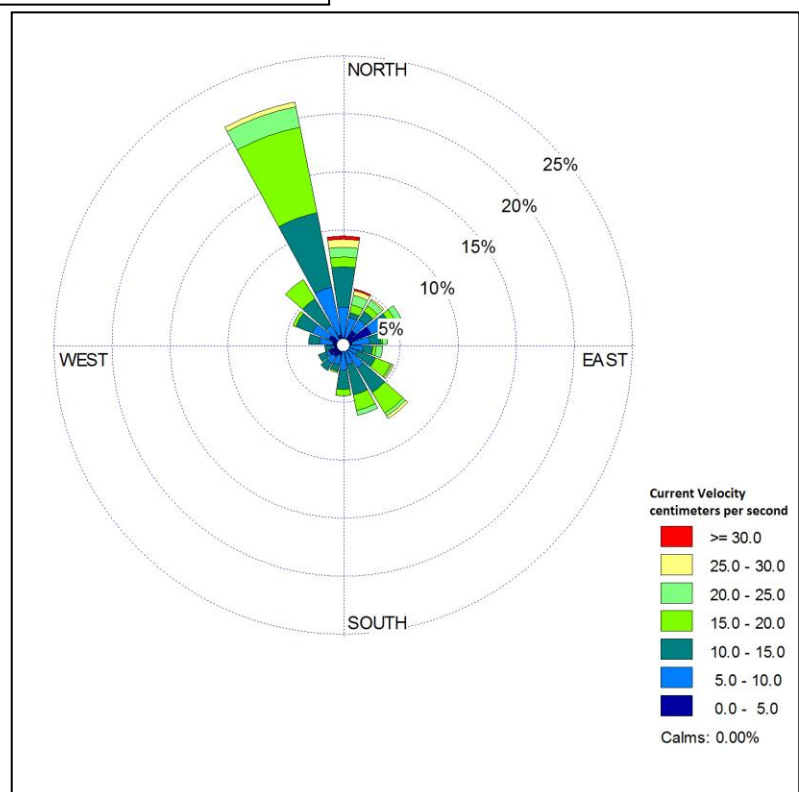


Figure 43. Frequency of occurrence of water currents in each of the specified direction sectors and velocity classes for a month long period at the simulated Site 4 location, using current velocity data extracted from the FVCOM model by AquaModel utilities with vectors showing the towards direction (not the from direction).

Figure 44. Frequency of occurrence of water currents in each of the specified direction sectors and velocity classes for a month long period at the simulated Site 8 location, using current velocity data extracted from the FVCOM model by AquaModel utilities with vectors showing the towards direction (not from direction).



Phytoplankton and Algal Effects

AquaModel's far field program is useful to estimate the effects of fish mariculture on nitrogen flux and resulting plankton standing stock in a designated modeling array. In this case, the modeled array is approximately 81 km long and 37 km wide, but the width includes some land as shown in previous screen prints of the model simulation area. The ideal finding is that no buildup of phytoplankton occurs in the simulation.

Table 8 presents the basic statistics of the final month of fish culture at several of the sites spanning the entire UAE east coast. The ambient (background or boundary condition) value was set at 0.2 $\mu\text{g/L}$ but the AquaModel NPZ model runs for thousands of iterations to stabilize the system before the viewer sees the first visual step. The system stabilized ambient value was then 0.09 $\mu\text{g L}^{-1}$, a value that is low relative to the nitrogen $\frac{1}{2}$ saturation constant for uptake and growth of most marine phytoplankton. This was intentionally done for worst case analysis.

Note in Table 8 that all the available data from worst case locations (i.e., the fish farm sites as indicated) were an immeasurably small value of less than 0.1 $\mu\text{g/L}$ above background conditions during the mid-fall time period in which the final month of fish culture was modeled. Chlorophyll values in many similar marine areas range from 0 to 10 $\mu\text{g L}^{-1}$ and in major blooms of phytoplankton to 50 $\mu\text{g L}^{-1}$, and it is very difficult to measure chlorophyll a at a precision level of 0.1 $\mu\text{g L}^{-1}$.

Table 8. Phytoplankton as chlorophyll ($\mu\text{g L}^{-1}$ = micrograms per liter) summary table for final month of fish culture at study sites from far field AquaModel simulation.

Site No. →	1	3	5	6	7	8
Mean ($\mu\text{g L}^{-1}$)	0.095	0.099	0.096	0.097	0.098	0.098
SD	0.003	0.004	0.003	0.003	0.004	0.004
Min	0.090	0.091	0.091	0.091	0.091	0.091
Max	0.103	0.106	0.103	0.104	0.105	0.105
5 th percentile	0.091	0.093	0.091	0.092	0.092	0.091
95 th percentile	0.100	0.104	0.101	0.102	0.103	0.103
Ambient	0.090	0.090	0.090	0.090	0.090	0.090

Figures 45 through 47 are snapshots of AquaModel showing the main image of phytoplankton at 3.5 m depth at the beginning, middle period and end of the final month of fish culture growout. In order to have any color show in the main image we adjusted the range of chlorophyll a values usually shown (i.e., 0 to 10 $\mu\text{g L}^{-1}$ or more) from 0 to 0.42 $\mu\text{g L}^{-1}$. Setting the top end at 0.43 $\mu\text{g L}^{-1}$ removed all color. This illustrates the tiny variation involved and the lack of apparent effect.

However the effect was generally nearshore, probably due to counter currents near shore and less advection related to nearshore currents. Accordingly, and because we are using tentative calibration factors for the NPZ model, we provide recommendations later in this report for improving the model accuracy with regard to fish farm carrying capacity estimates.

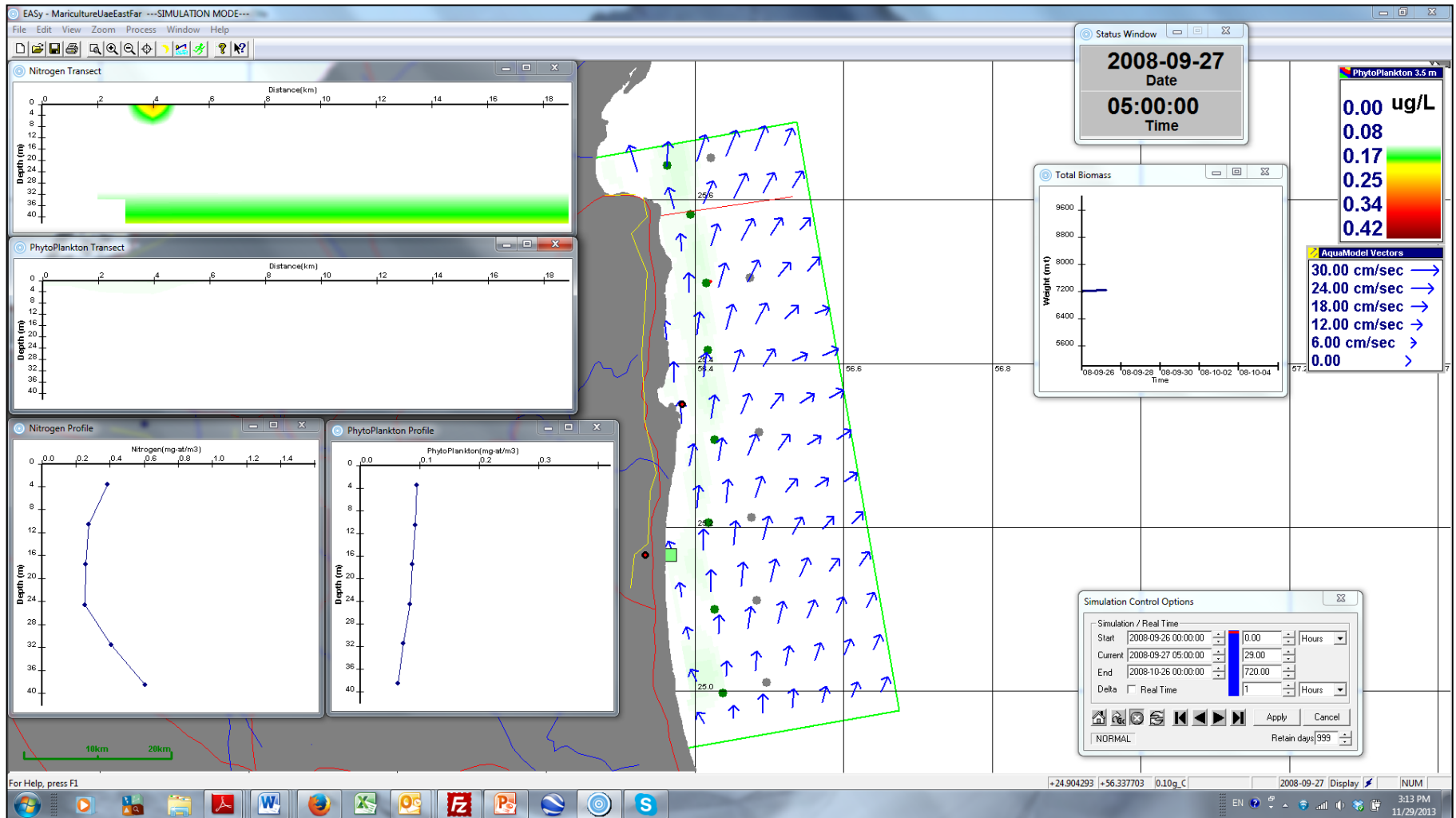


Figure 45. Beginning of last month of fish culture with images from top left to bottom right: Nitrogen transect (red line perpendicular from shore through Site 2, phytoplankton transect, nitrogen profile, phytoplankton profile, main image of phytoplankton standing stock (with very low range of concentration to only $0.42 \mu\text{g L}^{-1}$) and total fish biomass.

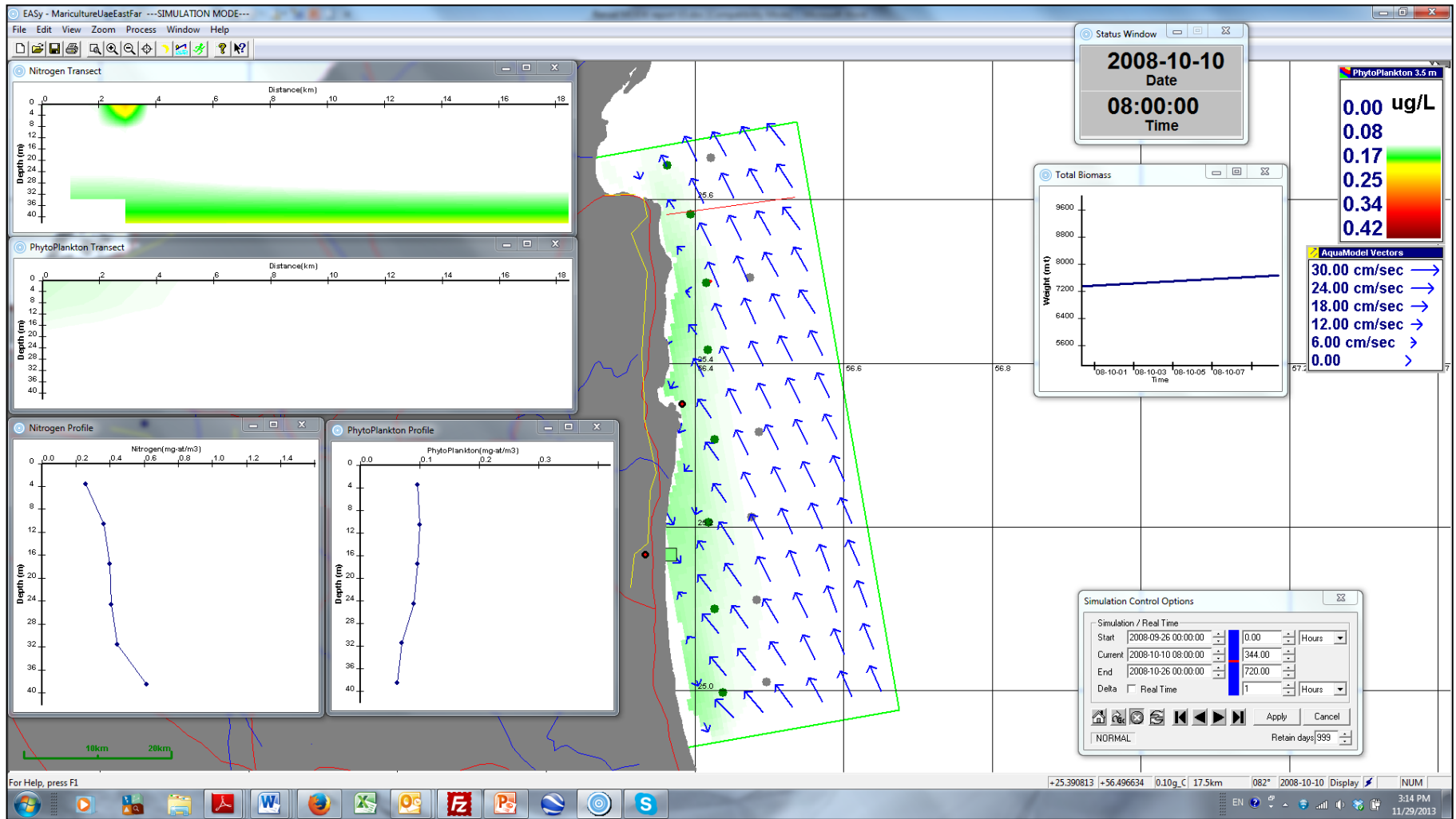


Figure 46. Midway through final month of fish culture with apparent increase of phytoplankton near shore but actual increase is no more than $0.02 \mu\text{g L}^{-1}$.

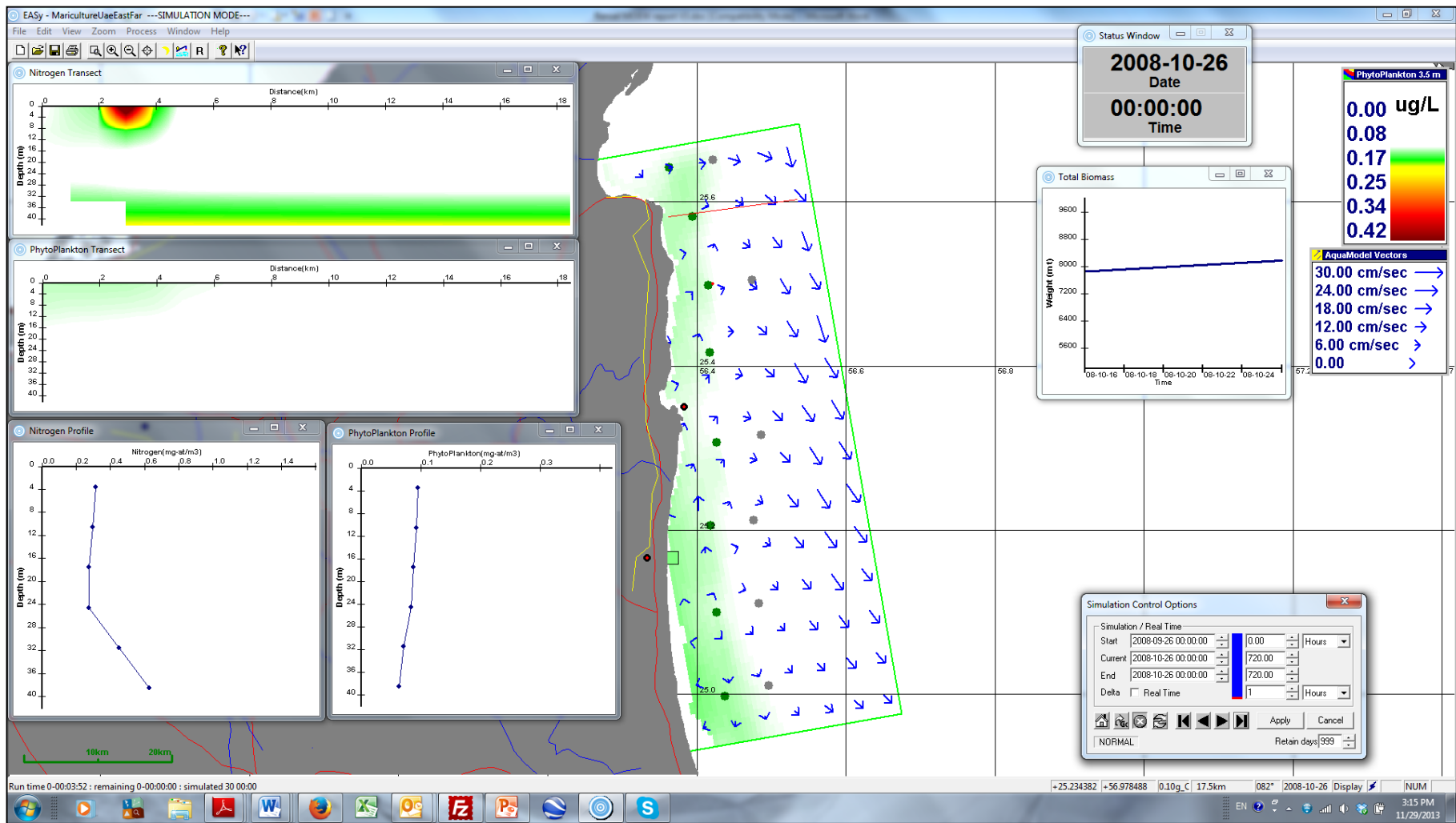


Figure 47. Completion of final month of fish culture with no change from the prior image two weeks before.

Decision Matrix for Net Pen Siting

Many factors are important in selecting and defending choices for net pen fish farm operations. Much quantitative and qualitative information may be gathered for net pen permitting siting proposals and there often is a need to organize and rank such information. Table 5 below lists two categories of information that may be considered including 1) data generated by AquaModel use, that is often quantitative in nature and 2) information gathered about possible use conflicts of the marine waters involved.

A matrix table such as that shown in Table 10 is useful to compare sites and decide how to weight differing types of information that involve conflicts or problems that might endanger successful permitting of a fish farm or result in poor performance after installation. It can also be used to rank candidate sites that have differing attributes, but in most cases will require a weighting factor for one type of criterion versus another. As in all such methods, the weighing of each factor is left to the analyst to apply to meet local situations.

Table 9. Example site selection matrix for various factors involved in site selection.

Category	Site A	Site B
Directly From AquaModel Use and Interpretation		
Current velocity distribution vs. optimum	X	X
Depth at selected site and nearby	X	X
Periods of low dissolved oxygen in pens	X	X
Periods of elevated (ammonia) N in pens	X	X
Amount of near shore N plume effect	X	X
Fish growth and feed conversion rates	X	X
From Other Sources of Information Entered Into AquaModel as Shapefiles or Data		
Navigation conflicts	X	X
Habitats of significance nearby	X	X
Sport and commercial fishing	X	X
Marine mammals	X	X
Marine fish resources	X	X
Shellfish resources	X	X
Ship anchorage zone	X	X
Aesthetics issues (shore side visual effects)	X	X
Neighboring country sovereignty issues	X	X
Security risks (piracy)	X	X
Logistics (distance to shore support)	X	X
Wind wave exposure and fetch	X	X
Water quality (e.g., temperature range)	X	X
Risk of harmful blooms (historical/probability)	X	X
Risk of permit legal appeal from neighbors	X	X
Total	XXX	XXX

Summary of Project Achievements

The goal of setting up AquaModel for initial use in the United Arab Emirates was achieved during this project. More remains to be done to insure the fully accurate calibration of the model, as described below in *Recommendations*. Achievements in this project include:

- Adaptation AquaModel to receive FVCOM circulation model outputs properly and some validation of that adaptation was initiated. This state-of-the-art circulation system is ideal for aquaculture modeling as the irregular grid structure allows for more modeling cells nearshore where fish farms are currently more likely to be placed.
- Development of a novel bathymetric data system that allows the user to merge or overlay differing data sets. In this case, we subcontracted for high resolution nearshore data and the new system integrated those data over the lower background resolution data (GEBCO) in order to increase AquaModel's resolution and accuracy.
- Implementation of a new user interface that should expedite use of the model by coastal managers or industry members. The "Mariculture Options Menu" (partially illustrated in this report) was re-designed, implemented and extensively tested during this project period.
- Alteration of software code and controls that manage mixed (surface) and stratified (deeper) layer vertical dispersion to properly control rates of flow between these nearly discrete compartments of our coastal oceans.
- Initial calibration of the model for the UAE east coast and preliminary determination of the suitability and carrying capacity for fish culture in the region.

While much was achieved, there are additional actions recommended to insure the accurate use of the model and usefulness to MOEW and the developing industry, as discussed next. We emphasize that the model may be used at this point as an approximate tool to manage fish farm development but with additional modest effort the model can be calibrated more accurately for local conditions, tuned and validated to demonstrate efficacy and optimum usefulness.

Recommendations

As with any model, it is necessary to fit the simulation with the best possible local data and calibration factors. It is also advisable to test the model against relatively well known outputs and this can be done on several levels, by component (i.e., one module at a time) or in total (i.e., the benthic or water column effects of primary modeling parameters like sediment total organic carbon and water column dissolved oxygen). Full validation of models is rarely done even in research mode, but there are certain components such as the current velocity and direction data that are best measured at a proposed fish farm site as insurance that the regional 3D model used in this instance has provided sufficiently accurate data for a commercial net pen operation.

We state recommendations as short or long-term goals as follows. The assumption is that MOEW staff would be directly involved in model calibration completion and application follow up, although those services can be provided if needed:

Short term (now and through 1 to 2 years' time line):

- Complete MOEW staff training on the use of AquaModel via internet share screen service such as Skype or Google+ or in person in the U.S. (in Seattle, Los Angeles/USC or at Woods Hole/WHOI).
- Collect or construct GIS shapefiles (from nautical charts and other sources) of potentially competing uses of the subject sea areas, e.g., anchorages, navigation channels, habitats of special significance, etc. for use in preparing an initial screening of suitable aquaculture areas.
- Obtain sufficient local hydrographic data to build an ambient condition (boundary input) file that would have weekly, semi weekly or monthly inputs of key parameters such as dissolved nitrogen, dissolved oxygen, water temperature, irradiance, phytoplankton and zooplankton biomass, mixed layer depths, etc. Some of these data are readily available from worldwide databases and some are being collected by MOEW presently. However, the worldwide databases are biased toward open ocean conditions, so an accurate calibration may involve the necessity of some additional data collection in the 25 to 100 m depth zone nearshore where fish net pens are more likely to locate.
- Obtain growth data for locally-reared gilthead sea bream to allow completion of the sea bream physiology model for AquaModel. Much of the sea bream model is completed, but we must validate it with local data from juvenile to adult fish sizes for fish fed to satiation on a daily basis.
- MOEW should consider obtaining a more recent and powerful PC computer to be able to complete this work. An example would be a Windows 7 desktop or laptop with a solid state hard drive of 500 GB or greater capacity. Existing MOEW computers that we installed the software in are adequate for preliminary testing and use, but higher computation power is needed if the modeling domain grid is to be improved (i.e., decreased) while maintaining the large, 3D modeling domain.

- MOEW may wish to consider obtaining better broadband cable or satellite internet connections to be able to work interactively with our modelers, transfer program and project updates and communicate via screen sharing software now commonly used throughout the world
- We recommend having an outreach seminar with the local fish farmers to inform them and demonstrate the utility of AquaModel. They could suggest possible candidate sites in advance and MOEW staff (with or without our assistance) could run the model to show the results for different locations and configurations.
- If new sites are to be occupied for fish farms, we recommend use of an acoustic Doppler current profiling current meter placed on the sea bottom to collect current flow and direction data throughout the water column and compare the results to seasonal results from the existing FVCOM model data as imported into aquamodel. These current meters can be leased from outlets who prepare them fully for deployment, while placed in a gimbaled bottom mount. Concurrently, drift object (drogue) surveys can easily be conducted to confirm the progressive water motion paths that the far field model suggests herein.

Long term (from now to > 2 years' time line)

- If interest in large scale fish farming in the region continues to grow, consider the need to have occasional routine benthic sampling to evaluate effects of the fish farms and the validity of the model to make projections. Samples for sediment grain size and total organic carbon and possibly other parameters may be collected easily with small grab samplers.
- Encourage fish farmers to routinely monitor and report quantitative and qualitative observations of harmful bloom occurrence. From prior HAB events, seek to establish a conceptual model of bloom occurrence that can be used to at least crudely forecast blooms of specific types or species of HABs.
- Expand the time series of the FVCOM model application: the existing FVCOM model only covers July through December 2008 that was an initiation period of a major harmful algal bloom period that killed wild and farmed fish. There is a need to complete an entire year of modeling as current flows are controlled not only by tides but by winds and ocean circulation patterns. This work may be possible through coordination with other activities in the region that Dr. Anderson and others are pursuing with regards to harmful algal bloom monitoring and prediction and sea water desalination plant protection.

References Cited

- Alexander, R.M. 1967. Functional Design in Fishes. Hutchinson University Library, London. 160 pp.
- Bertalanffy, L. von 1938. A quantitative theory of organic growth (Inquiries on growth laws. II). Human Biol. 10: 181-213.
- Beveridge, M. 1996. Cage aquaculture (2nd edition). Fishing News Books, London.
- Bertalanffy, L. von 1960. Principles and theory of growth, pp 137-259. In Fundamental aspects of normal and malignant growth. W. W. Wowinski ed. Elsevier's, Amsterdam.
- Brooks, K.M., 2001. An evaluation of the relationship between salmon farm biomass organic inputs to the sediments, physicochemical changes associated with those inputs and the infaunal response – with emphasis on total sediment sulfides, total volatile solids, and oxidation-reduction potential as surrogate endpoints for biological monitoring. Aquatic Environmental Services, 644 Old Eaglemount Road, Port Townsend, Washington, USA. 172pp.
- Brooks, K. and C.V.W. Mahnken. 2003. Interactions of Atlantic salmon in the Pacific Northwest environment II: Organic Wastes. Fisheries Research. 62:255-293.
- Chamberlain, J. & Stucchi, D. (2007) Simulating the effects of parameter uncertainty on waste model predictions of marine finfish aquaculture. Aquaculture 272, 296-311.
- Chen et al. 1999 Physical characteristics of commercial pelleted Atlantic salmon feeds and consideration of implications for modeling of waste dispersion through sedimentation Aquaculture International 7: 89–100.
- Chesney, E.J. 1993. A model of survival and growth of striped bass larvae *Morone saxatilis* in the Potomac River, 1987. Aquaculture 92: 15-25.
- City of San Diego. (2008). Annual Receiving Waters Monitoring Report for the Point Loma Ocean Outfall, 2007. City of San Diego Ocean Monitoring Program, Metropolitan Wastewater Department, Environmental Monitoring and Technical Services Division, San Diego, CA.
- Cromey, C.J. and K.D. Black. 2005. Modelling the impacts of finfish aquaculture. Chapter 7 in: The Handbook of Environmental Chemistry. Environmental Effects of Marine Finfish Aquaculture. Volume 5: Water Pollution. Springer, Berlin Heidelberg New York.
- Cromey, C.J., T.D. Nickell, and K.D. Black. 2002a. DEPOMOD - Modelling the deposition and biological effects of waste solids from marine cage farms. Aquaculture 214: 211-239.
- Cromey, C. J., T.D. Nickell, K.D. Black, P.G. Provost, and C.R. Griffiths. 2002b. Validation of a fish farm waste resuspension model by use of a particulate tracer discharged from a point source in a coastal environment. Estuaries 25: 916-929.
- Cromey, C.J. and K.D. Black (2005). Modeling the impacts of finfish aquaculture. Chapter 7 in: The Handbook of Environmental Chemistry. Environmental Effects of Marine Finfish Aquaculture. Volume 5: Water Pollution. Springer, Berlin Heidelberg New York.
- Cromey, C. P. Provost, K. Black. 2003. Development of monitoring guidelines and modelling tools for environmental effects from Mediterranean aquaculture. Newsletter 2. Scottish Association for Marine Science Dunstaffnage Marine Laboratory, Oban, Argyll, PA34 4AD, Scotland, UK

- Davidson, W. 1997. The effects of exercise training on teleost fish, a review of recent literature. *Comp. Biochem. Physiol.* 117A:67-75.
- Duston, J. T. Astatkie and P.F.MacIsaac. 2004. Effect of body size on growth and food conversion of juvenile striped bass reared at 16–28 °C in freshwater and seawater. *Aquaculture* 234:589-600.
- EAO (Environmental Assessment Office). 1997. British Columbia salmon aquaculture review. Environmental Assessment Office, Government of British Columbia, 836 Yates St., Victoria, BC V8V 1X4. http://www.eao.gov.bc.ca/epic/output/html/deploy/epic_project_doc_list_20_r_com.html
- EPA. 1982. Revised Section 301(h) Technical Support Document. Prepared by Tetra Tech. Inc. EPA Publication No. 430/9-82-011.
- EPA-PSEP. 1997. Recommended guidelines for sampling marine sediment, water column, and tissue in Puget Sound. Puget Sound water quality action team report prepared for Puget Sound Estuary Program, U.S. Environmental Protection Agency, Region 10, Seattle, Washington. 47 pp. http://www.psat.wa.gov/Publications/protocols/protocol_pdfs/field.pdf
- EPA 2002. EPA modeling QAPP Requirements for Research Model Development & Application Projects. On line recommendations for projects to receive EPA funding.
- Elberizon, I.R., Kelly, L.A., 1998. Empirical measurements of parameters critical to modelling benthic impacts of freshwater salmonid cage aquaculture. *Aquaculture Research* 29:669– 677.
- Findlay, RH, and L. Watling. 1997. Prediction of benthic impact for salmon net-pens based on the balance of benthic oxygen supply and demand *Marine Ecology Progress Series* 155:147-157.
- Fox, W. 1988. Modeling of particulate deposition under salmon net pens. Prepared for Washington Dept. of Fisheries by Parametrix, Inc. Bellevue, WA. (appendix to state PEIS)
- Fujii, M. S. Murashige, Y. Ohnishi, A. Yuzawa, H. Miyasaka, Y. Suzuki and H. Komiyama. 2002. Decomposition of Phytoplankton in Seawater. Part I: Kinetic Analysis of the Effect of Organic Matter Concentration *Journal of Oceanography*. 58: 433-438.
- Hargrave, B. 1994. Modeling benthic impacts of organic enrichment from marine aquaculture. Canadian Technical Report of Fisheries and Aquatic Sciences 1949. Fisheries and Ocean Canada.
- Hendrichs, S.M. and A.P. Doyle. 1986. Decomposition of ¹⁴C-labeled organic substances in marine sediments. *Limnology and Oceanography*. Vol. 31, pp. 765-778.
- Hickey, B.M. (1992) Circulation over the Santa Monica-San Pedro basin and shelf. *Progress in Oceanography* 30:37-115.
- Hung, S.S.O., F.S. Conte and E.F. Hallen. 1993. Effects of feeding rates on growth, body composition and nutrient metabolism in striped bass (*Morone saxatilis*) fingerlings *Aquaculture* 112:349-361
- Ikura, T., 1974. Sinking velocity of faecal pellet and left over food around yellowtail aquaculture. *Suisan Zoshoku* 22, 34– 39 (in Japanese with English abstract).
- Kiefer, D.A. and C.A. Atkinson. 1988. The calculated response of phytoplankton to nutrient loading by Dungeness Bay Sea Farm. Prepared for Sea Farm Washington and the Jamestown S’Klallam Tribe and presented to the Washington State Shorelines Hearing Board.

Kiefer, D.A., and C.A. Atkinson. 1984. Cycling of nitrogen by plankton: a hypothetical description based upon efficiency of energy conversion. *J. Marine Research*. 42: 655-675.

Kiefer, D.A. and C.A. Atkinson. 1989. The calculated response of phytoplankton in south Puget Sound to nutrient loading by the Swecker Sea Farm. Prepared for Swecker Sea Farm (Rochester Washington) and presented to the Washington State Shorelines Hearing Board. 28 pp.

Kiefer, D.A., J.E. Rensel, F.J. O'Brien, D.W. Fredriksson and J. Irish. 2011. [An Ecosystem Design for Marine Aquaculture Site Selection and Operation](#). (Gulf of Maine and Southern California Bight) NOAA Marine Aquaculture Initiative Program. Final Report. Award Number: NA08OAR4170859. by System Science Applications, Irvine CA in association with United States Naval Academy and Woods Hole Oceanographic Institution. 181 p.

Liao, I.C. et al. 2004. Cobia culture in Taiwan: current status and problems. *Aquaculture* 237:155-165.

Lemarié, G., A. Dosdat, D. Covès, G. Dutto, E. Gasset, and J. Person-Le Ruyet. 2004. Effect of chronic ammonia exposure on growth of European seabass (*Dicentrarchus labrax*) juveniles *Aquaculture* 229:479–491.

Magill, S.H., H. Thetmeyer and C.J. Cromey. 2006. Settling velocity of faecal pellets of gilthead sea bream (*Sparus aurata* L.) and sea bass (*Dicentrarchus labrax* L.) and sensitivity analysis using measured data in a deposition model. *Aquaculture* 251, 295-305.

Morelock, J., Winget, E. A., & Goenaga, C. (1994). Geologic maps of the Puerto Rico insular shelf, Parguera to Guanica. U.S. Geological Survey Misc. Investigations Map I-2387, scale 1:40,000 scale.

Nichols, F.H. 1975. Dynamics and energetics of three deposit-feeding benthic invertebrate populations in Puget Sound, Washington. *Ecol. Monogr.* 45:57-82.

Normandeau Associates and Battelle. 2003. Maine Aquaculture Review. Prepared for Maine Department of Marine Resources. Report R-19336. West Boothbay Harbor, Me, 54 pp. <http://mainegov-images.informe.org/dmr/aquaculture/reports/MaineAquacultureReview.pdf>

O'Brien, F., D. Kiefer and J.E. Jack Rensel. 2011. [Aquamodel: Software for Sustainable Development of Open Ocean Fish Farms](#). U.S. Department of Agriculture: Small Business Innovation Research Final Report Prepared by System Science Applications, Inc. Irvine, CA. Data provided by PacIOOS (www.pacioos.org), part of the U.S. Integrated Ocean Observing System (IOOS®), funded in part by National Oceanic and Atmospheric Administration (NOAA) Award #NA11NOS0120039. 124 p.

Ostrowski, A.C., J. Bailey-Brock and P. Leung. 2001. Hawaii offshore aquaculture research project (HOARP). Submitted to C.E. Helsley, Hawaii Sea Grant. University of Hawaii at Manoa and Oceanic Institute, Oahu, Hawaii. 78 pp.

Panchang, V., G. Cheng, and C.R. Newell. 1997. Modeling hydrodynamics and aquaculture waste transport in coastal Maine. *Estuaries* 20: 14–41.

Parametrix. 1990. Final programmatic environmental impact statement fish culture in floating net-pens. Prepared by Parametrix Inc, Rensel Associates and Aquametrix Inc. for Washington State Department of Fisheries, 115 General Administration Building, Olympia, WA 98504, 161 p.

- Pearson, T.H. and R. Rosenberg. 1978. Macrobenthic succession in relation to organic enrichment and pollution of the marine environment. *Oceanogr. Mar. Bio. Annu. Rev.* 16:229-311.
- Reid, G. K., Liutkus, M., Robinson, S. M. C., Chopin, T. R., Blair, T., Lander, T., Mullen, J., Page, F. and Moccia, R. D. 2009. A review of the biophysical properties of salmonid faeces: implications for aquaculture waste dispersal models and integrated multi-trophic aquaculture. *Aquaculture Research*, 40: 257–273.
- Rensel, J.E. 1987. Aquatic conditions at a proposed net-pen site in Northwest Discovery Bay, Washington. Milner-Rensel Associates for Jamestown S’Klallam Tribe and Sea Farm of Norway, Inc. 74 pp and appendices.
- Rensel, J.E. 1989a. Phytoplankton and nutrient studies near salmon net-pens at Squaxin Island, Washington. in technical appendices of the State of Washington's Programmatic Environmental Impact Statement: Fish culture in floating net-pens. Washington Department of Fisheries. 312 pp. and appendices.
- Rensel, J.E. 1989b. Dissolved nutrients, water quality and phytoplankton studies near the Swecker Sea Farms net-pen site in Lower Case Inlet, and in southern Puget Sound, Washington. Prepared for Swecker Sea Farms, Inc. Tumwater, Washington. 24 pp. plus.
- Rensel, J.E. 2001. Salmon net pens in Puget Sound: Rules, performance criteria and monitoring. An overview of net pen permitting and monitoring in Washington State. *Global Aquaculture Advocate* 4(1):66-69. <http://www.wfga.net/SJDF/reports/regulations.pdf>
- Rensel, J.E., D.A. Kiefer and F.J. O’Brien. 2006. Modeling Water Column and Benthic Effects of Fish Mariculture of Cobia (*Rachycentron canadum*) in Puerto Rico: Cobia AquaModel. Prepared for Ocean Harvest Aquaculture Inc., Puerto Rico and The National Oceanic and Atmospheric Administration, Washington D.C. by Systems Science Applications, Inc. Los Angeles, CA. 60 pp. http://www.lib.noaa.gov/docuqua/reports_noaaresearch/cobia_aquamodel_final_report.pdf
- Rensel, J.E., D.A. Kiefer, J.R.M. Forster, D.L. Woodruff and N.R. Evans. 2007. Offshore finfish mariculture in the Strait of Juan de Fuca. *Bull. Fish. Res. Agen.* No. 19, 113-129, <http://www.fra.affrc.go.jp/bulletin/bull/bull19/13.pdf>
- Rensel, J.E. (Chapter Editor), A.H. Buschmann, T. Chopin, I.K. Chung, J. Grant, C.E. Helsley, D.A. Kiefer, R. Langan, R.I.E. Newell, M. Rawson, J.W. Sowles, J.P. McVey, and C. Yarish. 2006. Ecosystem based management: Models and mariculture. Pages 207-210 in J.P. McVey, C-S. Lee, and P.J. O'Bryen, editors. *The Role of Aquaculture in Integrated Coastal and Ocean Management: An Ecosystem Approach*. The World Aquaculture Society, Baton Rouge, Louisiana, 70803. United States
- Rensel, J.E. 2007. Fish kills from the harmful alga *Heterosigma akashiwo* in Puget Sound: Recent blooms and review. Prepared by Rensel Associates Aquatic Sciences for the National Oceanic and Atmospheric Administration Center for Sponsored Coastal Ocean Research (CSCOR). Washington, D.C. 59 pp.
- Rensel, J.E. and J.R.M. Forster. 2007. Beneficial environmental effects of marine net pen aquaculture. Rensel Associates Aquatic Sciences Technical Report prepared for NOAA Office of Atmospheric and Oceanic Research. 57 pp. http://www.wfga.net/documents/marine_finfish_finalreport.pdf

- Riedel, R. and C. Bridger. 2003. Simulation for Environmental Impact. Mississippi-Alabama Sea Grant Consortium software, Ocean Springs, MS. MASGP-03-001-01.
- Sanderson, J.C. , C.J. Cromey, M.J. Dring and M.S. Kelly. 2008. Distribution of nutrients for seaweed cultivation around salmon cages at farm sites in north-west Scotland. *Aquaculture* 278:60-68.
- Trusty, M.F., K Snook, V.A. Pepper and M.R. Anderson. 2000. The potential for soluble and transport loss of particulate aquaculture wastes. *Aquaculture Res.* 31:745.
- WDF (Washington Department of Fisheries). 1991. Programmatic Environmental Impact Statement: Fish culture in floating net-pens. Prepared by Parametrix, Battelle Northwest laboratories and Rensel Associates. Olympia WA. 61 pp.
- Weber, M., D. de Beer, C. Lott, L. Polerecky, K. Kohls, R. M. M. Abed, T.G. Ferdelman, and K.E. Fabricius. 2012. Mechanisms of damage to corals exposed to sedimentation. *PNAS* 109: E1558-E1567.
- Weston, D.P. 1990. Quantitative examination of macrobenthic community changes along an organic enrichment gradient. *Mar. Ecol. Prog. Ser.* 61:233–244
- Weston, D. and R. Gowen. 1988. Assessment and prediction of the effects of salmon net pen culture on the benthic environment. Tech. Appendix to the State of Washington’s Programmatic Environmental Impact Statement: Fish culture in floating net pens. Washington Dept. of Fisheries. 312 pp.
- Westrich, J.T., Bernier, R.A., 1984. The role of sedimentary organic matter in bacterial sulphate reduction: the G model tested. *Limnol. Oceanogr.* 29, 236– 249.
- Wroblewski, J.S., J. L. Sarmiento, and G. R. Flierl. 1988. An Ocean Basin Scale Model of Plankton Dynamics in the North Atlantic 1. Solutions for the Climatological Oceanographic Conditions in May. *Global Biogeochemical Cycles*, vol. 2(3): 199-218.